Localizing selected endocytosis protein candidates in *Plasmodium falciparum* using GFP-tagged fusion constructs

Prepared by:

TRAVIS BASSON

Under the supervision of:

PROFESSOR HEINRICH C. HOPPE

Submitted in fulfilment of the academic requirements for the degree of:

MASTER OF SCIENCE IN BIOCHEMISTRY

Department of Biochemistry and Microbiology

Rhodes University, Grahamstown, South Africa

RHODES UNIVERSITY

Grahamstown • 6140 • South Africa

FEBRUARY 2016

ABSTRACT

Malaria is a mosquito-borne infectious disease caused by several obligate intracellular protozoan parasites in the *Plasmodium* genus, with *Plasmodium falciparum* causing the most widespread cases and malaria deaths. In 2013 there were approximately 190 million cases of the disease and between 584,000 and 855,000 deaths. It is essential to identify novel drug targets and develop novel drug candidates due to the increase in resistance of *P. falciparum* parasites to the current arsenal of antimalarial drugs. Endocytosis is an essential process in eukaryotic cells in which the external environment is internalized by the cell in order to obtain various particles from the extracellular space. This extracellular cytoplasm is internalized in membrane-bound invaginations at the plasma membrane. During the blood stage of malaria infection, the parasite requires nutrients from the host red blood cell. To obtain these nutrients, the parasite internalizes haemoglobin in large amounts and degrades it in an acidic, lysosome-like organelle, known as the digestive vacuole. Whilst the exact molecular mechanism of malaria parasite endocytosis is not yet fully understood, a number of proteins have been suggested to be involved. The most expedient approach in identifying candidate endocytosis proteins is to investigate parasite homologues of proteins known to be involved in endocytosis in mammalian cells. The three proteins selected for investigation in this study were the *P. falciparum* homologues of coronin, dynamin 2, and μ4.

The coding sequences for the candidate endocytosis proteins were amplified by PCR and cloned into the pARL2-GFP expression vector. *P. falciparum* 3D7 parasites were transfected with these vectors and the episomal expression of full-length GFP-tagged fusion protein was confirmed by Western blot analysis using commercially available anti-GFP antibodies. Microscopic analysis of live parasites using fluorescence and confocal microscopy was used to determine the localization of the candidate endocytosis proteins. Coronin appeared to display diffuse cytoplasmic GFP localization during the trophozoite stage, arguing against a role in endocytosis. However, distinct localization during the schizont stage at what appears to be the inner membrane complex was observed. Coronin is thus likely required to coordinate the formation of

the actin network between the merozoite IMC and the plasma membrane on which the glideosome is dependant for generating the motile forces required for the merozoite motility and invasion of RBCs.

Dynamin 2 displayed localization at three potential locii: the parasite periphery (plasma membrane), punctuate regions within the cytoplasm (potentially at membrane bound organelles) and at the parasite food vacuole. The data suggested that dynamin 2 is involved in endocytosis and membrane trafficking in a similar manner to classical dynamins, potentially as a vesicle scission molecule at the plasma membrane, mediating vesicle formation at the food vacuole to recycle membrane to the plasma membrane, and possibly mitochondria organelle division. μ4 displayed transient localization, cycling between cytosolic localization, and localization to distinct regions at the plasma membrane and the food vacuole. Localization of *Pf*μ4 to the plasma membrane is indicative of a role for μ4 as a part of an adaptor protein (AP) complex which may be responsible for recruitment of clathrin to initiate endocytosis in a manner similar to mammalian AP-2. As was observed with *Pf*DYN2, *Pf*μ4 localizes to the FV, which suggests that *Pf*μ4 forms part of a coat complex that mediates the formation of vesicles that recycle membrane from the FV to the parasite plasma membrane. This study showed that expressing proteins as full-length GFP-tagged fusion constructs is an effective approach in the early stages of determining the localization and function of *P. falciparum* proteins *in vitro*, and distinguishing between candidates that have a potential role in endocytosis and those that are unlikely to do so.

TABLE OF CONTENTS

LIST OF FIGURES

LIST OF TABLES

LIST OF ABBREVIATIONS

BLAST	basic local alignment search tool
a.a	amino acid
AP	adaptor protein
BFA	brefeldin A
bp	base pair
BSA	bovine serum albumin
CCP	clathrin-coated pit
CCV	clathrin-coated vesicle
cDNA	complementary DNA
crt	chloroquine resistance transporter protein
DAPI	diamidino-2-phenylindole
Dlp	dynamin-like protein
DMSO	dimethylsulfoxide
DRP	dynamin-related protein
DV	digestive vacuole
E. coli	*Escherichia coli*
EDTA	ethylenediaminetetraacetic acid
ER	endoplasmic reticulum
FITC	fluorescein isothiocyanate
FP	ferriprotoporphyrin IX
fRBC	fresh red blood cell
FV	food vacuole
gDNA	genomic DNA
GED	GTPase effector domain
GFP	green fluorescent protein
hDHFR	human dihydrofolate reductase
HEPES	*N*-(2-hydroxyethylpiperazine-*N*'-2 ethanesulfonic acid
IMC	inner membrane complex
iRBC	infected red blood cell
Kb	kilobase
kDa	kilo dalton
LB	luria broth
NPF	nucleation promoting factor
OD	optical density
ORF	open reading frame
PH	pleckstrin homology
Pi	inorganic phosphate
PlasmoDB	*Plasmodium* genome database
PMT	photomultiplier tube
PPM	parasite plasma membrane
PRD	proline rich domain

PVM	parasitophorous vacuole membrane
RE	restriction enzyme
SCAR	suppressor of cAMP receptor
SIM	SUMO 2/3 interacting motif
Tm	melting temperature
WASP	Wiskott-Aldrich syndrome protein
WHO	World health organization
WT	wild-type
YFP	yellow fluorescent protein

ACKNOWLEDGEMENTS

The completion of this degree has been a great challenge and would not have been possible without a number of key people.

I would like to express my sincere gratitude to my supervisor, Professor Heinrich Hoppe. His guidance, patience, teaching, understanding, support and advice were vital, and much appreciated.

My sincere appreciation goes to my loving wife, Amanda, for her continuous support and motivation, the recipient of all my outpourings of frustration during the difficult moments. To my parents Anita and Tony Basson, and my family that supported and encouraged me, as well as assisted me financially during my studies, I am forever grateful.

My thanks to the members of Lab 309, especially Dustin Laming and Tarryn Swart, for their friendship, expertise and support in the lab. I thank Dr. Ben Loos and Prof. Marina Rautenbach for their hosting at Stellenbosch University and support with the confocal microscopy. I thank Prof. Dr. Jude Przyborski for his hosting at Phillips-Universität Marburg, Germany, and his assistance with the generation of mCherry expression vectors.

I thank the following organizations for financial support: DST-NRF Innovations Master Scholarship, Medical research council of South Africa, Rhodes University and the Deutsche Forschungsgemeinschaft**.**

CHAPTER ONE: INTRODUCTION

1.1. Introduction to Malaria

Malaria is a life-threatening, mosquito-borne infectious disease caused by several obligate intracellular protozoan parasites in the genus *Plasmodium*, including *Plasmodium falciparum, Plasmodium ovale, Plasmodium knowlesi, Plasmodium vivax,* and *Plasmodium malariae* (Fattorusso & Taglialatela-Scafati 2009). *P. falciparum* is responsible for most severe disease and most fatal cases in humans across sub-Saharan Africa (Fidock *et al*. 2004; Kappe *et al*. 2010). *P. vivax* is the most prevalent parasite in most other malaria-endemic areas of the world. *P. vivax* malaria has historically been categorized as benign, but recent data suggests that severe disease caused by infection of this strain is common (Price *et al*. 2007).

1.1.1. Extent of Malaria

The extent of malaria is vast; according to the World Health Organization (WHO malaria report, 2013) there were approximately 198 million cases of disease, and between 584,000 and 855,000 deaths in 2013 and it accounted for 2.23% of worldwide deaths in that year. The WHO further states that half of the world's population is at risk of malaria infection and majority of deaths caused by malaria are children under the age of 5 years. Although most of the cases and deaths due to malaria occur in sub-Saharan Africa (up to 90%), malaria also affects Asia, Latin America and the Middle East.

1.1.2. Life cycle of Plasmodium falciparum

The life cycle is complex (Van Agtmael *et al*. 1999) with the asexual stage of development and multiplication occurring within the liver and red blood cells (RBCs) of the human host, followed by the sexual stage of the life cycle taking place within the midgut of the female *Anopheles* mosquito (Figure 1) (Beier 1998). While there are many species of *Anopheles* mosquito that transmit the disease, *Anophele gambiae* is the chief vector of *P. falciparum*.

Infection in humans begins when sporozoite stage parasites from the saliva of a malaria infected anopheline mosquito are injected into the blood stream during a blood meal (Beier 1998). The

sporozoites remain in circulation in the blood (Van Agtmael *et al*. 1999; Beier 1998) before they enter the liver of the host and invade hepatocytes (Lopez-Antunano & Shmunis, 1980). The sporozoites mature and undergo drastic changes, and multiply over the following two weeks to form schizonts, and ultimately burst from the infected hepatocytes as thousands of haploid forms called merozoites into the bloodstream where they proceed to infect healthy RBCs (Van Agtmael *et al*. 1999).

The blood phase of the life cycle is initiated when free merozoites from the liver schizonts are released into circulation where they invade RBCs and develop into early trophozoites (also known as ring stage parasites) (Beier 1998). These trophozoites are ring shaped, vacuolated and uninucleated (Trampuz *et al*. 2003). The rings develop into trophozoites, which have high metabolic activity that includes extensive endocytosis of host cell haemoglobin and cytoplasm, glycolysis and production of parasite genetic material and proteins (Martin *et al*. 2005). During this trophozoite stage, the parasites produces secretory proteins which are exported across the parasite plasma membrane and the PVM (parasitophorous vacuole membrane) to the red blood cell in order to modify the membrane of the RBC and the RBC cytosol (Taraschi *et al*. 2003). Trophozoite stage parasites mature to form schizonts, which undergo nuclear division to produce up to 32 daughter merozoites, a process known as blood schizogony (Trampuz *et al*. 2003). Eventually the infected RBCs are lysed by protease-dependant lysis, and the released merozoites subsequently invade other healthy RBCs, starting a new cycle of asexual reproduction (Talman *et al*. 2004). The duration of time from infection of the liver cells to the development of disease symptoms is between 10 and 15 days, and the duration of each cycle of asexual reproduction is approximately 48 hours in *P. falciparum* infected humans (Giobbia *et al*. 2005).

After several cycles, some of the merozoites that do not follow the normal asexual cycle develop into male and female gametocytes (macrogametocytes and microgametocytes), the sexual stage of malaria, which is infective for mosquitoes when they take a blood meal (Kooij & Matusch 2007; Trampuz *et al*. 2003). The parasite numbers passing from mosquito to human and back to mosquito have been found to be exceedingly low in comparison to parasite populations in an infected individual during asexual blood stage replication (Kappe *et al*. 2010), but is nonetheless sufficient to maintain the cycle.

The gametocytes from a blood meal are haploid cells and differentiate into gametes in the mosquito midgut (Gerald *et al*. 2011) where a small number of male gametes will fuse with female gametes to create diploid zygotes (Gerald *et al*. 2011). These diploid zygotes develop into motile ookinetes that penetrate the midgut epithelium (Janse *et al*. 1986) and ultimately become embedded in the basal lamina beneath the midgut epithelial wall and develop into oocysts on the exterior of the gut wall (Beier 1998). Over the course of several days a single oocyst undergoes multiple cycles of DNA synthesis and mitosis to create a sporoblast (Carreno *et al*. 1997). In a large cytokinesis event, thousands of haploid daughter sporozoites are formed and migrate to the salivary glands of the mosquito where they are available for transmission to a new human host to complete the life cycle (Kooij & Matusch 2007; Schrevel *et al*. 2008).

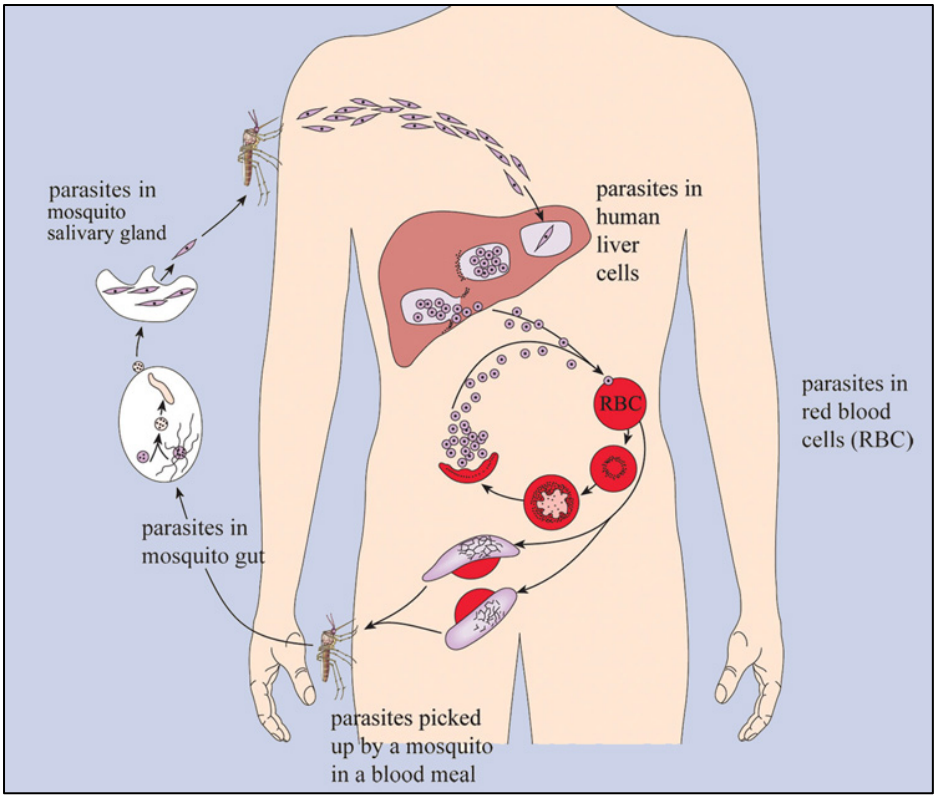

Figure 1. Simplified life cycle of the malaria parasite *P. falciparum*

(Adapted from: The Open University, 2003, *Infectious disease*, Book 5: *Evolving Infections*, Figure 3.4).

1.1.3. Symptoms and Effects of the Disease

Initial symptoms of malaria usually present 8-25 days following infection, although these symptoms could occur later in patients that have taken antimalarial medication as preventative measure. Symptoms include, but are not limited to: headache, fever, vomiting, joint pain and shivering (Fidock *et al*. 2004). The parasite invasion and destruction of red blood cells of the human host causes anaemia. The rupturing of infected erythrocytes is associated with the release of cell debris into the blood stream (Fidock *et al*. 2004) which is responsible for the fever spike patterns in intervals of 48 hours. This cyclical occurrence of coldness and shivering followed by fever and sweating occurring in 48-hour intervals is a hallmark symptom of malaria, known as paroxysm (Fidock *et al*. 2004).

The parasite evades the immune system by invading and residing inside red blood cells, and the modification of the RBC causes the cytoadherence of the infected RBC to the endothelium of capillaries, which allows them to avoid destruction by immune clearance by spleen macrophages (Fidock *et al*. 2004; Haldar 1998)**.** The parasite regularly changes the amino acid sequence of the proteins that it presents on the surface of the red blood cell in order to further protect them from the immune system (Fidock *et al*. 2004). Due to the changes in the adhesion properties of the RBC, it can lead to the sequestration of infected RBCs to the blood-brain barrier endothelia and other organs. This also causes an obstruction of blood vessels and associated inflammatory responses (Fattorusso & Taglialatela-Scafati 2009). In some cases this can lead to severe anaemia, organ failure and cerebral malaria.

1.2. Endocytosis in eukaryotic cells

1.2.1. Vesicular trafficking in Eukaryotic cells

Vesicular trafficking in eukaryotic cells is made up of the endocytic system, where cells internalise macromolecules (such as proteins) from the extracellular space and the exocytic systems, where molecules are systematically exported from the cell.

The internalization of macromolecules by endocytosis from the extracellular environment occurs at specialized sites on the plasma membrane. The function of this process is to internalize cargo that is to unable to pass through the membrane by passive diffusion or via membrane transport proteins (Sigismund *et al*. 2012). Invaginations are formed at the plasma membrane to assemble coated transport vesicles which are internalized into the cell (Ungewickell & Hinrichsen 2007).

Endocytosis can be roughly characterized into two categories; firstly, phagocytosis and macropinocytosis and secondly, pinocytosis. Phagocytosis is the process by which large particles (above 500 nm) are internalized. This is the general case for bacteria and apoptotic cells (Sigismund *et al*. 2012). These large particles are engulfed by membrane extensions or pseudopods, and this process is usually limited to specialized cells such as *Dictyostelium* amoeba and mammalian macrophages (Doherty & McMahon 2009).

Macropinocytosis is a GTPase regulated process in which large actin-driven membrane protrusions engulf large amounts of the extracellular environment into endocytic vesicles known as macropinosomes (Conner & Schmid 2003b). The formation of these membrane pseudopods and membrane protrusions into the extracellular environment is facilitated by extensive remodelling of the actin cytoskeleton, and coordinated by Rho-GTPases and signalling cascades (Insall & Machesky 2009; Niedergang & Chavrier 2004).

Pinocytosis occurs in all eukaryotic cell types and is characterized by the invagination of specific regions of the plasma membrane that gives rise to pinocytic vesicles. These pinocytic vesicles are used for the uptake of fluids and small solutes into the cell (Doherty & McMahon 2009; Kerr & Teasdale 2009). There are multiple pathways by which pinocytosis occurs, based on the size of the extracellular cargo to be internalized (Doherty & McMahon 2009). These pathways

include clathrin-mediated, caveolae-mediated, and clathrin- and caveolae-independent endocytosis (Conner & Schmid 2003b).

Caveolae are less common in eukaryotic cell types than clathrin-mediated processes and present as small, flask shaped invaginations at sphingolipid and cholesterol rich membrane domains, or lipid rafts in the plasma membrane (Kirkham & Parton 2005). Caveolae-mediated endocytosis is dependent on dynamin for fission of vesicles from the plasma membrane (Kirkham & Parton 2005). Caveolae and clathrin-independent endocytosis is not as well defined, but also involves lipid rafts to facilitate the internalization of lipids and fluids from outside the cell. Like caveolae and clathrin-dependent endocytosis, internalization is a transient process, activated by cargo, which is dependent on cholesterol and the actin cytoskeleton, but is independent of dynamin for vesicle scission (Kirkham & Parton 2005).

1.2.2. Clathrin-mediated membrane budding:

Clathrin-mediated endocytosis (CME) is the prominent pathway for the uptake of nutrients as well as signalling molecules in higher eukaryotic cells. In fibroblasts for example, according to Bretscher (1982), the high efficiency of clathrin-mediated endocytosis machinery has been estimated to endocytose almost the equivalent of the cell's total plasma membrane within one hour. A wide variety of transmembrane receptors and their ligands are packaged with the use of cargo adaptors into clathrin-coated vesicles (CCVs) (Doherty & McMahon 2009). CCV formation isn't limited to the plasma membrane; they can also bud from a variety of intracellular compartments by using different adaptor proteins (Schmid & McMahon 2007). This means that there are various forms of CCVs within the cell at any given time (Doherty & McMahon 2009). For CCP (clathrin-coated pit) and CCV formation at the plasma membrane, there is a large range of possible cargo adaptors and accessory proteins that can be used. This means that the diversity of adaptor and accessory proteins used to implement vesicle formation reflect the pathway's adaptions to the materials being packaged (Doherty & McMahon 2009).

The processing of an endocytic coated vesicle starts with the recruiting of clathrin-adaptors and endocytic accessory proteins to the plasma membrane where they are observed to form clumps ranging from 10 nm to more than 500 nm. According to an electron microscopy study

performed by Heuser (1980), clathrin networks are polygonal in shape at multiple stages of invagination which culminates in an almost completely closed polyhedral structure that surrounds the coated membrane invaginations. This study provided visuals of the dynamic process which provided the basis for a widely accepted membrane budding model in which the internalization process begins with primarily flat, hexagonal lattices that become curved (Heuser 1980). In order to promote the polymerization of clathrin into curved lattices, adaptor and accessory proteins coordinate clathrin nucleation at sites of the plasma membrane destined for internalization (Schmid *et al*. 2006). This nucleation also stabilizes the deformation of the attached plasma membrane (Doherty & McMahon 2009). Clathrin polymerization aids in the development and constriction of the vesicle neck. This forces the membranes surrounding the vesicle neck into close proximity (Doherty & McMahon 2009). The clathrin encased vesicles eventually separate by fission from the plasma membrane (Ungewickell & Hinrichsen 2007). This separation of the vesicle from the plasma membrane is due to the membrane scission protein, dynamin. Dynamin is a large GTPase that forms a helical polymer surrounding the neck of this constricted membrane neck, and upon GTP hydrolysis, mediates the irreversible fission of the vesicle from the plasma membrane, releasing the CCV to the interior of the cell (Doherty & McMahon 2009; Praefcke & McMahon 2004).

Before these vesicles fuse with endosomes, clathrin and the adaptors are released from the vesicles membrane by auxilin and hsc70. The now soluble coat proteins can then be involved in a subsequent round of clathrin coated vesicle formation (Doherty & McMahon 2009; Ungewickell & Hinrichsen 2007). The vesicle then undergoes further trafficking within the cell, before delivering the cargo contained within through fusion with the destination intracellular compartment, early endosomes (Doherty & McMahon 2009). Some of the internalized bulk membrane and associated transmembrane proteins are re-cycled back to the plasma membrane. The early endosomes mature into late endosomes that ultimately fuse to lysosomes where the endocytosed cargo is degraded.

1.3. Endocytosis in *Plasmodium falciparum* parasites

During the blood stage of malaria infection, the parasite requires nutrients from the host red blood cell and extracellular environment. The parasite internalizes host RBC haemoglobin and degrades it in large amounts (Elliott *et al*. 2008). It is during the trophozoite stage of the parasite life cycle that the parasite is most metabolically active, synthesizing genetic material (DNA and RNA) and proteins. *P. falciparum* parasites digest more than 80% of the RBC haemoglobin in order to support parasite growth and replication during the blood stage (Ginsburg 1990).

Haemoglobin is internalized from the host cell and transported to the digestive vacuole (DV) or food vacuole (FV), an acidic compartment comparable to the mammalian lysosome (Elliott *et al*. 2008; Lazarus *et al*. 2008). The internalization of RBC cytoplasm is facilitated by double-membrane invaginations of the PPM (parasite plasma membrane) and the PVM (parasitophorous vacuole membrane) known as the cytostome (Lazarus *et al*. 2008). The cytostome is the specialized site of haemoglobin endocytosis and is characterized by the presence of sub-membranous electron-dense material flanking the cytostome neck (Lazarus *et al*. 2008). Following the budding of the double-membrane cytostome derived vesicles, they pinch off and the vesicles are proposed to be trafficked to, and fuse with the FV for degradation of the enclosed haemoglobin (Lazarus *et al*. 2008). While this is the widely accepted view of the mechanism of haemoglobin uptake and transport to the FV, the exact identity and characteristics of the transport machinery, the biochemical characterization of the cytostomes and haemoglobin transport structures is not fully understood (Cooke *et al*. 2004; Elliott *et al*. 2008; Lazarus *et al*. 2008).

Haemoglobin is digested in the acidic parasite FV by two aspartic proteases, plasmepsin I and II, and a calcium-dependent cysteine protease, falcipain (Lazarus *et al*. 2008). The haemoglobin is hydrolyzed into heme, and globin. The amino acids attained from the globin are exported into the parasite cytoplasm, and the resulting toxic heme moiety, ferriprotoporphyrin IX (FP) is detoxified by its polymerization and sequestration as an inert crystalline pigment known as the haemozoin crystal (Elliott *et al*. 2008; Hempelmann 2007; Roberts *et al*. 2008). Antimalarials such as chloroquine accumulate in the FV where they interfere with the polymerization of heme, by dimerizing with the FP, causing an inhibition of haemozoin formation, and therefore causing a toxic accumulation of FP and chloroquine-FP complexes (Roberts *et al*. 2008).

1.4. Coronin

1.4.1. Introduction to coronin

Coronins are a highly conserved family of actin cytoskeleton regulators (Uetrecht & Bear 2006). They promote cell motility and have been shown to modulate other actin-dependent processes (Chan *et al*. 2011). Cell motility has a vital role in the causation of a variety of disease states, such as cancer, and many autoimmune disorders. In a majority of cases, cell motility is dependent on the re-organization of the actin cytoskeleton (Uetrecht & Bear 2006). Coronin was originally identified as a component of a contracted actin-myosin preparation from *Dictyostelium* (de Hostos *et al*. 1991). During this initial identification, antibodies raised against coronin were used to localize the protein to 'crown-like' structures on the dorsal surface of the cells. Coronin-deficient cells showed a 50% reduction in cell migration speed (Uetrecht & Bear 2006). Additionally, cytokinesis (cell division), fluid-phase endocytosis uptake and growth was significantly impaired (de Hostos *et al*. 1991; Ishikawa-Ankerhold *et al*. 2010).

1.4.2. Structure of coronin

The most defining characteristic of structure for the coronin family of proteins is the presence of WD40 domain repeats that form a β-propeller. Originally, the five WD40 repeats were thought to form a five-bladed β-propeller which is flanked by highly conserved N- and C-terminal extensions (de Hostos 1999). However, according to Appleton *et al*. (2006), most of the sequence in the highly conserved extensions form the first and last blades of a seven-bladed β-propeller. The initial predictions regarding the N- and C-terminal extensions was found to be partially correct- there are short highly conserved stretches in both the N- and C-terminal extensions that do not participate directly in the β-propeller structure. These are thought to be involved in the regulation of coronin interaction with binding partners and potentially also involved in the stabilisation of the β-propeller (Chan *et al*. 2011). Indeed, according to Cai *et al*. (2007) the N-terminal extension contains a crucial phosphorylation site that regulates the interaction of coronin with binding partners. Following the C-terminal extension there is a unique region that links the coiled-coil domain to the β-propeller. Based on phylogenetic analysis, mammalian coronin genes are grouped into three types: Type I, II, and III. The basic

structural arrangements apply to all coronins of Type I and Type II classes. However Type II coronins contain several blocks of conserved residues in predicted loops in the β-propeller, as well as unique regions that distinguish them from the Type I coronins (Chan *et al*. 2011). The Type III class of coronins also contain the N- and C-terminal extensions, but are unusual because they have two complete β-propeller units, which are linked by a sequence that has been predicted to be flexible (Chan *et al*. 2011). These coronins lack the coiled-coil domain, but have a highly acidic region at the C-terminus (Uetrecht & Bear 2006).

1.4.2.1. Mechanism of Type I coronin function

The main defining characteristic of type I coronins is their ability to bind F-actin (Chan *et al*. 2011). Targeted strategies to determine the surface patches of the β-propeller that associate with F-actin were employed and it was found that a charged patch on the upper surface of the β-propeller is critical for high affinity F-actin binding (Gandhi *et al*. 2010). A single conserved residue located in this patch, R30 (arginine at position 30) has been found to be critical for F-actin binding (Cai *et al*. 2007; Chan *et al*. 2011). This was discovered because Arg30 can be mutated to Aspartic acid (R30D), which results in the loss of F-actin binding (Chan *et al*. 2011).

Actin proteins have native ATPase activity that is triggered by polymerization into filaments. A by -product of this reaction is inorganic phosphate (Pi), which is released slower than hydrolysis occurs, leading to a segment of filament that retains this bound phosphate (Chan *et al*. 2011). Once phosphate is released, the actin filament takes on an ADP conformation that favours depolymerisation at the pointed end of the actin filament (Pollard *et al*. 2003). According to Chan *et al*. (2011), type I coronins have a definite preference for ATP/ADP+Pi F-actin, over the ADP-bound form of F-actin. A stark example of this is human Cor1B, which has a binding affinity for F-actin that is approximately 50-fold higher for newly polymerized actin that is enriched for ATP/ADP+Pi F-actin relative to actin filaments polymerized from pure ADP-bound monomers (Cai *et al*. 2007). According to Gandhi *et al*. (2009), the same has been observed in budding yeast coronin. This suggests that this preference for F-actin is a conserved property of Type I-like coronins.

Coronins of the type I class also interact with the Arp2/3 complex (Marshall *et al*. 2009). The Arp2/3 complex is a crucial component in the regulation of actin polymerization. This complex associates with the side of a growing actin filament, where it nucleates the formation of a daughter filament at a 70° angle to the mother filament, and this activity results in the formation of a branched actin network (Appleton *et al*. 2006; Insall & Machesky 2009). The Arp2/3 complex consists of seven subunits, with Arp2 and Arp3 being very similar in structure and sequence to actin. The remaining 5 subunits are unique, and highly evolutionarily conserved (Insall & Machesky 2009). The actin-nucleating and actin-branching activities of Arp2/3 are activated by nucleation promoting factors (NPFs), including the "suppressor of cAMP receptor and the Wiskott-Aldrich syndrome protein (WASP)-family verprolin homology protein" (SCAR/WAVE) and WASP families of proteins (Uetrecht & Bear 2006). According to Insall & Machesky (2009), Arp2/3 in its biochemically pure form is biochemically inactive, and is maximally activated via its interactions with the WASP family protein C-terminal sequence (known as VCA), as well as an actin filament. The V domain of the WASP protein interacts with actin monomers while the CA region associates with the Arp2/3 complex to create a nucleation core. Since the complex only shows maximal activity as part of this multimolecular structure, and due to this tight regulation of the activity of the Arp2/3 complex, it has been difficult to visualize the activated state of the complex *in vitro*. The polymerization of actin filaments is limited to the region activated by the Arp2/3 complex by capping proteins, and once actin filaments have elongated, the ends are recapped to prevent the depolymerisation in order to conserve the actin filament (Bear & Gertler 2009). Uetrecht & Bear (2006) suggest that coronin (which binds F-actin and the Arp2/3 complex) could also play a role in the tight regulation of the activity of Arp2/3.

1.4.2.2. Type II coronin

Distinct from type I coronins are the type II and III coronins. Coro2A is a widely expressed type II coronin isoform that localizes to focal adhesions in MTLn3 adenocarcinoma cells, and has been implicated in the regulation of focal adhesion turnover events during cellular migration (Chan *et al*. 2011). Marshall *et al*. (2009) showed that the depletion of Coro2A resulted in impaired focal adhesion turnover and slower cell migration. Additional to its role in focal adhesion and cell migration, Cor2A has also been identified as a component of the Nuclear Co-repressor (NCor) complex in nuclear extracts of HeLa cells (Yoon *et al*. 2003). At the time it was not known what the function of Cor2A in the NCor complex was, until Huang *et al*. (2011) discovered that there is a SUMO 2/3 interacting motif (SIM) at the C-terminal end of Cor2A. This SIM was the target of SUMOylated Liver X Receptors, and this uncovered a mechanism for Cor2A in macrophages in the Toll-like receptor inflammation response pathway (Huang *et al*. 2011). This implicated Cor2A as a key regulator of NCor clearance from target gene promoters. This NCor clearance is an essential step before transcription by Toll-like Receptors can occur. The binding of nuclear actin to putative actin-binding residues in Cor2A facilitated the clearance of nuclear actin from the target gene promoters, whilst the binding of nuclear actin to SUMOylated Liver X receptors via the SIM blocked this mechanism (Huang *et al*. 2011).

1.4.2.3. Type III coronin

In addition to type II coronins, most eukaryotes also encode a long coronin, which is distinct in both structure and function. Type III coronin is known as Pod1 in *C. elegans* and *Drosophila*, and as Cor7 in *Dictyostelium* and humans. While this type III coronin is highly conserved across species, the function of it has changed across species, and is thought to have adapted to meet new needs in mammalian cells (Chan *et al*. 2011). Non-mammalian type III coronin functions in actin-dependent processes. It was shown that mutation of Pod-1 in *C. elegans* causes the mis-localization of Par proteins and as a result disrupts single cell embryo polarity. The abnormal vesicle trafficking, defects in the cellular membrane and defects in eggshell development caused by the lack of Pod-1 in *C. elegans* suggests multiple cytoskeleton-linked roles (Rappleye *et al*. 1999). In *Dictyostelium*, *Dd* coro7 accumulates with actin at surface cell projections and binds

to F-actin. Shina *et al*. (2010) showed that the knockout of *Dd* coro7 led to defects in migration response, but an increase in phagocytosis. Human coro7 was found to localize to the Golgi complex where it plays a role in maintenance of the Golgi morphology and membrane trafficking. However, this protein does not interact with the actin cytoskeleton (Uetrecht & Bear 2006; Rybakin *et al*. 2004). The targeting of coro7 to the Golgi membrane is reliant on tyrosine phosphorylation of coro7. Rybakin *et al*. (2004) also showed that redistribution of coro7 to the cytosol following treatment with the Src kinase inhibitor SU6556 implies that Src is the key kinase in this phosphorylation dependent membrane targeting.

1.4.3. Coronin in Plasmodium falciparum

In order to successfully invade the red blood cell of its host, *Plasmodium* has evolved molecular machinery that has multiple components involved in a set of interactions with the host cell. *Plasmodium* as well as other members of the Apicomplexa share a polarized apical structure made up of a set of secretory organelles such as rhoptries and micronemes which is very important during the genesis as well as maturation of the parasitophorous vacuole shaped by the parasites (Tardieux *et al*. 1998). There is a multistep process of sequential events involving a series of distinct receptor-ligand binding steps. This process is reviewed in detail by Weiss *et al*. (2015).

Electron micrographs, video microscopy and pharmacological data from the related genera *Plasmodium*, *Eimeria* and *Toxoplasma* have indicated that the sequential events leading to the internalization closely resemble each other (Pimenta *et al*. 1994). The driving force amongst these similarities underlying parasite motility and host cell invasion has been shown to be an actin based event (Riglar *et al*. 2011). The role that the *P. falciparum* homologue of coronin plays in the parasite is currently not well defined. *Pf* coronin is considered to be a type I coronin, due to the presence of the critical residue R30 (arginine at position 30) for actin binding - this residue is not conserved in type II and III coronins, which would therefore suggest that these coronins have an alternative actin-binding surface with different characteristics, or no actin interactions at all (Cai *et al*. 2007). Type III coronins expressed in some cell types (human type

III coronin for example) does not appear to have any interaction with the actin cytoskeleton (Chan *et al*. 2011).

Tardieux *et al*. (1998) first identified a *P. falciparum* homologue of coronin that showed very strong homology with coronin sequences from amoeba, bovine and human. This homology also lay within the C-terminal domain and not only within the N-terminus containing the five WD repeats which have been shown to characterise coronins. Tardieux *et al*. (1998) identified a single copy *P. falciparum* gene that displays strong homology with the *Dictyostelium discoideum* actin binding protein (known as *Dd* coronin).

Tardieux *et al*. (1998) used an affinity-purified monoclonal antibody against *D. discoideum* coronin. The anti-*Dd* coronin antibody was used to detect the *Pf* coronin in a co-sedimentation assay. *Pf* coronin was found to co-sediment with parasite actin filaments. Additional functions for coronin have been suggested in *Dd* coronin, which could also apply to *P. falciparum*. *Dd* coronin can speed up the disassembly of the actin network, and can balance the actin nucleating activity that occurs during cytokinesis and cell locomotion (De Hostos *et al*. 1993), and cells lacking coronin display a 60% decrease in phagocytic uptake levels. Based on the latter involvement of *Dd* coronin in phagocytosis, it was included in the current study as a potential mediator of endocytosis in *P. falciparum*, keeping in mind its additional potential roles in cytokinesis and locomotion.

1.5. Dynamin

1.5.1. Introduction to the dynamin super-family of proteins

Dynamin proteins are a super-family of conserved large GTPase (guanosine triphosphatase) proteins that exist in many eukaryotic cells (Praefcke & McMahon 2004; Gaechter *et al*. 2008). They are involved in multiple processes including the budding of transport vesicles, division of organelles, endocytosis, cytokinesis and pathogen resistance (Konopka *et al*. 2006; Zhou *et al*. 2009). Members of the dynamin superfamily are broadly divided into classical dynamins and dynamin-related or dynamin-like proteins (DRPs or DLPs). Classical dynamins are distinguished from DRPs by the presence of five distinctive domains (Ramachandran 2011). A large N-terminal GTPase domain, a middle domain that has involvement in self-assembly, a pleckstrin homology (PH) domain that has binding specificity to membrane phosphoinositides, a GTPase effector domain that is involved in self-assembly, and in the allosteric regulation of GTPase activity, and finally, a C-terminal proline and arginine-rich (PR) domain, that is involved in binding to Src-homology 3 domains of accessory proteins that act in targeting dynamin to multiple sites (Ramachandran 2011). Dynamin-related proteins lack two of these distinctive domains; the PH domain, as well as the PR domain (Niemann *et al*. 2001; Ramachandran 2011). DRPs instead rely on other motifs for their localization and in order to confer specificity, for example, *D. discoideum* has a glutamine-rich domain (Praefcke & McMahon 2004).

1.5.2. Known Functions of dynamin

The most well known function of dynamin is its involvement in clathrin-mediated endocytosis. This was initially observed in the *Drosophila* genus of small flies, and mammalian cells (Zhou *et al*. 2009). The role of dynamin in endocytosis was first established when a human homologue of the *Drosophila shibire* dynamin was overexpressed in mammalian cells, and a mutated dynamin, deficient in GTP binding (K44A point mutation) was also expressed in mammalian cells (Damke *et al*. 1994). Induction of the mutant dynamin specifically blocked endocytic coated vesicle formation. This led to the conclusion that dynamin plays an important role in vesicle formation at the plasma membrane (Zhou *et al*. 2009).

During the early stages of the endocytosis process dynamin localizes at the plasma membrane of the cell at clathrin-coated invaginations. It then self-assembles into rings at the neck of the invagination buds that become stacked and interconnected (Bottomley *et al*. 1999). These rings then constrict to pinch off the clathrin-coated vesicles (Sweitzer & Hinshaw 1998). This pinching activity was given the name, pinchase (Hinshaw & Schmid 1995). This vesicle scission function (pinchase) of dynamin to pinch off clathrin-coated vesicles was the main motivation for including dynamin in this study. Vesicle scission is however, not the only important cellular function that dynamin has been implicated in. Dynamin has also been shown to be involved in organelle division and fusion, and cytokinesis. Smirnova *et al*. (1998) expressed mutant Drp1 (dynamin-related protein 1) in COS-7 cells and observed that this mutant Drp1 resulted in profound changes to mitochondrial morphology.

Mitochondria are made up of inner and outer membranes; the inner membrane is highly invaginated and forms cristae. Mitochondria undergo a constant process of fission and fusion to ensure the appropriate distribution of mitochondria in the cell, and to ensure the distribution of mitochondrial DNA (mDNA) in dividing cells (Wong *et al*. 2003). Three families of dynamin-related proteins have been shown to be involved in mitochondrial dynamics: Dlp, OPA1 and mitofusin (Smirnova *et al*. 1998). OPA1 and mitofusion have been found to be involved in mitochondria fusion, whilst Dlp has been shown to be involved in fission (Smirnova *et al*. 1998). Dlp has the GTPase, middle and GED domains. Mutations in Dlp based on conserved residues in the dynamin superfamily which have been well characterised in dynamin 1, lead to changes in the dynamic structure of mitochondria (Labrousse *et al*. 1999; Wong *et al*. 2003). The best proof of the involvement of Dlp in mitochondria fission is the discovery that Dlp localizes to sites of constriction on mitochondria, as well as the fact that Dlp GTPase mutants are found to be defective in mitochondrial division (Wong *et al*. 2003). Labrousse *et al*. (1999) found remarkable proof of the importance of Dlp in mitochondrial division in in *C. elegans*. A GTPase mutant of *C. elegans* produced two daughter cells (that migrate after division), that were found to be connected by a narrow band mitochondrial membrane - this was caused by the failure of mitochondrial division, due to the lack of Dlp activity (Labrousse *et al*. 1999).

Dynamin has been shown to localize to the spindle midzone and the subsequent intercellular bridge and plays an essential role in successful cytokinesis (Feng 2002; Thompson *et al*. 2002).

Thompson *et al*. (2002) showed that insertion of membrane at the cleavage furrow is an important component of cyotkinesis. Using immunofluorescence confocal microscopy, they analyzed the distribution of dynamin during mitosis in Clone 9 cells (Clone 9 cells are a normal rat liver cell line). They found that dynamin was localized as punctate spots surrounding the microtubual organizing centers as they began to separate during the early stages of cell division, as well as around the disassembling nuclear membrane. During the final stages of cytokinesis (telophase), Thompson *et al*. (2002) observed that dynaim accumulated at the intercellular bridge near the protein dense midbody. This dynamin localization was not detected along the entire bundle of intercellular bridge microtubules, but was instead located at regions near the midbody where the final sepearation would be thought to occur (Thompson *et al*. 2002). This provides insight into the proposed involvement of dynamin in cytokinesis events. This data suggested a novel function for dynamin in cytokinesis in mammalain cells.

Following this finding, the authors tested if dynamin played a role in cytokinesis in other eukaroytes. Thompson *et al*. (2002) decided to look at the nematode *C. elegans* since it is more amenable to genetic manipulation. They made use of RNA interference (RNAi), as well as a temperature sensitive dynamin mutant, dyn-1(ky51). Early embryos were immunostained with a specific antibody for *C. elegans* dynamin. Immunostaining of the wild-type dynamin showed that localization accumulated at the midbody as the embryos progressed through the early and late stages of cytokinesis. Thompson *et al*. (2002) analysed embryos with the temperature sensitive dynamin mutant, and found that this resulted in consistent embryonic cytokinetic failures. They also found that targeting dynamin using RNAi resulted in the blocking of the late phase of cytokinesis in *C. elegans*. The data presented by Thompson *et al*. (2002) in mammalian rat liver cells, as well as the eukaryote, *C. elegans* presents convincing evidence that dynamin is an essential requirement for cytokinesis.

1.5.3. Essential GTP binding action of dynamin

The GTP binding domain of dynamin has been shown to be essential for its function. The conserved core of related GTP-binding proteins is a GTPase domain of approximately 160 amino acid residues. The biochemical properties, and biological functions of GTP-binding proteins are influenced by the insertion of residues in their GTPase domain (Vetter & Wittinghofer 2001). Within the dynamin family of GTP-binding proteins, the GTPase domain is extended to approximately 300 amino acids (Niemann *et al*. 2001). While GTPase activity is essential for dynamin function, they are characterized by their low affinity for GTP and an even lower affinity for GDP (Lenz *et al*. 2009). Stowell *et al*. (1999) showed that GTPase activity requires the oligomerization of dynamin. Whilst oligomerization usually refers to a complex of more than one monomer, the basic dynamin building block is a dimer or tetramer. Oligomerization in this case refers to the ordered assembly of these dynamin building blocks into helices or rings (Stowell *et al*. 1999). For many regulatory GTPases (such as Ras-like GTPases), the GTPase activity is stimulated by the binding of GTPase-activating proteins (GAPs). For the oligomerized form of dynamin, dynamin itself is the GAP (Praefcke & McMahon 2004).

As mentioned above, Ras-like GTPase activity is controlled by GAPs, whereas the GTPase activity of dynamin is controlled by self-oligomerization. This would provide a risk factor for the cell as cycles of dynamin GTP hydrolysis would not be able to be prevented (Konopka *et al*. 2006). There is however a pre-requisite step that prevents unnecessary cycles of dynamin GTP hydrolysis, due to the fact that the oligomerization of dynamin is regulated by membrane recruitment of dynamin to its sites of action. The PH domain of classical dynamins is responsible for their interaction with negatively charged lipid membranes (Ramachandran 2011). A single point mutation (K44A) has been shown to abolish GTPase activity of dynamin; the same approach was employed to show that a single point mutation (K535A) in the PH domain of mammalian dynamin 1 has a dominant-negative effect on endocytosis in cells (Lee *et al*. 1999; Damke *et al*. 1994). It is due to this low affinity of unassembled dynamin for lipids and its oligomerization only after lipid binding that ensures that there is tight control of GTPase activation.

1.5.4. Dynamin in Plasmodium falciparum

The *P. falciparum* genome encodes two dynamin-like proteins, *Pf*DYN1 and *Pf*DYN2. According to Li *et al*. (2004) *Pf*DYN1 is expressed during the entire erythrocytic life cycle of the parasite, while *Pf*DYN2 expression is limited to the schizont stage of the parasite life cycle (Dourado *et al*. 2007). According to Zhou *et al*. (2009), *Pf*DYN1 plays an important role in the haemoglobin uptake pathways.

Zhou *et al*. (2009) hypothesized that treating parasites with dynasore inhibits haemoglobin uptake. Hydroxy-dynasore is a small molecule that inhibits the GTPase activity of dynamin (Zhou *et al*. 2009). The authors explored the effect this had on haemoglobin uptake by treating parasites with 80 μmol/L dynasore, in combination with 100 μmol/L leupeptin, which is an inhibitor of serine/cysteine proteinase that blocks the degradation of haemoglobin (Rosenthal 1995). Following incubation with these inhibitors for 24 hours, cells were removed and saponin lysed to release the parasites from the red blood cells. Following a washing step of intact parasites in PBS, the samples were analysed by Tris-tricine SDS-PAGE and haemoglobin was evaluated by Western blotting with mouse monoclonal anti-haemoglobin antibody. Based on their SDS-PAGE and Western blotting results, haemoglobin was clearly visible in parasites treated with leupeptin without dynasore, but almost no haemoglobin was seen in the parasite treated with both leupeptin and dynasore. Following up from this, Zhou *et al*. (2009) also monitored FITC-dextran uptake by parasites. Parasites incubated with FITC-dextran and treatments with dynasore for 24 hours were viewed by fluorescence microscopy to evaluate the levels of FITC-dextran that had entered the parasite. They found from this data, that the uptake of FITC-dextran was also inhibited in parasites treated with dynasore. Since the authors showed that inhibition of dynamin resulted in reduced levels of haemoglobin and FITC-dextran uptake, they reached the conclusion that *Pf*DYN1 plays an important role in the haemoglobin uptake pathway of *P. falciparum*.

According to Dourado *et al*. (2007), *Pf*DYN2 localizes in punctuate structures within the parasite cytoplasm. They performed immunofluorescence assays using anti-*Pf*DYN2 polyclonal antisera produced in mice. To attempt to further determine the compartments to which *Pf*DYN2 may be recruited, Dourado *et al*. (2007) performed co-localization analysis using specific marker

antibodies of the endoplasmic reticulum (*Pf*BIP), Golgi apparatus (*Pf*ERD2) and the apicoplast (ACP).

Based on the immunofluorescence data, *Pf*DYN2 appeared to co-localize with all of these three markers. Based on phylogenetic analysis, Dourado *et al*. (2007) found that *Pf*DYN1 and *Pf*DYN2 belong to distinct groups, *Pf*DYN2 appears to be more related to the well-characterized yeast dynamin-like proteins, VSP1 and DNM1, and to human DRP1. Yeast VSP1 mediates vesicular transport to the Golgi apparatus, and has also been implicated in the division of the peroxisome (Nothwehr 1995; Hoepfner *et al*. 2001). Yeast DNM1 has been shown to be involved in both mitochondrial outer membrane division and endosome dynamics (Sesaki 1999; Hoepfner *et al*. 2001). Human DRP1 was initially shown to regulate mitochondria and ER divisions, and was also shown to be essential to the division of the peroxisome (Pitts *et al*. 1999; Li & Gould 2003). *Pf*DYN2 clusters close to an *Arabidopsis* Dlp (ADL2a) and a *Trypanosoma brucei* Dlp (*Tb*Dlp) in the phylogenetic tree. The *Arabidopsis* Dlp has been involved in plant mitochondrial division, and *Tb*Dlp is the unique Dlp found in the kinetoplastid *T. brucei* that has been involved in both mitochondrial fission, and endocytosis (Arimura 2004; Chanez *et al*. 2006).

The mitochondrion and the apicoplast occur as single organelles during the asexual stage of the *P. falciparum* life cycle (Kobayashi *et al*. 2007). During parasite growth and division, these two organelles grow and elongate into highly branched structures in late-stage parasites. The fission of these elongated organelles is an ordered process that occurs in late-stage parasites (Dourado *et al*. 2007). Divided mitochondrion associate with divided apicoplasts and they separate as pairs into daughter merozoites (Van Dooren *et al*. 2005).

Dourado *et al*. (2007) concluded that, based on the phylogenetic clustering of *Pf*DYN2 with well characterized Dlps involved mainly in the division of mitochondria and the peroxisome, as well as in vesicular transport in eukaryotic cells, *Pf*DYN2 should be suggested as a candidate for these functions in *P. falciparum*.

The dynamin in question for this thesis was *Pf*DYN2. The nomenclature used here is based on the PlasmoDB designations of the dynamin genes and their closet sequence homologues in

humans. *Pf*DYN2 is most homologous to human dynamin 2 which is the dominant dynamin isoform present in most human cell types (Tse *et al*. 2003).

1.6. μ4 chain of the Adaptor Protein 4 (AP-4) complex

1.6.1. Introduction

Clathrin-coated vesicles carry cargo between intracellular membrane-bound compartments; clathrin is the framework that assembles the vesicular coat. In order to load the cargo into nascent coated vesicles in clathrin-coated pits, adaptor proteins which interact with the clathrin lattice, as well as the cargo molecules are required (Heldwein *et al*. 2004).

The organization and sorting of integral membrane proteins during the various stages of the endocytic and secretory pathways is mediated by the interaction of signals found within the cytosolic domains of these proteins with cargo receptors recruited to the cytoplasmic face of budding transport vesicles (Aguilar *et al*. 2001; Marks *et al*. 1997). These signals are made up of short, linear stretches of amino acids that are situated within these cytosolic domains of the proteins. The majority of these fall into groups of consensus sequences known as motifs (Marks *et al*. 1997). There are two main types of signal motifs that have been implicated in a variety of sorting processes in mammalian cells. These are known as tyrosine-based and dileucine-based signals (Canagarajah *et al*. 2013). The processes implicated include the internalization of cargo from the plasma membrane during endocytosis, transport from early to late endosomes, antigen processing compartments and lysosomal targeting (Dell'Angelica *et al*. 1999; Marks *et al*. 1997; Trowbridge *et al*. 1993). Dileucine- and tyrosine-based signals have both been shown to interact with heterotetrameric adaptor protein (AP) complexes (Canagarajah *et al*. 2013; Kirchhausen *et al*. 1997). The analogous subunits of AP complexes are structurally related. The β chains interact with clathrin. The functions of the γ/α/δ and the σ subunits are less clear, although AP-2 α has been shown to interact with components of the protein sorting machinery, such as amphiphysin, dynamin, Eps15 and epsin (Dell'Angelica *et al*. 1999). The μ chains are involved in the recognition of tyrosine-based motifs with a YXXϕ consensus sequence (ϕ refers to a bulky hydrophobic amino acid, x refers to any amino acid) within the cytoplasmic tails of cargo proteins. This allows for their main function of trapping and concentrating transmembrane cargo proteins in budding transport vesicles (Canagarajah *et al*. 2013).

1.6.2. Adaptor Proteins complexes

The adaptor proteins are a group of five closely related heterotetrameric complexes that have been shown to have key functions in vesicle trafficking (Aguilar *et al*. 2001; Hirst *et al*. 2013). Three of the adaptor protein complexes, known as AP-1, AP-2, and AP-3, have been well characterized and their roles broadly established (Dell'Angelica *et al*. 1999; Hirst *et al*. 2013). Comparatively, much less is known about the more recently discovered AP-4 and AP-5 complexes (Hirst *et al*. 2013). Adaptor proteins 1 to 5 are made up of two large chains (γ/α/δ/ε/ζ and β1-5, ~90-13 kDa), one medium chain (μ1-5, ~50 kDa), and one small chain (σ1-5, ~20kDa) (Dell'Angelica *et al*. 1999; Hirst *et al*. 2013). Each chain of the AP complex serves a different function. For example; the α chain of AP-2 interacts with many regulators of coat assembly, and vesicle formation (Owen & Luzio 2000). The γ/δ/ε chains are assumed to interact with proteins that play a similar regulatory role to the α chain. β chains interact with clathrin (β1 and β3 of AP-1 and AP-3 respectively, also bind a subset of dileucine-based sorting signals) (Rapoport *et al*. 1998). σ1 and σ3 have been found to be required for the functional integrity of AP-1 and AP-3 complexes, respectively (Mullins *et al*. 2000; Shim *et al*. 2000).

AP-1 and AP-2 were initially identified and described as 'assembly polypeptides' that were involved in the promotion of assembly of clathrin *in vitro* (Keen *et al*. 1979). AP-3, AP-4, and more recently AP-5 were consequently identified *in silico* based on their sequence similarity to AP-1 and AP-2 (Hirst *et al*. 2011).

The AP complexes associate with clathrin as well as accessory molecules to produce coated membrane transport vesicles (Canagarajah *et al*. 2013). They are positioned in the space between clathrin and the membrane and function to bridge the gap between the transmembrane cargo proteins and clathrin (Hirst *et al*. 2013).

According to Aguilar *et al*. (2001) AP-1, AP-2, AP-3, and AP-4 associate with the cytosolic face of organelles of the endocytic and secretory pathways. All of the adaptor proteins are thought to have a function as coat proteins that are transiently recruited to membrane in order to selectively recruit cargo to be included into nascent transport vesicles (Hirst *et al*. 2013). The direct interaction of the AP complex with sorting signals allows them to be involved in the induction of

formation of coated vesicles, as well as the concentration of cargo molecules within the vesicles (Aguilar *et al*. 2001).

AP-1 has a role in sorting of proteins from the *trans*-Golgi network (TGN) and endosomes to compartments of the endosomal and lysosomal systems (Traub 2009). AP-2 is specifically associated with the plasma membrane and mediates rapid internalization of endocytic receptors (Aguilar *et al*. 2001; Marks *et al*. 1997) through clathrin mediated endocytosis. AP-3 is associated with endosomes (Dell'Angelica *et al*. 1997; Simpson *et al*. 1997) and/or the TGN (Aguilar *et al*. 2001; Simpson 1996). AP-3 is also involved in the recruitment of integral membrane proteins for their transport to lysosomes and lysosome-related organelles (Borgne & Hoflack 1998). Mammalian AP-4 has been shown to have a role in signal-mediated trafficking of integral membrane protein in mammalian cells (Hirst *et al*. 2013). AP-4 is thought to associate with the cytoplasmic face of the *trans*-Golgi network (TGN), and unlike the other adaptor proteins, as part of a non-clathrin coat (Hirst *et al*. 2013). The AP-5 complex appears to be involved in endosomal dynamics, but its precise localization and function are, at present, still inconclusive (Hirst *et al*. 2013). It does appear, however, that AP-5 deficiency is associated with progressive spastic paraplegia, indicating that it plays a fundamental role in neuronal development and homeostasis (Hirst *et al*. 2013).

1.6.3. Adaptor protein 4 complex (AP-4)

Dell'Angelica *et al*. (1999) raised antibodies to new mammalian adaptor protein homologues (found using searches through cDNA databases), as well as the AP μ-related protein, μ-ARP2 (described by Wang & Kiliman 1997). This allowed them to identify a novel heterotetrameric adaptor-like complex. They named it AP-4 (Dell'Angelica *et al*. 1999), and it is a closely related complex to AP-2, which is involved in clathrin-mediated endocytosis.

As is the case with other AP complexes, AP-4 is composed of two large chains (ε and β4), a medium chain (μ-ARP2, and subsequently referred to as μ4), and a small chain (σ4). AP-4 is widely expressed in mammalian tissues and has been found to associate with membrane as a peripheral membrane protein (Dell'Angelica *et al*. 1999). They localized the AP-4 complex by immunofluorescence in the HeLa cell line; they found that it localized to the *trans*-Golgi network

(TGN) or a neighbouring compartment. Dell'Angelica and colleagues (1999) also found that AP-4 is sensitive to the Golgi-disrupting agent brefeldin A (a compound that also affects the distribution of AP-1 and AP-3). The properties of AP-4 complexes are similar to those of other AP complexes, which suggests that it would be a component of the cellular machinery that sorts integral membrane proteins in mammalian cells (Dell'Angelica *et al*. 1999). The four subunits of the AP-4 complex are thought to adopt a mouse head-like structure with a "head" comprising the μ and σ subunits, and the amino-terminal "trunk" domain of the two large subunits (ε and β), and the two "ears" that correspond to the carboxyl-terminal domains of the large subunits, and are linked to the head by flexible "hinges" (Dell'Angelica *et al*. 1999).

1.6.4. Medium (μ) chains of adaptor proteins

As previously mentioned, the μ chains of the AP complexes are involved in the recognition of transmembrane cargo adaptors by binding to specific motifs in their cytoplasmic tail domains, notably, the YXXΦ motif (Aguilar *et al*. 2001; Kibria *et al*. 2015). μ1 and μ2 exhibit a bipartite structure, with the N-terminal third involved in interactions with the corresponding β chains, and the C-terminal two-thirds involved in recognition of YXXΦ type signals (Aguilar *et al*. 2001). The tyrosine and Φ residues fit into hydrophobic pockets in the banana shaped YXXΦ-binding domain of μ2 which is composed entirely of β-sheets (Owen 1998). Similarly to the μ2 subunit of AP-2, the μ4 subunit consists of two structural domains, the N-terminal domain that interacts with the β4 subunit, and a C-terminal domain that binds to specific subsets of tyrosine-based sorting signals through the YXXΦ-binding site (Φ represents a bulky hydrophobic amino acid, and X represents a non-specified residue) (Boehm *et al*. 2001; Aguilar *et al*. 2001). μ4 has been shown to interact weakly with the YXXΦ signals from lysosomal membrane proteins LAMP-1, CD63 and the *trans*-Golgi network protein TGN38 (Stephens & Banting 1998). Aguilar *et al*. (2001) found that a reporter integral membrane protein bearing a μ4-specific YXXΦ signal was delivered to the endosomal/lysosomal system, without being internalized from the plasma membrane.

1.6.5. Adaptor protein complexes in eukaryotic cells

The adaptor protein complexes are expressed in most eukaryotic systems. There are, however, a number of exceptions - genes for the AP-3 complex are absent from *Toxoplasma gondii* (Ngô *et al*. 2003), AP-4 complexes are absent in the yeast, *S. cerevisiae, S. pombe*, the nematode, *C. elegans*, and the fruit fly, *D. melanogaster* (Boehm *et al*. 2001). Identification of adaptor protein complexes in organisms outside of the well studied mammalian homologues is achieved by comparing genetic information to identify homologues (Robinson & Bonifacino 2001). The *P. falciparum* µ4 medium chain adaptor protein used in this project was identified by BLAST analysis of the *P. falciparum* genome with the mammalian homologue for µ4. According to PlasmoDB searches, *P. falciparum* has genes encoding AP-1, AP-2, AP-3, and AP-4, however the more recently described AP-5 complex has yet to be described in malaria parasites.

1.6.6. Adaptor protein functions in parasites

The localization and function for the adaptor protein complex 1 of *P. falciparum* was investigated by Kibria *et al*. (2015). Using GFP-tagged fusion constructs for live cell imaging, and fixed parasites for immunofluorescence analysis, they found that *Pf*µ1 showed similar localization to that of several Golgi/ER markers, indicating Golgi and ER localization. The treatment of transgenic parasites with brefeldin A affected the localization of the Golgi-associated *Pf*µ1 (Kibria *et al*. 2015). They went on to perform co-localization studies that showed considerable co-localization of *Pf*µ1 with the resident rhoptry organelle protein, rhoptry associated protein 1 (RAP1).

1.7. Aims and Objectives

Endocytosis of the extracellular environment and protein trafficking within the malaria parasite is vital for parasite survival and growth. Whilst these pathways have been described at the morphological level, the molecular mechanisms remain poorly understood.

The aim of this study was to characterise, through sub-cellular localization, *P. falciparum* homologues of the endocytosis candidate proteins coronin, dynamin 2, and the medium chain adaptor protein, μ4. These are proteins expressed during the blood stage of the parasite life cycle. These proteins were identified by genome searches of the *Plasmodium* sequence database, PlasmoDB. These proteins were chosen due to amino acid sequence homology to proteins involved in endocytosis in other organisms. The goal was to localize these proteins in order to investigate whether the parasite homologues of these proteins are involved in endocytosis in the malaria parasite, or in other trafficking events, such as cytokinesis.

To accomplish the goal of localization, the three endocytosis candidate proteins were expressed as full-length GFP-tagged fusion proteins in *P. falciparum* 3D7 cells. The coding sequences for the genes of interest were cloned into pARL2-GFP expression vectors. Success of cloning was determined by running restriction-digested plasmids on agarose gels, as well as plasmid DNA sequencing. Parasites were transfected with the expression vectors, and full-length GFP-tagged fusion protein expression was confirmed by Western blotting. Proteins were localized by viewing live parasites using fluorescence and confocal microscopy.

CHAPTER TWO: METHODS AND MATERIALS

Compositions of non-commercial reagents are listed in appendix A.

2.1. *In vitro* cultivation of *Plasmodium falciparum* parasites

2.1.1. Washing and diluting erythrocytes

Blood was collected from a healthy volunteer (blood type: A-) using 9 mL Vacuette K3EDTA (Greiner Bio-One, Austria) tubes. In a laminar flow hood, freshly collected blood was transferred to sterile 50 mL centrifuge tubes and diluted with an equal volume of incomplete RPMI 1640 culture medium. These tubes were centrifuged in a swing-out rotor at 3500 xg for 5 minutes with the brake set to low, to pellet the red blood cells (RBCs). The blood separates into three layers. The upper two layers; plasma supernatant from the pelleted RBCs, as well as the buffy coat layer were aspirated using a Pasteur pipette (Marienfield, Germany) and discarded. The RBCs that remained were then gently resuspended in incomplete culture medium by inverting the tube. Centrifugation was repeated, followed by aspiration of the supernatant and the buffy coat. This washing step was performed twice. The fresh RBCs (fRBCs) were stored at 4°C, for up to 1 month.

2.1.2. Routine culture media composition and parasite maintenance

The drug sensitive *P. falciparum* parasite strain 3D7 was cultured using the protocol outlined by Karl *et al*. (2009). Cultures were maintained in RPMI 1640 with HEPES and Glutamine media (Lonza, Belgium) supplemented with 4 g/L glucose (Sigma-Aldrich, USA), 5 g/L Albumax II (Life Technologies, USA), 0.088 g/L hypoxanthine (Sigma-Aldrich, China) and 60 µg/mL Gentamicin solution (Sigma-Aldrich, USA). These supplementary components were dissolved in 50 mL incomplete media and filter sterilized using a 0.22 µm filter into the remaining 450 mL of incomplete media. In instances where transfected parasites were maintained, complete media was supplemented with 2.5 nM WR99210 (Jacobus Pharmaceuticals, USA) or 5 µM Blasticidin S (Sigma-Aldrich). Cultures were maintained with daily changes of fresh medium at

approximately 3% haematocrit (volume of RBCs in the total volume of culture). Cultures were diluted with blood type A- RBCs to maintain the parasitaemia (percentage of infected RBCs to the total number of RBCs in the culture) at approximately 2% when the culture was in the trophozoite/schizont stage of their life cycle. The health of parasites as well as the parasitaemia was determined using a Giemsa (Sigma-Aldrich, Switzerland) stained thin smear. Giemsa stain was made up in PBS buffer (Sigma-Aldrich, USA). When parasitaemia reached levels above 3% for trophozoite/schizont stage parasites, the culture was diluted. When the parasitaemia was above 3%, it was diluted between 5 and 10-fold. For example, when diluting the infected RBCs (iRBCs) 5-fold with fRBC for a 10 mL culture; 240 µL fresh RBCs (fRBCs) was added to 60 µL iRBC. When the parasitaemia was lower than 3%, the media was replaced with fresh, complete media, with no dilution of RBCs necessary. Fresh media (10 mL) was added and the culture returned to the culture flask. Cultures were maintained in non-vented T75 culture flasks. Flasks were gassed with 5% CO_2, 5% O_2, balance N_2 (Afrox, South Africa) and incubated at 37°C in a shaking incubator at 45 rpm.

2.1.3. Cryopreservation of parasitized red blood cells

2.1.3.1. Preparation of culture from frozen stocks

Frozen stocks, stored in cryotubes (Greiner Bio-One, Germany), were removed from the -80 °C storage freezer. The cryotubes were incubated at 37°C until they were fully thawed. Immediately once thawed, the suspension was transferred to a 15 mL tube. Fresh RBCs (500 µL) were added to the thawed cells in order to dilute the number of infected RBCs that lyse during the thawing process. For every millilitre of thawed cells, 0.2 mL 12% sodium chloride was added drop-wise, whilst constantly swirling. The suspension was incubated at room temperature for 2 minutes before the addition of 10 mL 1.2% sodium chloride (the first 5 mL added drop wise with swirling between drops). The suspension was then centrifuged in a swing-out rotor at 1000 xg for 5 minutes. The supernatant was aspirated using a sterile Pasteur pipette, followed by the addition of 10 mL fresh culture medium to the thawed RBC pellet. The suspension was incubated at room temperature for 3 minutes before pelleting the RBCs in a swing-out rotor centrifuge at 1000 xg for 2 minutes. The supernatant was carefully aspirated,

ensuring not to aspirate the small pellet of thawed RBCs. Fresh RBCs (100 μL) , followed by 5 mL of complete culture medium were added to the pellet. The culture was transferred to a sterile T25 culture flask, gassed and returned to the 37°C incubator. For the first two days following thawing, the cultures were incubated without shaking, to allow for recovery of the parasites.

2.1.3.2. Freezing culture stocks

When the pelleted RBCs predominantly contained ring stage parasites at a parasitaemia of between 5% and 10% they could be cryopreserved. Preparation of frozen stocks was performed using the method described by Nomark (2008). To 1 volume of parasitized RBC pellet, 1 volume of ice-cold freezing solution was added. The freezing solution was added drop wise with 10-second intervals between each drop. The mixture was constantly swirled in order to produce a homogenous suspension. The RBCs were then transferred to sterile cryotubes and stored at -80°C.

2.1.4. Giemsa stained smear preparation

Smears were prepared daily to determine the health and parasitaemia of parasite cultures. Using a P1 pipette with a sterile P1 pipette tip, 1 μL was removed from the iRBC pellet after centrifugation. An alternative and quick method of obtaining a small sample of RBCs is also possible; the culture flask was tilted at an angle allowing the culture medium to flow back and expose a thin layer of RBCs on the surface of the flask. A sterile Pasteur pipette was then used to take up a drop of RBCs by capillary action. This small drop was placed on a microscope slide; a second microscope slide was used to smear a thin layer of the RBCs on the surface of the slide. The smear was briefly incubated at room temperature inside the laminar flow hood and allowed to air dry. The cells were then fixed briefly using methanol before staining with Giemsa stain (Sigma-Aldrich, Switzerland) freshly prepared in phosphate buffered saline (1 part Giemsa to 10 parts PBS). The slides were incubated for 3 minutes before removing the Giemsa stain by rinsing under running water. The slides were then viewed at 100x magnification under oil-immersion on an upright light microscope (Olympus CX22LED, Japan).

2.1.5. Calculating parasitaemia

In order to determine percentage parasitaemia (the number of infected RBCs out of the total number of RBCs in the culture) it is important to search for a field on the slide where the RBCs were evenly spread with at least 100 RBCs per field. Five to ten fields of evenly spread RBCs were viewed to determine percentage parasitaemia as follows:

$$\%\, Parasitaemia = \frac{Number\ of\ infected\ RBCs}{Total\ number\ of\ RBCs} \times 100$$

The average of five to ten calculations was taken as an estimate of parasitaemia for the entire culture.

2.1.6. Synchronization of parasite life cycles

2.1.6.1. Sorbitol treatment

Effective experimentation with *P. falciparum* usually requires the parasites to be in the same stage of development. The cultures were therefore synchronized when predominantly ring stage parasites were present at a high parasitaemia (above 5%). The RBCs were harvested from culture by centrifugation at 1000 xg for 2 minutes. The spent media was aspirated off using a sterile Pasteur pipette. The pellet was resuspended in 10 volumes 5% D-sorbitol (Sigma-Aldrich, USA) prepared in sterile water and filter sterilized. The suspension was incubated for 10 minutes at 37°C. The RBCs were pelleted again by centrifugation; the sorbitol-containing supernatant was then removed by aspiration with a sterile Pasteur pipette. The erythrocytes containing viable parasites were resuspended in culture medium; this change in osmotic pressure causes the RBCs containing trophozoite and schizont stage parasites to lyse. The suspension was returned to the culture flask, gassed and incubated as described in 2.1.2.

2.1.6.2. Parasite enrichment using Percoll Gradient Centrifugation

This method of parasite enrichment was only performed when the parasite culture contained predominantly trophozoite and/or schizont stage parasites. iRBCs were harvested from a 20-30 mL culture by centrifugation at 1000 xg for 2 minutes. The supernatant was aspirated off using a sterile Pasteur pipette. Into a sterile microfuge tube 1 mL 60% Percoll in 2.5x RPMI/12.5% was pipetted. A sample of 300 μL iRBCs were carefully pipetted on top of the Percoll (if there was more than 300 μL packed RBCs, additional microfuge tubes containing 1 mL Percoll each were used). It is vitally important that the microfuge tubes are handled carefully to ensure the RBCs do not mix with the Percoll. The microfuge tubes were then centrifuged at 9000 xg for 15 minutes. Post centrifugation, the microfuge tube had three layers present: a RBC pellet at the bottom of the tube (this pellet contains uninfected and ring stage parasite-infected RBCs); a layer of pink Percoll; finally, a thin, brown layer of RBCs on top of the Percoll (this contains trophozoite and schizont stage parasite-infected RBCs). This top brown layer was carefully removed and pipetted into a 15 mL tube. 10 mL of fresh culture medium was added to the tube (the first 2 mL of medium was added drop wise, with careful stirring between drops); this was to prevent excessive RBC lysis due to the sorbitol in the 60% Percoll. The RBCs were pelleted by centrifugation at 1000 xg for 2 minutes. A small, brown pellet of enriched RBCs was observed. The supernatant was aspirated using a sterile Pasteur pipette. To confirm that the enrichment procedure has been successful, 5-10 μL of the pellet was pipetted under a cover slip on a microscope slide, and viewed with a 100x oil-immersion objective on an upright light microscope. 5 mL of complete culture medium was added to the pellet, the culture transferred to a new, sterile T25 culture flask, gassed and incubated as described in 2.1.2.

2.2. Preparation of nucleic acids

2.2.1. Total P. falciparum parasite RNA extraction

A non-synchronized 20 mL culture with a parasitaemia above 5% was used for RNA extraction. The experiment was carefully carried out in sterile conditions with special care to ensure prevention and elimination of RNase contamination. Cultures were transferred to 15 mL centrifuge tubes and centrifuged at 1000 xg for 2 minutes to pellet the iRBCs. The supernatant was aspirated using a Pasteur pipette, and the pellet was resuspended in 3.4 mL 0.3% saponin (204 µL 5% saponin in 3.196 mL 1x PBS). The suspension was incubated at room temperature for 5 minutes to allow for the RBCs to be fully lysed. Following this incubation, the suspension was centrifuged at 1000 xg for 2 minutes. The supernatant containing free haemoglobin and ghost RBC membranes was aspirated using a Pasteur pipette. The parasite pellet was washed with 1x PBS and centrifuged at 1000 xg for 2 minutes to produce a pellet containing pure parasites. This washing step was repeated until the supernatant was clear.

Total RNA was extracted from the saponin-lysed parasites using a SV Total RNA Isolation System (Promega, USA: Cat# Z3101). The recommended manufacturer's protocol was followed.

2.2.2. cDNA synthesis

Promega ImProm-II™ Reverse Transcription System (Promega, USA: Cat# A9281) was used to convert the isolated mRNA into cDNA. The recommended protocol was followed. PCR reactions using the newly synthesized cDNA as template was performed to ascertain the success of the nucleic acid synthesis.

2.3. Polymerase chain reaction (PCR)

2.3.1. Primer design

Primers were designed by preparing forward and reserve primers with similar melting temperatures of approximately 65°C. Melting temperatures were determined by the addition of 2 °C for each A/T (Adenine/Thymine), and 4°C for each G/C (Guanine/Cytosine). Restriction sites dependent on the particular requirement of each primer were added at the 5' ends, along with an additional 2 to 3 bases to aid restriction digests of PCR products (the nucleotides of the restriction site and additional bases were not included in the melting temperature calculation). Preferably, primers contained Guanine and/or Cytosine (known as GC clamp) at the 3' end to aid in primer binding. Particular care is required when designing reverse primers to ensure that the primers are the reverse compliment of the gene sequence they are required to bind to. Table 1 below indicates sequences of the primers used in this research project.

Table 1: Designer primers used for PCR reactions (restriction sites are underlined).

Primer	Sequence	Melting Temperature
COR_SalI_F	5'- GAG GTC GAC ATG TAT AAT GTT CCT TTA ATC AAG -3'	60°C
COR_KpnI_R	5'- GAG GGT ACC TAA TAC CGT TGC TGT ACT TTT ACA C -3'	68°C
DYN1_XhoI_F	5'- GAG CTC GAG ATG GAT AAA TTA GTA CCG ATT GTA ACC -3'	70°C
DYN1_AvrII_R	5'- GAG CCT AGG AAC TTC TTG GTT TCT AAT TTC GGC -3'	66°C
MU4_XhoI_F	5'- GAG CTC GAG ATG GTG ATA TCC CAA TTT TAT ATT TTG -3'	68°C
MU4_KpnI_R	5'- GAG GGT ACC GTT CAA ACG GTA AAC ATA TGA AG -3'	62°C
GAP45_ATG_XhoI_F	5'- CC CTC GAG ATG GGA AAT AAA TGT TCA AGA AGC -3'	67°C
GAP45_TAA_XmaI-R	5'- TAA CCC GGG TTA GCT CAA TAA AGG TGT ATC GG -3'	68°C
GAP45+30_AvrII_F	5'- GC CCT AGG CAA TCT GAA GAA ATA ATT GAA GAA AAA CC -3'	67°C
mCherry_noTAA_AvrII_R	5'- TG CCT AGG CTT GTA CAG CTC GTC CAT G -3'	68°C
GAP_cherry_sew_F	5'- GCT GAA CGT GAA AAT TTA AAA AAA ATG GTG AGC AAG GGC GAG GAG -3'	72°C
GAP_cherry_sew_R	5'- CTC CTC GCC CTT GCT CAC CAT TTT TTT TAA ATT TTC ACG TTC AGC -3'	72°C

2.3.2. Primer preparation

Primers were synthesized by IDT (Integrated DNA technologies, USA) and were supplied as lyophilized preparations. These preparations were resuspended in TE (Tris-EDTA, pH 8.0) buffer to a concentration of 100 μM. Upon addition of the required amount of TE buffer, the suspension was vortexed vigorously to completely resuspend the primers. Once resuspended, the primers were stored at -20°C.

2.3.3. PCR reaction

PCR reactions were performed in 200 μL thin-walled PCR tubes using the KAPA HiFi PCR kit (KAPA Biosystems, South Africa). The reaction mixture was prepared with 38.5 μL molecular grade water, 10.0 μL 5 x KAPA HiFi buffer A, 1.0 μL dNTP mix, 2.0 μL cDNA template, and 1.5 μL of each primer. The reaction mix was heated at 94°C for 2 minutes in the PCR thermocycler (BioRad MJ-Mini, USA) and 0.3 μL KAPA HiFi DNA polymerase was added. This allows for the PCR reaction to have a "hot start" and reduce non-specific amplification during the initial heating phase. The PCR cycle was then resumed with the conditions as outlined in the Table 2 below.

Table 2: PCR conditions

Phase	**Temperature**	**Time**
Denaturation	94°C	0:40 minutes
Annealing	62°C	0:45 minutes
Extension	70°C	2:00 minutes
Denaturation, annealing and extension were repeated 30 times		
Final extension	70°C	5:00 minutes
Cooling	4°C	Holding temperature

Following the PCR reaction, the products were stored at 4 °C for the short term or at -20°C for long term. The PCR products were run on a 0.8% agarose gel to confirm the correct sizes of the product based on the predicted sequences. Once PCR products were verified, they were then cleaned using the Wizard SV gel and PCR clean-up system (Promega, USA). The methodology was followed as outlined by the kit protocol (section 2.5.1).

2.4. Agarose Gel electrophoresis

0.8% agarose gels were used by preparing 0.4 g agarose (Seakem LE; Lonza, Switzerland) in 50 mL 1x TBE buffer. The solution was heated in a microwave until fully dissolved. 12 µL ethidium bromide from a 1 mg/mL stock solution was added to this suspension. The gel was then allowed to set at room temperature in a gel tray, with the gaskets attached and the comb inserted. Once the gel was set, it was submerged in 1x TBE buffer in the gel buffer tank. For each gel run, 5 µL of 1kB DNA ladder (Promega, USA) was run as the standard. For every 10 µL of sample to be run, it was diluted with 10 µL 1x TBE buffer, and 3 µL sample loading buffer. Gels were run at 100 V for approximately 1 hour to allow for adequate fragment separation. Gels were visualized under UV using a Chemidoc XRS+ system (BioRad, USA), and images were edited using Image Lab™ software.

2.5. PCR product and plasmid purification

Linearized plasmids as well as PCR products were purified using the Wizard SV gel and PCR clean-up system (Promega, USA). The purification was followed as per the manufacturer's guidelines.

2.5.1. PCR product purification

PCR product was added to Membrane binding solution at an equal ratio. This solution was added to a SV minicolumn, the minicolumn was then inserted into a collection tube. The solution was incubated at room temperature for 1 minute to allow for the DNA to bind the minicolumn. The minicolumn was centrifuged at 18,000 xg for 1 minute; the flow through from the collection tube was then discarded. 700 µL of Membrane wash solution was added to the minicolumn, centrifugation was repeated and the flow through discarded. An additional washing step using 500 µL of the Membrane was solution was then performed; following centrifugation, the flow through was discarded. The minicolumn was then centrifuged empty to allow for the evaporation of excess ethanol which was present in the wash solution. The minicolumn was transferred to a sterile microfuge tube, and 50 µL nuclease-free water was added to the minicolumn, after 1 minute incubation at room temperature, the DNA was eluted from the column by centrifugation. The concentration and purity of the eluted DNA was determined using the NanoDrop 2000 spectrophotometer apparatus (Thermo Scientific, USA). The eluted DNA was stored at 4°C for the short term or at -20°C for long term.

2.5.2. Plasmid purification

Once a plasmid was linearized by restriction digest, and run on an agarose gel, the DNA band of interest was excised from the gel. Excision of the band was carried out in the shortest possible time, since the UV light can damage the nucleic acids. This excised band was then purified using the clean-up kit. The excised band was weighed, for each mg of gel, 1 µL of Membrane binding solution was added. This mixture was then heated at 60 °C until the gel was fully dissolved. This solution was then transferred to a SV minicolumn, and the protocol followed, as outlined in 2.5.1.

2.6. Cloning PCR products into cloning vector

2.6.1. Ligation of PCR product into pGEM-T Easy plasmid

Ligation into a cloning vector was performed using the pGEM-T Easy system (Promega, USA). The ligation reaction was prepared in a sterile microfuge tube containing 5 µL of 2x Rapid ligation buffer, 1 µL of the pGEM-T Easy plasmid (50 ng), a 3-fold molar excess of purified PCR product. The reaction mix was made up to a total volume 10 µL using molecular grade water. A negative control ligation was also prepared, where the reaction was PCR product deficient; a corresponding volume of water was used as a replacement for the PCR product. The reaction was carried out overnight, in a slurry of ice (the ice melts overnight, resulting in a gradual temperature gradient from just above 0^{o}C to room temperature). The ligated plasmid was then stored at 4°C.

2.6.2. Transformation

The ligated pGEM-T Easy products were used to transform *E. coli* XL10-Gold competent cells. A 50 µL stock of competent cells was thawed on ice per transformation. To the competent cells, 10 µL of plasmid or ligation mix was added. This mixture was incubated on ice for 20 minutes. The mixture was heat shocked at 42.5°C for 75 seconds using a heating block. After the heat shock, the cells were incubated on ice for 5 minutes. To this, 500 µL of LB broth (without antibiotic) was added. The mixture was incubated at 37°C for 1 hour to allow the bacteria cells to recover and express antibiotic resistance. After this 1 hour incubation, 100 µL of the suspension was plated on agar plates containing 100 µg/mL ampicillin. The plates were incubated, inverted overnight (at least 18 hours) at 37°C.

2.7. Verification of transformation products

It is important to verify that the bacterial colonies present on the LB-broth agar plates contain the plasmid insert of interest. Colonies from the plates were scraped using sterile P200 pipette tips; 5 mL of LB broth supplemented with 50 μg/mL ampicillin was inoculated from these scrapings. This was performed for 5 colonies from the experimental plate. These broth cultures were incubated overnight at 37°C on a shaker.

2.7.1. Alkaline Lysis miniprep

3 mL from an overnight broth culture was centrifuged at 1500 xg for 3 minutes in sterile microfuge tubes using a microfuge. The bacterial pellet was resuspended in 100 μL GTE buffer. 200 μL NaOH/SDS lysis solution was added and completely mixed by pipetting. This suspension was incubated on ice for 5 minutes. An aliquot of 150 μL 5 M potassium acetate was added and mixed completely. This was incubated on ice for an additional 5 minutes. To pellet the bacterial debris from the suspension, the solution was centrifuged at 18,000 xg for 8 minutes. From the supernatant, 400 μL was aseptically transferred to a sterile microfuge tube and 850 μL absolute ethanol (molecular grade) was added to precipitate the plasmid DNA. To pellet the DNA, the suspension was centrifuged at 18,000 xg for 6 minutes. The pellet was washed in 70% ethanol. Once the pellet had dried for 20 minutes, to allow for any excess ethanol to evaporate, the plasmid DNA pellet was resuspended in 50 μL 5mM TE buffer. The plasmid DNA was then stored at 4°C for the short term or -20°C for long term.

2.7.2. Restriction digests

Restriction digests were performed using restriction enzymes and restriction buffers supplied by New England Biolabs (USA). The reaction mix was made up of 11.5 μL water, 2.5 μL 10x restriction buffer, 0.5 μL of each restriction enzyme, and 10 μL of plasmid to be digested. For diagnostic digests, the reaction mixture was incubated at 37°C for 30 minutes. For digestions to be used in subcloning reactions, reaction mixtures were incubated over night at 37°C to ensure that the plasmids were completely digested. After the restriction digestions, the digested products were run on a gel, as outlined in 2.4 in order to separate the DNA fragments.

2.7.3. Cryopreservation of transformed E. coli cells

E. coli cultures transformed with the correct inserts (confirmed by diagnostic restriction digest) were cryopreserved by the addition of sterile glycerol to a final concentration of 35% v/v. This suspension was transferred to cryotubes and stored at -80°C.

2.8. Subcloning of coding region into pARL2-GFP

2.8.1. Restriction digestion of insert and target vector

The pARL2-GFP plasmid as well as the pGEM-T Easy vector containing the inserts of interest were digested with restriction enzymes that introduced compatible "sticky ends". The reaction mixtures were prepared as outlined in 2.7.2. The digested plasmids were then run on a 0.8% agarose gel, the insert (DNA band cut out of pGEM-T Easy) and the target vector (linearized pARL2-GFP) were excised from the gel and purified as outlined in 2.5.2. The concentration and purity of the eluted DNA was determined using the NanoDrop 2000 spectrophotometer apparatus (Thermo Scientific, USA).

2.8.2. Ligation reaction

Between 50 and 100 ng of purified target vector was used in the subcloning ligation reactions. A 3-fold molar excess of purified insert DNA was required. To calculate the volume of insert required, the following equation was used:

$$Volume\ of\ insert = \frac{\frac{Insert\ size\ (bp)}{Plasmid\ size\ (bp)}\ x\ 3\ x\ mass\ of\ plasmid\ (ng)}{Concentration\ of\ insert\ DNA\ (ng/\mu L)}$$

The insert DNA and plasmid were combined and made up to a volume of 10 µL with molecular grade water. An aliquot of 10 µL 2x KAPA rapid ligation buffer (KAPA Biosystems, South Africa) and 1.0 µL KAPA T4 DNA ligase were added to the reaction mixture. A negative control reaction was also prepared by excluding the DNA insert from the reaction mixture. This mixture was incubated overnight in an ice slurry.

2.8.3. Post ligation reactions

Competent *E. coli* cells were transformed with the reaction products as explained in 2.6.2. The transformation products were verified by restriction digestion as outlined in 2.7.

2.9. Plasmid MaxiPrep

A plasmid MaxiPrep was performed using the QIAfilter kit (Qiagen, Germany) in order to purify up to 500 μg of plasmid at a high purity to be used in parasite transfections. Glycerol stocks stored at -80°C of *E. coli* cells transformed with the expression vector of interest were required for the plasmid MaxiPrep.

A sterile solution of LB broth (2 mL) supplemented with antibiotic selection marker (ampicillin) was inoculated with a scraping from the glycerol stock; this broth culture was then incubated at 37°C with shaking for 8 hours. From this 2 mL culture, 200 μL was used to inoculate a 200 mL LB broth (with antibiotic) culture in an Erlenmeyer flask. This broth culture was incubated overnight with shaking at 37°C.

The 200 mL overnight culture was transferred to a sterile centrifuge tube and centrifuged at 4500 xg for 15 minutes using a JA-10 rotor. The bacterial pellet was processed as outlined in the Qiagen QIAfilter manufacturing instructions without deviation from this protocol. Following isolation of the plasmid DNA, it was resuspended in 1 mL 5 mM Tris buffer (preheated to 37°C). The concentration and purity of the purified plasmid DNA was determined using the NanoDrop 2000 spectrophotometer apparatus, and stored at 4°C for the short term or -20°C for long term.

2.10. Transfection of *P. falciparum* blood-stage parasites by "RBC preloading"

2.10.1. Preparation of parasites: Percoll gradient centrifugation

Parasites were enriched as outlined in 2.1.6.2. A 20 mL culture, containing a high parasitaemia trophozoite and schizont stage parasites was required for each transfection. A small drop of enriched parasites was viewed under oil immersion using a light microscope to confirm the success of the enrichment as well as the integrity of the enriched parasites.

2.10.2. Preparation of plasmid for transfection

A very pure sample of plasmid (75 µg) was required per transfection. Sufficient volume of plasmid (obtained using the MaxiPrep procedure in 2.9) was pipetted into a sterile microfuge tube. To this, 0.5 volumes of 5 M potassium acetate was added, followed by 3 volumes of absolute ethanol (molecular grade). This suspension was pelleted in a centrifuge at 18,000 xg for 7 minutes. The DNA pellet was washed 3 times in 70% ethanol, taking care to remove all supernatant between washes. Following the washing steps, the DNA pellet was allowed to air dry in a laminar flow hood, to ensure that the DNA remains sterile. The pellet was dissolved in 100 µL 25 mM Hepes. Once fully resuspended, the plasmid was ready for transfection.

2.10.3. Preparation of red blood cells for transfection

A sterile aliquot of 300 µL fRBCs were required for each transfection. The RBCs were resuspended in 5 mL 1x cytomix to remove culture media. The RBCs were centrifuged at 900 xg for 2 minutes and the cytomix supernatant was completely removed by aspiration.

2.10.4. Transfection methodology

In a 0.2 cm electroporation cuvette, the following was added: 100 µL 2x cytomix, 100 µL plasmid DNA, and 200 µL washed fRBCs. The components were mixed thoroughly by carefully pipetting the mixture up and down. The electroporation cuvette was incubated on ice for 5 minutes, followed by electroporation under normal conditions (310V, 950 µF) using a Bio-Rad Gene Pulser Xcell^{TM} electroporator. The cuvette was incubated on ice for an additional 5 minutes, followed by re-electroporation under the same conditions and an additional incubation on ice for 5 minutes. The electroporated RBCs were resuspended, and the mixture transferred to a T25 culture flask containing the enriched parasites. The parasites were gassed and incubated at 37°C, without shaking.

On the day following transfection (day 2), the medium was replaced with fresh medium (all pipetting and centrifuge steps were carried out with great care, as the RBCs are fragile following electroporation). On day 3, 150 µL fresh RBCs were added, and the media was replaced with fresh media containing 2.5 nM of the selection drug WR99210, or 5 µM Blasticidin S (depending on the expression plasmid used). Parasites that had successfully taken up the plasmid gained resistance to the WR99210 drug due to the presence of the human dihydrofolate reductase gene (hDHFR) in the pARL2-GFP expression plasmid. Parasites successfully transfected with pARL2-mCherry plasmids containing the Blasticidin S deaminase gene gain resistance to the selection marker, Blasticidin S. From day 4 onwards, the transfected cultures were kept under continual drug pressure with bi-weekly medium changes and Giemsa stained smear preparations to monitor the presence of parasites. When necessary, fresh RBCs were added in order to maintain a 3% haematocrit. This continued until parasitaemia increased to the point that cultures were maintained routinely (section 2.1.2). It took, on average, approximately 3 weeks of culturing transfected parasites in selection media for parasitaemia to increase to the levels where parasites were visualized in Giemsa stained smears.

2.11. Confirmation of transfection of *P. falciparum* parasites by Western blotting

2.11.1. Preparation of parasite lysate

iRBCs (150 µL) were harvested from parasite culture and resuspended in 1350 µL 0.1% saponin solution. The suspension was mixed by pipetting, followed by centrifugation at 2300 xg for 5 minutes. The parasite pellet was washed in PBS twice to remove free haemoglobin and ghost RBC membranes. The pellet was then dissolved in 100 µL 1x sample buffer. Immediately before the sample was to be run on the gel, it was boiled for 5 minutes.

2.11.2. SDS-PAGE gel electrophoresis

A 10% resolving gel was poured by combining 3.33 mL 30% acrylamide, 2.5 mL lower gel buffer and 4.16 mL water, followed by the addition of 35 µL of 10% ammonium sulphate (APS) and 7 µL TEMED. The gel solution was poured between glass plates mounted in the gel apparatus. A small amount of isopropanol was added to the top of the gel while it was incubated at room temperature to polymerize. The stacking gel, which was poured on top of the resolving gel, was prepared by combining 0.7 mL acrylamide, 1.25 mL stacking buffer, 3.0 mL water, 25 µL 10% APS and 6 µL TEMED. The comb was inserted into the stacking gel. The gel was incubated at room temperature for it to polymerise and fully set.

The gel was mounted in the gel apparatus and submerged in 1x SDS running buffer. A 15 µL volume of each sample was added, as well as 5 µL molecular weight marker (Colour Prestained Broad Range Protein ladder; New England Biolabs, USA). The gel was run at 20 mA constant current until sufficient separation had been achieved (separation can be monitored based on the Colour Prestained marker).

2.11.3. Western blotting

2.11.3.1. Transblotting

The SDS-PAGE gel was incubated in transblot buffer for 15 minutes. The transblotting was performed in a Bio-Rad transblot sandwich by arranging (starting from the black side): the sponge, Bio-Rad mini trans-blot filter paper, the soaked SDS-PAGE gel, Amersham Hybond-ECL membrane (GE Healthcare, Germany) an additional layer of filter paper, and an additional sponge. The Bio-Rad transblot sandwich was placed in the Bio-Rad apparatus, placed in the gel tank and submerged in fresh transblotting buffer.

The transblot was performed with cooling, and stirring with a magnetic stirrer at 100 V for 1 hour. Following the transblotting, the Hybond blot was rinsed in water, followed by staining in Ponceau S staining solution for 5 minutes. The blot was then destained using Ponceau S destain solution. Ponceau staining allows the bands on the blot to be visualized.

2.11.3.2. Antigen detection

The blot was incubated with incubation buffer (TBS-Tween containing 1% BSA and 2% milk powder) for 40 minutes at room temperature, followed by an overnight incubation at 4°C with gentle shaking, with monoclonal mouse anti-GFP primary antibody (KPL, USA), diluted to a final concentration of between 0.2 and 1 μg/mL with incubation buffer. The blot was washed 4 times in washing buffer (TBS + 0.1% Tween 20) to ensure that all unbound antibody was removed. Incubation with anti-mouse-HRP secondary antibodies (KPL, USA) diluted 1:5000 with incubation buffer was performed for 1 hour at room temperature. The blot was then washed thoroughly 5 times in washing buffer to ensure that all unbound secondary antibody was removed. The blot was visualized using the colorimetric reagent, TMB membrane peroxidase substrate (KPL, USA). A volume of 1 mL of the substrate was used per 10 cm^2 membrane. The membrane was incubated until colour developed to the desired level. To stop the reaction the membrane was rinsed with water for 30 seconds. The blot was then photographed using a Chemidoc XRS+ system (BioRad, USA), and images were edited using Image Lab™ software.

2.12. Microscopy studies

In order to determine the localization of fluorescently labelled proteins (either fluorescently tagged fusion proteins, proteins tagged with fluorescent antibodies or cells treated with a fluorescent compound), cells were prepared as described below on microscope slides an analysed by fluorescence light microscopy as well as Confocal fluorescence microscopy.

2.12.1. Live cell imaging of P. falciparum parasites

A 1 mL volume of culture was centrifuged at 400 xg for 2 minutes to pellet 30 μL iRBC. The iRBC were incubated at room temperature for 5 minutes with PBS containing 1 μg/mL Hoechst (supplied as *bis*-Benzemide H 33258 by Sigma-Aldrich, USA), or PBS containing 1 μg/mL DAPI. The RBCs were pelleted again and washed with 1x PBS. The iRBCs were resuspended in 100 μL incomplete medium, ready for viewing by fluorescence microscopy.

iRBC (1 μL) suspension was pipetted onto a microscope slide; this drop was covered by a glass cover slip. The cells were then viewed using a Carl Zeiss AxioVert A.1 FL-LED Inverted microscope, with an N-Achroplan 100x/0.13 Ph0 M27 oil immersion objective, and an AxioCam Mrm camera. Microscopy was also performed using confocal microscopy, with a Carl Zeiss LSM780 Elyra S1 microscope, with an alpha Plan-Apochromat 100x/1.46 Oil DIC M27 Elyra objective. Images were processed and edited using Zen 2011 Blue edition software (Zeiss, Germany).

CHAPTER THREE: MOLECULAR CLONING AND TRANSFECTION

3.1. Introduction

One of the possible approaches in characterising candidate proteins potentially involved in endocytosis is to identify parasite genes based on homology to mammalian counterparts. For this project, homologues of coronin, dynamin and medium chain (μ) adaptins were investigated, based on their roles in mammalian cells, as discussed in Chapter 1 – coronin is thought to be involved in actin dynamics during phagocytosis and macropinocytosis, dynamin mediates endocytic vesicle fission during clathrin-dependent and –independent endocytosis and μ adaptins form part adaptor protein complexes (particularly AP-2) that recruit clathrin to sites of clathrin-dependent endocytosis. *P. falciparum* homologues of coronin, dynamin 2 and μ4 were identified by BLAST searches of the parasite genome and verified by their annotations in PlasmoDB (Coronin: PF3D71251200, Dynamin-like protein (DYN2): PF3D71037500, AP-4 complex subunit μ, putative: PF3D71119500). The nomenclature employed in this thesis is based on the PlasmoDB designations of the genes and their closest sequence homologues in humans – dynamin 2 is most homologous to human dynamin 2 (the dominant dynamin isoform present in most human cell types) and μ4 to the human μ4 adaptin (forms part of the AP-4 complex that mediates trafficking between the Golgi and endosomes/lysosome-like organelles and is closely related to the AP-2 complex involved in endocytosis (Conner & Schmid 2003). Homology was confirmed by sequence alignment and, importantly, the conservation of critical amino acid residues required for protein function (see section 3.2.1).

The overall goal of this project was to assess the functions of the three candidate endocytosis proteins by employing fluorescence microscopy to determine their sub-cellular localization in blood stage parasites. Localization may be achieved by two main approaches: immuno-localization using custom antibodies raised against the proteins of interest, or the generation of transgenic parasites expressing fluorescent protein fusions of the proteins of interest, for which variants of the *Aequorea* Green Fluorescent Protein (GFP) is most commonly used. The preparation of antibodies for immuno-localization requires purified recombinant antigen (usually

expressed in *E. coli*) for animal immunization, which is a lengthy process and preparing recombinant antigen by expressing malaria genes in heterologous systems may be fraught with difficulties (Birkholtz *et al*. 2008). Alternatively, custom antibodies raised against peptides based on predicted surface epitopes of the proteins may be obtained from commercial companies. However, this approach is expensive and the epitopes in question may not always be recognised with sufficient affinity to produce robust immuno-localization results, particularly after cell fixation. In addition, the cell fixation/permeabilization required in immuno-affinity procedures may disrupt the normal architecture of the cell and produce staining artefacts, while antibody specificity (i.e. the possibility that immuno-staining patterns are produced by the recognition of related epitopes in non-relevant proteins) is always a concern.

By comparison, the approach of expressing GFP fusion constructs in transgenic parasites does not suffer from these drawbacks and has the main advantage that protein localization may be studied in live cells, without the need for fixation/permeabilization procedures. In addition, large selections of commercial anti-GFP antibodies are available, should further co-localization studies with antibodies be required. Admittedly, there are also conceivable pitfalls associated this approach: the fusion of GFP to the protein of interest may disrupt its normal function and localization; overexpression of the protein in the cell may alter cell function and homeostasis and indeed be toxic to the cell, making it difficult or impossible to obtain transgenic cells (particularly with malaria parasites, where the poor transfection efficiency using current methods necessitates weeks or months of culturing and drug selection to obtain a population of stable transgenic parasites). Depending on the promoter used to drive fusion protein expression, the protein may be expressed at parasite life cycle stages that do not accurately reflect the timing of expression of the endogenous protein, thus contributing to toxicity or producing erroneous localization results. Nonetheless, given the comparative advantages of the GFP fusion protein approach, it was adopted for the localization of the proteins of interest in this study.

The preparation of transgenic parasites expressing GFP fusions of the proteins of interest requires the cloning of their coding sequences into an expression plasmid. The coding sequences for these three homologues chosen for this study were amplified by PCR. PCR was performed using cDNA as the template, because coronin and μ4 were predicted to contain introns. Genes

amplified by PCR were cloned using the pGEM-T Easy vector system, followed by subcloning into the parasite expression plasmid pARL2-GFP.

The pGEM-T Easy vector system was used as it is a convenient system to clone PCR products. The system is convenient as the vectors are just 3015 bp in size which makes them easier to transform competent *E. coli* cells, and they are high copy number plasmids with the T7 and SP6 RNA polymerase promoters flanking the multiple cloning site. In this application, PCR products were ligated into the cloning vector using TA cloning. The PCR inserts were created by using KAPA high fidelity polymerase because it has a proofreading function. Following the purification of the PCR products, the products were briefly incubated with *Taq* polymerase and nucleotides. This polymerase adds a single 3'-adenine overhang to each end of the DNA product (Holton & Graham, 1991). The pGEM-T Easy vector contains a single 3'-thymidine at each end of the DNA which allows for rapid ligation of PCR products. This makes it possible for linear strands of DNA with 3'-adenine tails to be ligated into the pGEM-T Easy vector. The presence of the ampicillin resistance gene allows the plasmid to be amplified in transformed *E. coli* cells.

Subcloning of the coding sequences involved the double digestion of plasmids using the restriction sites introduced by the specific primers. These digestion products were then ligated into the parasite expression vector pARL2-GFP. The plasmid map in Figure 2 below illustrates the pARL2-GFP vector. This plasmid is commonly used in *P. falciparum* parasite transfections (e.g. Przyborski *et al*. 2005) because it encodes the necessary components to optimise GFP-tagged fusion protein expression.

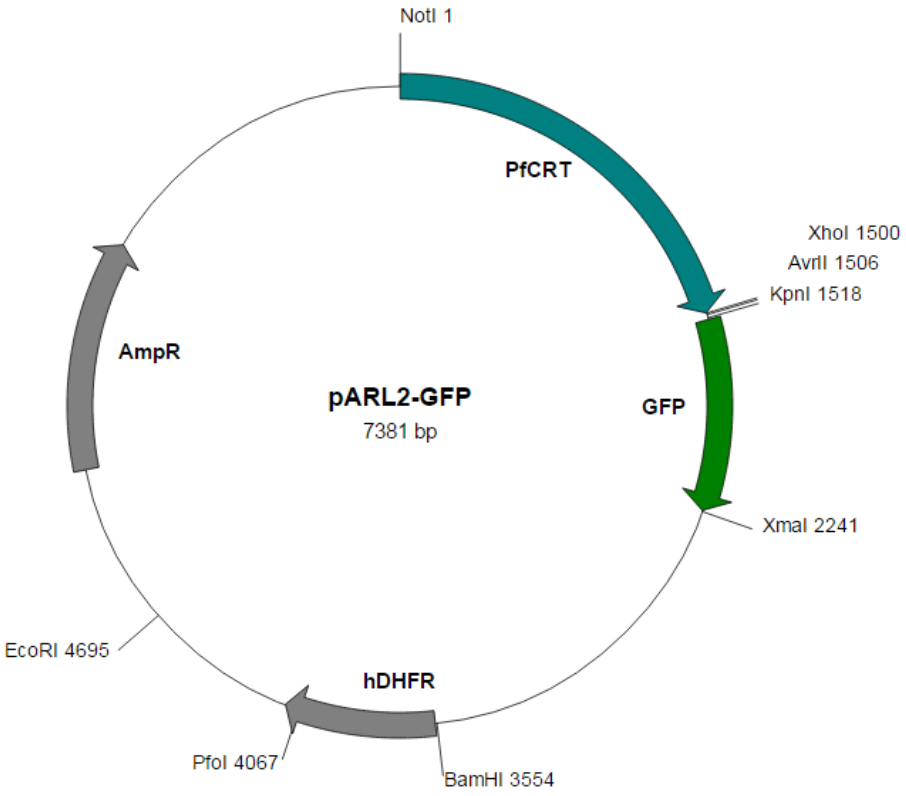

Figure 2. pARL2-GFP expression vector.
Plasmid map showing the 7381 bp pARL2-GFP expression vector used for the transfection of *P. falciparum* 3D7 parasites. Plasmid map was generated using the online Savvy-Scalable vector graphic generator.

As can be seen above, the pARL2-GFP plasmid encodes the *Pf*CRT promoter sequence. This promoter allows expression throughout the intra-erythrocytic life stages of *P. falciparum* parasites (Van Dooren *et al*. 2005). In order to express GFP-tagged fusion proteins, the genes of interest were cloned between the *Pf*CRT promoter and the GFP coding sequence using the multiple cloning site, which contains the restriction sites: *Xho*I, *Avr*II and *Kpn*I. This results in expression of the gene of interest as a GFP-tagged fusion construct with GFP expressed at the C-terminal end of the protein. The plasmid contains the coding sequence for the ampicillin resistance gene, a selectable marker which confers resistance to the antibacterial agent, ampicillin. This results in rapid amplification of the vectors in transformed competent *E. coli* cells. In addition, the plasmid encodes the gene for the hDHFR (human dihydrofolate reductase) enzyme. This is a selectable marker which confers resistance to the antifolate inhibitor, WR99210. As a result, only parasites successfully transfected with the complete plasmid are able to grow in RPMI 1640 media supplemented with WR99210.

Transfection of *P. falciparum* parasites with expression plasmids is achieved by electroporation, followed by culturing in RPMI medium supplemented with WR99210. There are two electroporation strategies that could be employed: the first possibility is the direct electroporation of red blood cells (RBCs) infected with ring-stage parasites (Wu *et al*. 1995). The second option is the "spontaneous uptake" method (Deitsch *et al*. 2001). The "spontaneous uptake" method involves electroporating uninfected RBCs with the expression plasmids. These pre-loaded RBCs are then added to parasite cultures. When the parasites invade the pre-loaded RBC they internalize the plasmid. We chose to employ the "spontaneous uptake" methodology for the transfection in this project. Previous work by a student in our research group made use of firefly luciferase expression plasmids to repeatedly, and consistently demonstrate that obtaining transgenic parasite cell lines is considerably accelerated using this approach, compared to the direct electroporation of ring-stage parasites methodology (T. Moyo, B.Sc. (Hons) report). We employ a number of modifications to the method established by Deitsch *et al* (2001): two electroporation pulses are used, with brief incubations on ice between pulses; in addition, electroporated RBCs are added to enriched trophozoite/schizont stage parasites in order to maximise transfection efficiency.

Once WR99210-resistant parasites were obtained, the expression of full-length GFP-tagged fusion proteins of the predicted sizes needed to be confirmed. This confirmation was achieved by Western blotting. Parasite lysates were run on SDS-PAGE gels and transblotted onto Western blot membranes. Commercially available anti-GFP antibodies were used to probe the lysates to determine the size of the GFP-tagged fusion proteins, and compared with a protein size marker.

The first aim of these experiments in this chapter was to successfully clone the coding sequences for the endocytosis candidate proteins into the pARL2-GFP expression vector. Once the plasmids were successfully cloned, they were sent for sequencing to confirm that the inserts were in frame, orientated correctly, and without mutation. The second aim was to use these plasmids to prepare transgenic parasites expressing the relevant GFP fusion proteins. *P. falciparum* parasites were transfected with the expression plasmids using the RBC preloading method. SDS-PAGE and Western blotting was used to confirm the expression of full-length GFP-tagged fusion proteins.

3.2. Results

3.2.1. Sequence alignments

The predicted amino acid sequences of the three *P. falciparum* coding regions (coronin: PF3D71251200, dynamin-like protein (DYN2): PF3D71037500, AP-4 complex subunit μ, putative: PF3D71119500) were downloaded from the PlasmoDB website (www.plasmodb.org) and aligned with the sequences of their closest human homologues – coronin 1A (NCBI reference number NP_001180262.1), μ4 adaptin (UniProt O00189) and dynamin 2 isoform 3 (NP_004936.2) using the DNAMAN alignment program. Regions of amino acid identity and similarity are denoted in the alignments.

The alignments indicated for coronin an identity of 27% and 51% positives over a 448 amino acid sequence. For dynamin 2, an identity of 32% and 54% positives over a 695 amino acid sequence. For μ4, an identity of 30% and 59% positives over a 459 amino acid sequence.

3.2.1.1. Coronin

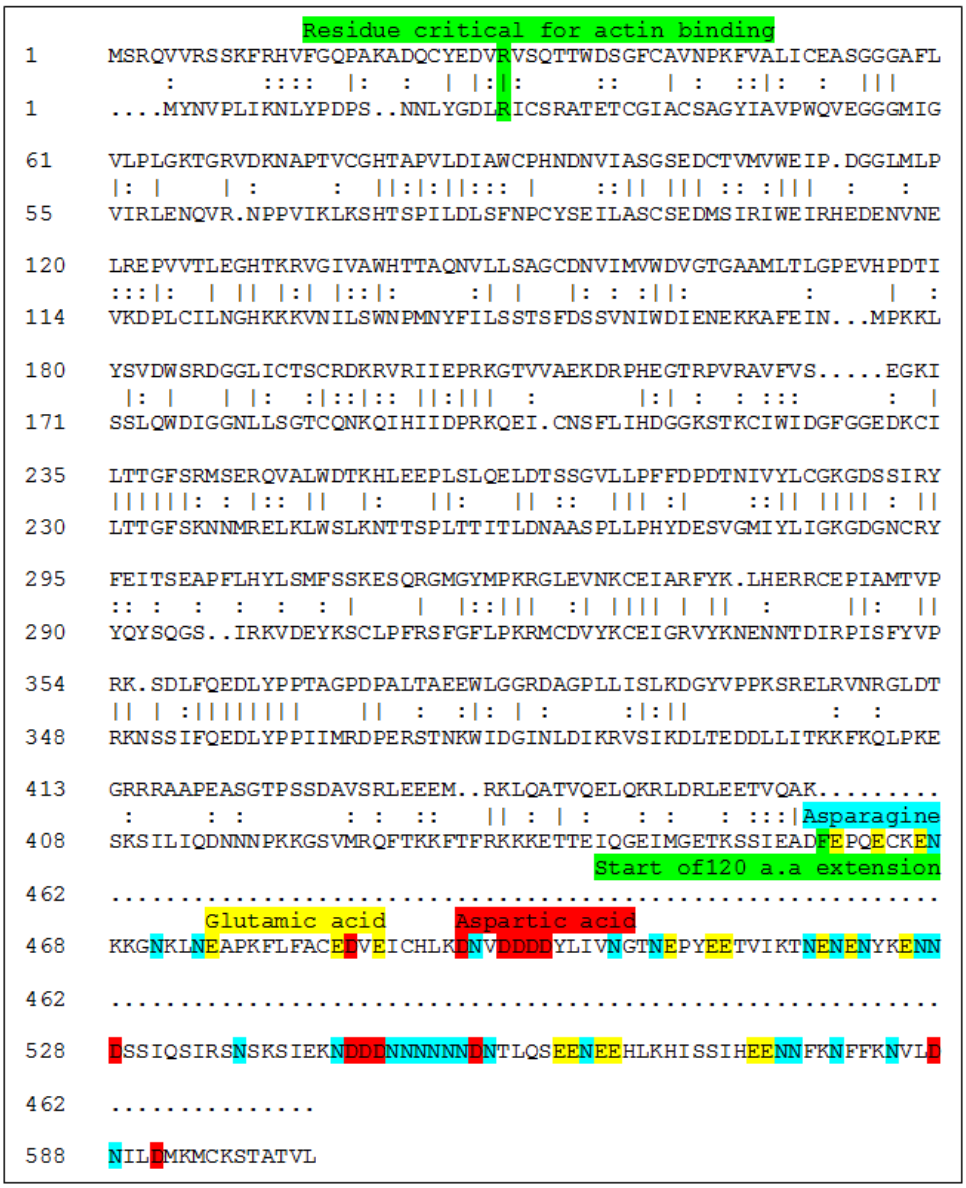

Figure 3. Coronin protein sequence alignment

Protein sequence alignment of human (upper line) and *P. falciparum* (lower line) coronin using DNAMAN© alignment program. Identical residues are denoted by a vertical line, conserved amino acid substitutions are denoted by a colon, and a dot denotes the absence of the residue in that position.

3.2.1.2. Dynamin 2

Figure 4. Dynamin 2 protein sequence alignment

Protein sequence alignment of human (upper line) and *P. falciparum* (lower line) dynamin 2 using DNAMAN© alignment program. Identical residues are denoted by a vertical line, conserved amino acid substitutions are denoted by a colon, and a dot denotes the absence of the residue in that position.

3.2.1.3. µ4 adaptin

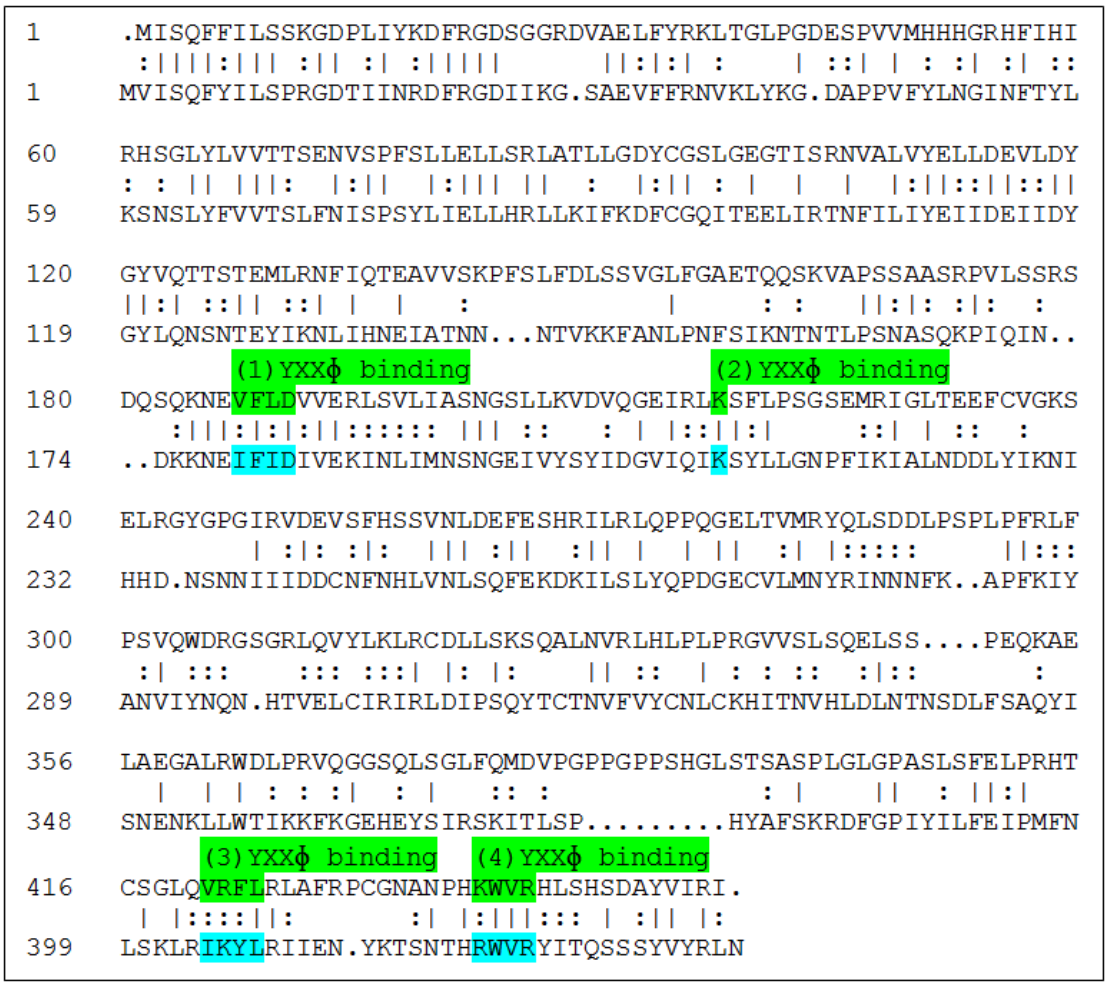

Figure 5. µ4 adaptin protein sequence alignment

Protein sequence alignment of human (upper line) and *P. falciparum* (lower line) µ4 adaptin using DNAMAN© alignment program. Identical residues are denoted by a vertical line, conserved amino acid substitutions are denoted by a colon, and a dot denotes the absence of the residue in that position.

3.2.2. Total P. falciparum RNA isolation and cDNA synthesis

The first step in amplifying the coding sequences for the proteins of interest was to purify the total complementary DNA (cDNA) from the *P. falciparum* 3D7 strain parasites. To achieve this, RNA was isolated from parasites in the erythrocytic cycle, followed by RT-PCR to synthesise total cDNA.

In order to achieve maximum yield of RNA, non-synchronised parasites were harvested from 20 mL cultures with a haematocrit of 4% and a parasitaemia of above 5%. Non-synchronised parasites were used to ensure that mRNA from all RBC parasite life stages was isolated. The Promega SV Total RNA Isolation System was used as per the manufacturer's instructions. The total yield of RNA was determined spectrophotometrically at 260 nm. One absorbance unit (A_{260}) is equivalent to 40 μg of single-stranded RNA/mL of sample. The average yield of RNA per preparation was between 50 and 100 μg. The RNA purified with the SV Total RNA Isolation System was generally free of DNA and protein contaminants, determined by visualizing nucleic acids on agarose gels, and by checking the purity using the A_{260}/A_{280} ratio. The average range for a pure RNA preparation is between 1.8 and 2.1, and the RNA isolated here had ratios between 2.0 and 2.1. This purified RNA was subsequently used as a template for single-stranded cDNA synthesis using RNA-dependant DNA polymerase using the Promega ImProm-II™ Reverse Transcription System, making use of Oligo-dT and random hexamer primers.

3.2.3. *Polymerase chain reaction (PCR) amplification*

Gene amplification was performed by PCR using cDNA as the template. Primers were designed to amplify the full-length coding sequences of Coronin, Dynamin 2, and μ4 (Designer primers used for PCR reactions (restriction sites are underlined).

Table 1 in section 2.3.1). Restriction sites were introduced using these primers to allow for subsequent cloning steps. The pARL2-GFP expression vector contains *Xho*I, *Avr*II and *Kpn*I sites. Coronin primers introduced *Sal*I (produces an *Xho*I compatible cohesive sticky end) and *Kpn*I restriction sites with the forward and reverse primers respectively. Dynamin 2 primers introduced *Xho*I and *Avr*II restriction sites with the forward and reverse primers respectively. μ4 primers introduced, *Xho*I and *Kpn*I restriction sites using the forward and reverse primers respectively.

The predicted sizes of PCR amplification products based on the genome sequences obtained are outlined in Table 3 below.

Table 3. Expected sizes of PCR amplification products

Size (bp)		
Coronin	Dynamin 2	μ4
1809	2130	1311

PCR amplification reactions followed standard PCR protocols as previously outlined (2.3.3) using the KAPA HiFi PCR kit (to reduce the possibility of polymerase errors), followed by the addition of dA tail to the 3' end of the PCR product using the KAPA2G Robust PCR kit. These reactions yielded DNA of accurate sizes. The correct size was scrutinized by agarose gel electrophoresis and compared to a 1kb DNA marker. A second reason for running the products on an agarose gel is to confirm that there are no non-specific PCR products. As can be seen on the agarose gels in Figure 6, PCR yielded only the band of interest. For subsequent cloning steps, PCR products were purified using the Promega Wizard SV PCR clean-up system. The purpose of the purification step was to remove any residual primers, nucleotide bases, and excess polymerases.

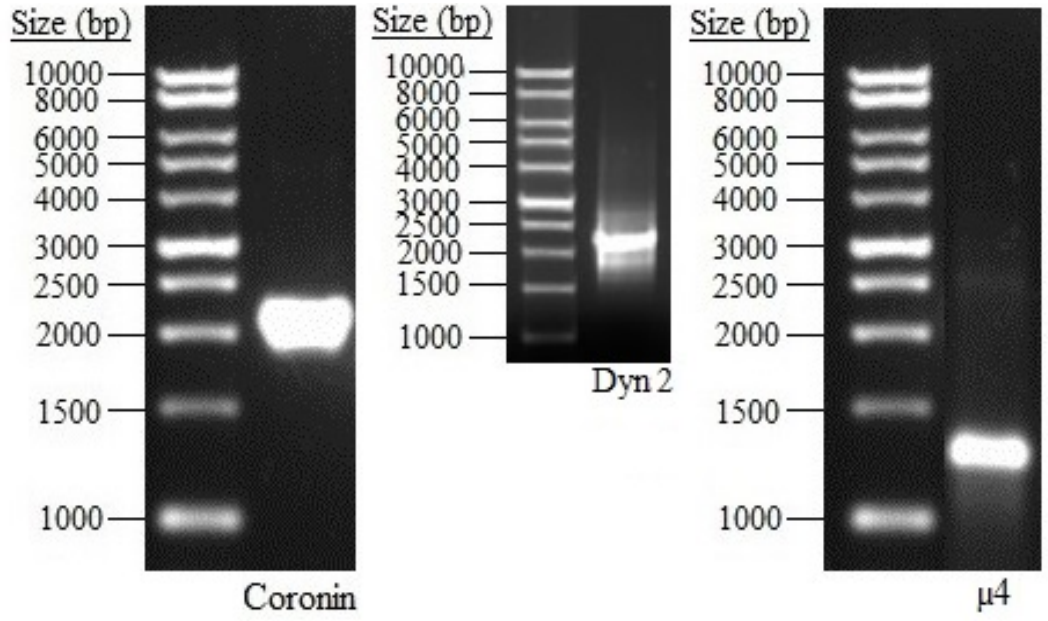

Figure 6. PCR amplification products

0.8% agarose gel electrophoresis showing the PCR products of predicted size alongside a 1kb DNA ladder per gel. Gene products for Coronin (1809 bp), Dynamin 2 (2130 bp) and μ4 (1311 bp) are shown in the gels on the left, middle, and right, respectively.

3.2.4. Cloning into pGEM-T Easy Vector

After the PCR products were purified and the purity and concentration established by absorbance at 260 nm and A_{260}/A_{280} ratios > 1.8, the PCR products were diluted to the correct volume and ligated to the pGEM-T Easy vector (Promega) using a 3:1 molar ratio of insert vs. plasmid. Competent XL10-Gold *E. coli* cells were transformed with the recombinant plasmid DNA. Transformed cells were spread plated on LB-Agar plates containing ampicillin to allow for the selection of single colonies containing the plasmid with insert DNA. Colonies from these plates were grown overnight in liquid broth cultures, and the plasmids isolated by alkaline lysis miniprep. Restriction digest analysis confirmed which plasmids contained the inserts of the expected size. Restriction digests were performed with *Sal*I and *Kpn*I for coronin (Figure 7): coronin has an internal *Xho*I site, therefore the *Sal*I site was introduced using the forward primer, to produce compatible sticky ends with the *Xho*I site in the pARL2-GFP expression vector, and *Kpn*I was introduced using the reverse primer. Dynamin 2 has an internal *Kpn*I site, therefore *Xho*I and *Avr*II sites were introduced using the forward and reverse primers respectively and

used for the diagnostic digests (Figure 8). For μ4, *Xho*I and *Kpn*I sites were introduced using the forward and reverse primers respectively and used for the diagnostic digests (Figure 9). As previously mentioned, these restriction sites were introduced to allow subsequent cloning into the pARL2-GFP expression vector which contains *Xho*I, *Avr*II and *Kpn*I sites in the multiple cloning site.

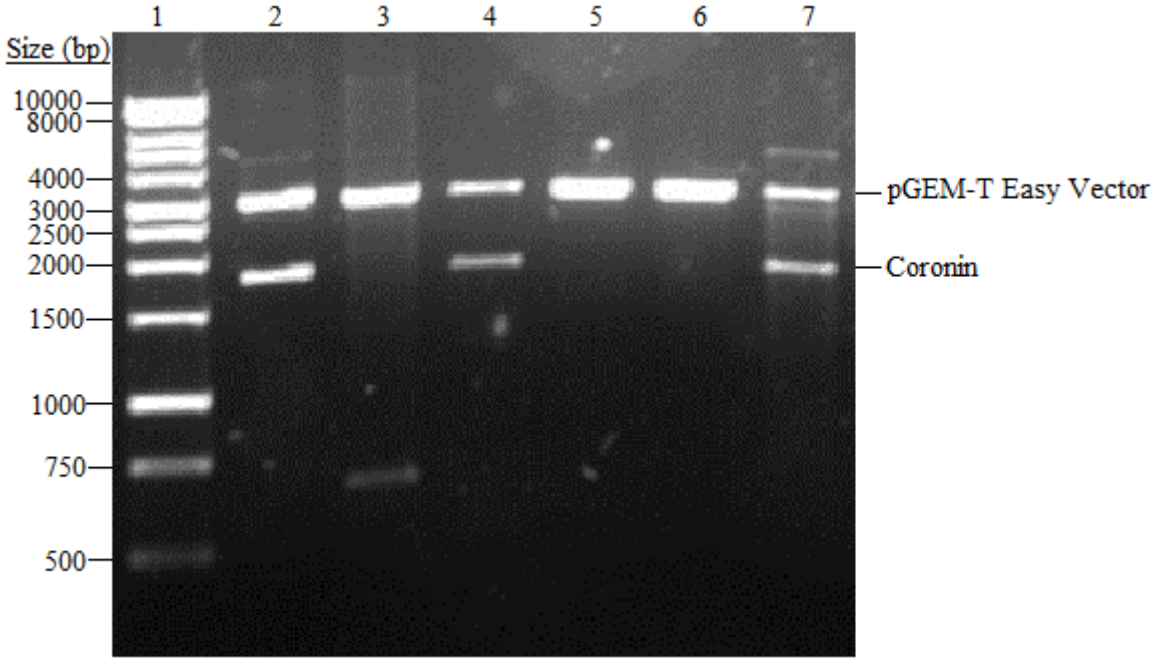

Figure 7. Restriction digest analysis of coronin coding sequence in pGEM-T Easy cloning vector.

0.8% agarose gel representing the coronin insert excised from recombinant pGEM-T Easy plasmids isolated from six individual *E. coli* colonies. The restriction digest was performed using the restriction enzymes *Sal*I and *Kpn*I. The restriction sites for *Sal*I and *Kpn*I were introduced into the coronin sequence with the forward and reverse primers respectively. This results in a predicted DNA fragment of 1809 bp. The remaining plasmid backbone has a size of approximately 3015 bp. Lane 1: 1 kB DNA ladder. Lanes 2, 4, and 7: Restriction digest containing insert of predicted size. Lanes 3, 5, and 6: Restriction digests of plasmids lacking insert.

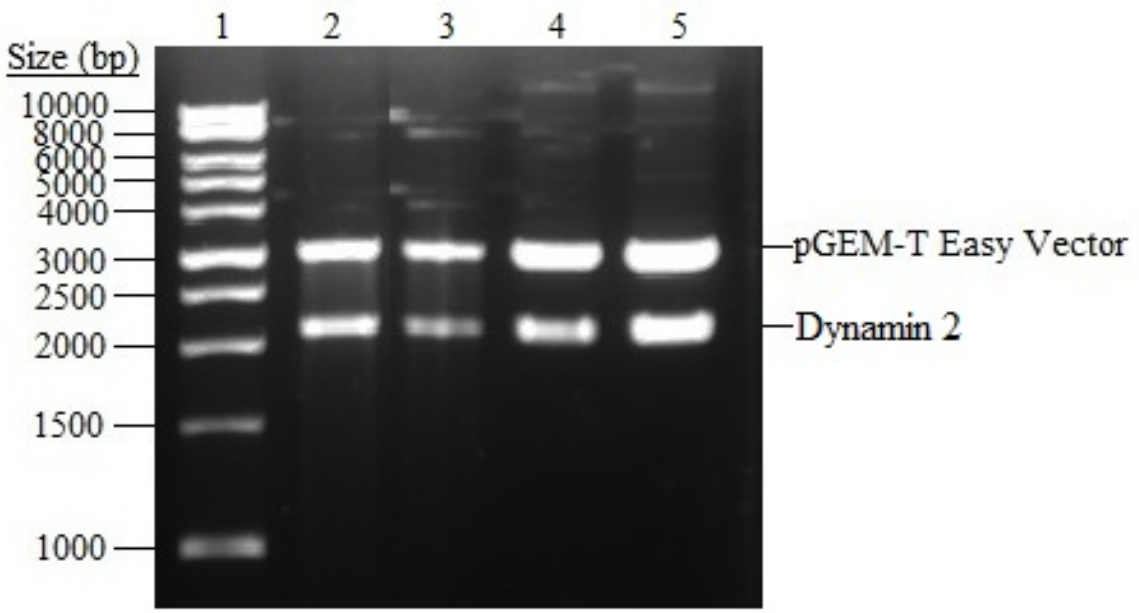

Figure 8. Restriction digest analysis of dynamin 2 coding sequence in pGEM-T Easy cloning vector.

0.8% agarose gel representing the dynamin 2 insert excised from pGEM-T Easy plasmids isolated from four *E. coli* colonies. The restriction digest was performed using the restriction enzymes *Xho*I and *Avr*II. The restriction sites for *Xho*I and *Avr*II were introduced into the dynamin 2 sequence with the forward and reverse primers respectively. This results in a predicted DNA fragment of 2130 bp. The remaining plasmid backbone has a size of approximately 3015 bp. Lane 1: 1 kB DNA ladder. Lanes 2-5: Restriction digest containing insert of predicted size.

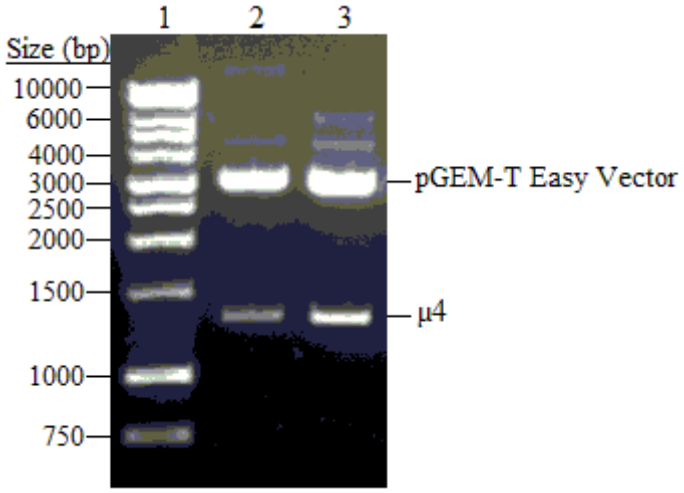

Figure 9. Restriction digest analysis of µ4 coding sequence in pGEM-T Easy cloning vector.

0.8% agarose gel representing the µ4 insert excised from pGEM-T Easy plasmids isolated from two *E. coli* colonies. The restriction digest was performed using the restriction enzymes *Xho*I and *Kpn*I. The restriction sites for *Xho*I and *Kpn*I were introduced into the µ4 sequence with the forward and reverse primers respectively. This results in a predicted DNA fragment of 1311 bp. The remaining plasmid backbone has a size of approximately 3015 bp. Lane 1: 1 kB DNA ladder. Lanes 2 and 3: Restriction digest containing insert of predicted size.

3.2.5. Cloning into pARL2-GFP

After the prescence of correct inserts was verified by restriction digest, digestions were carried out on a larger scale to obtain the insert DNA from the pGEM-T Easy vectors for subcloning. The vectors were digested with *Sal*I and *Kpn*I for coronin, *Xho*I and *Avr*II for dynamin 2, and *Xho*I and *Kpn*I for µ4. The pARL2-GFP target vector was also digested on a large scale with corresponding restriction enzymes to ensure compatible sticky ends for the insert DNA and target expression plasmid. These restriction sites were selected to ensure that the genes were cloned into the plasmid in frame and in the correct orientation. The restriction digests for the inserts and the target vectors were run on an agarose gel to achieve separation; the bands were excised from the gel and purified using the Promega Wizard SV gel clean-up system.

The yield and purities of the purified DNA fragments was determined spectrophotometrically by A_{260} and A_{260}/A_{280} ratios. The insert DNA and target vectors were concentrated by vacuum centrifuging or diluted to the correct concentrations and volumes to achieve a 3:1 molar ratio of

insert vs. vector and 50 µg vector per ligation reaction, and ligated using the KAPA Rapid Ligation system. Competent XL10-Gold *E. coli* cells were transformed with the ligated pARL2-GFP plasmids and grown overnight on LB-Agar plates containing ampicillin. Single colonies were then grown overnight in liquid broth. Recombinant plasmids were isolated by alkaline lysis miniprep from broth cultures. Restriction digests were performed on isolated plasmids to confirm the plasmids contained the inserts of the expected size. These digestions were performed using *Xho*I and *Kpn*I for coronin, *Xho*I and *Avr*II for dynamin 2, *Xho*I and *Kpn*I for µ4. All digests yielded DNA fragments of the expected size.

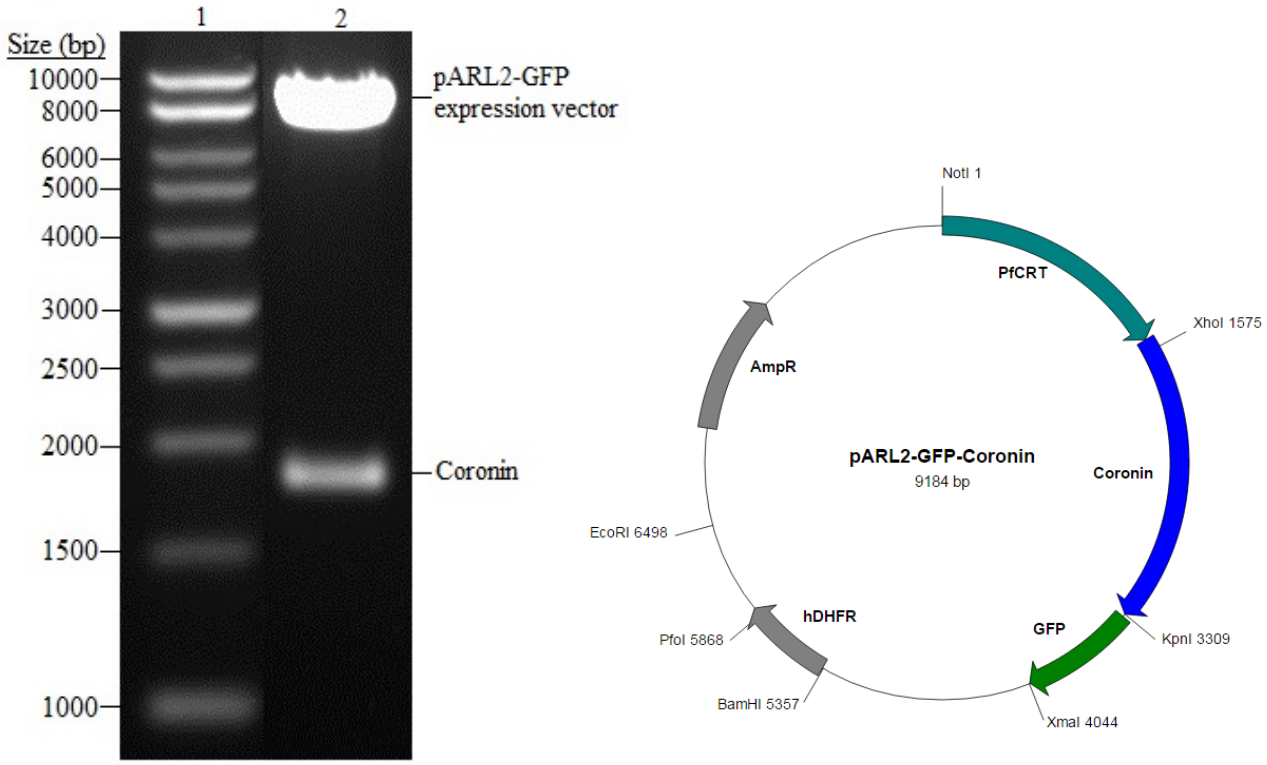

Figure 10. Restriction digest analysis of pARL2-GFP-coronin expression vector.

0.8% agarose gel showing the coronin gene excised from the pARL2-GFP expression vector. The plasmid was digested with the restriction enzymes *Xho*I and *Kpn*I. The restriction site for *Kpn*I is found at the 3' end of the insert sequence. The coronin gene contains an internal *Xho*I restriction site found within the insert sequence, 69 base pairs downstream from the 5' end. This results in a fragment of 1740 bp, and the plasmid with the remaining fragment of the gene has a size of approximately 7450 bp. Lane 1: 1 kB DNA ladder. Lane 2: Restriction digest containing DNA fragments of predicted size.

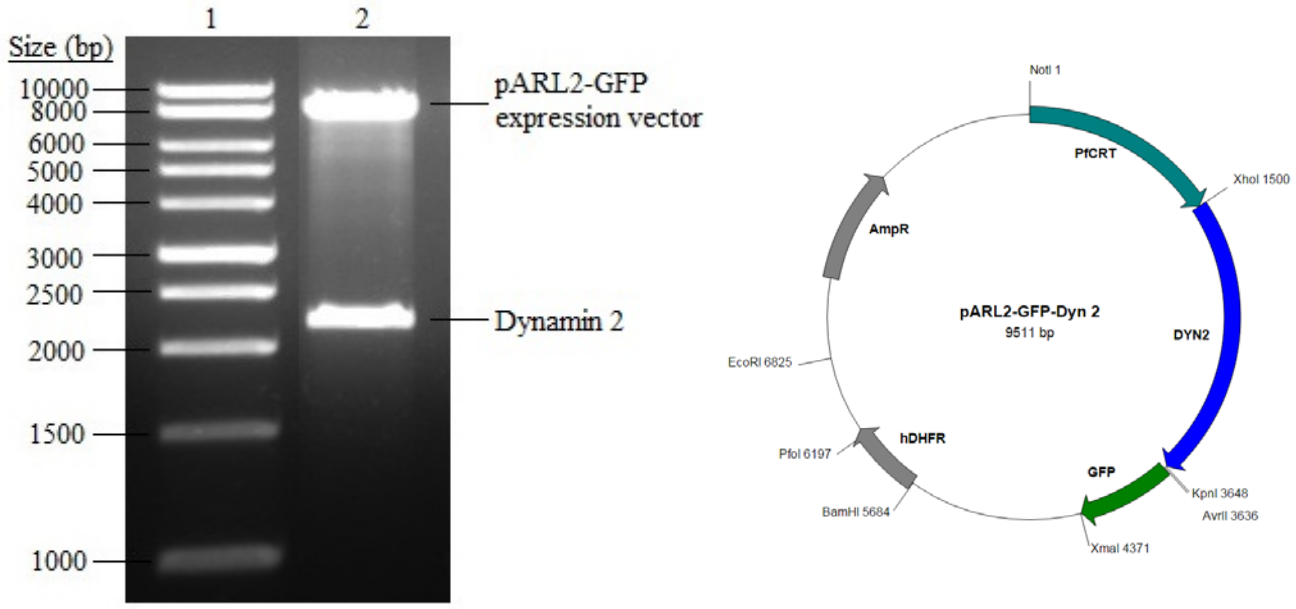

Figure 11. Restriction digest analysis of pARL2-GFP-Dynamin 2 expression vector.

0.8% agarose gel showing the dynamin 2 gene excised from the pARL2-GFP expression vector. The plasmid was digested with the restriction enzymes *Xho*I and *Avr*II. The restriction sites for *Xho*I and *Avr*II are found at the 5' and 3' end of the insert sequence respectively. This results in a fragment of 2130 bp, and the plasmid backbone has a size of approximately 7381 bp. Lane 1: 1 kB DNA ladder. Lane 2: Restriction digest containing DNA fragments of predicted size.

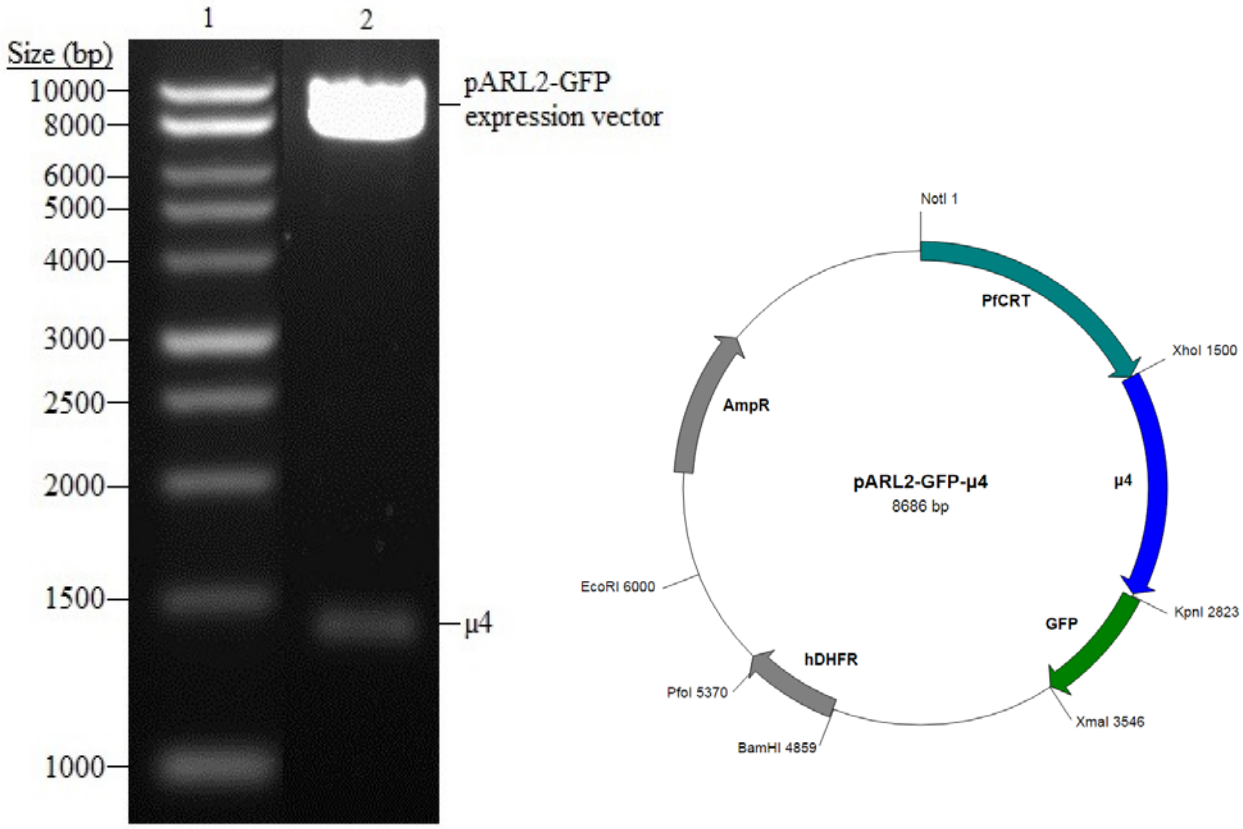

Figure 12. Restriction digest analysis of pARL2-GFP-μ4 expression vector.

0.8% agarose gel showing μ4 gene excised from the pARL2-GFP expression vector. The plasmid was digested with the restriction enzymes *Xho*I and *Kpn*I. The restriction sites for *Xho*I and *Kpn*I are found at the 5' and 3' end of the insert sequence respectively. This results in a fragment of 1311 bp, and the plasmid backbone has a size of approximately 7375 bp. Lane 1: 1 kB DNA ladder. Lane 2: Restriction digest containing DNA fragments of predicted size.

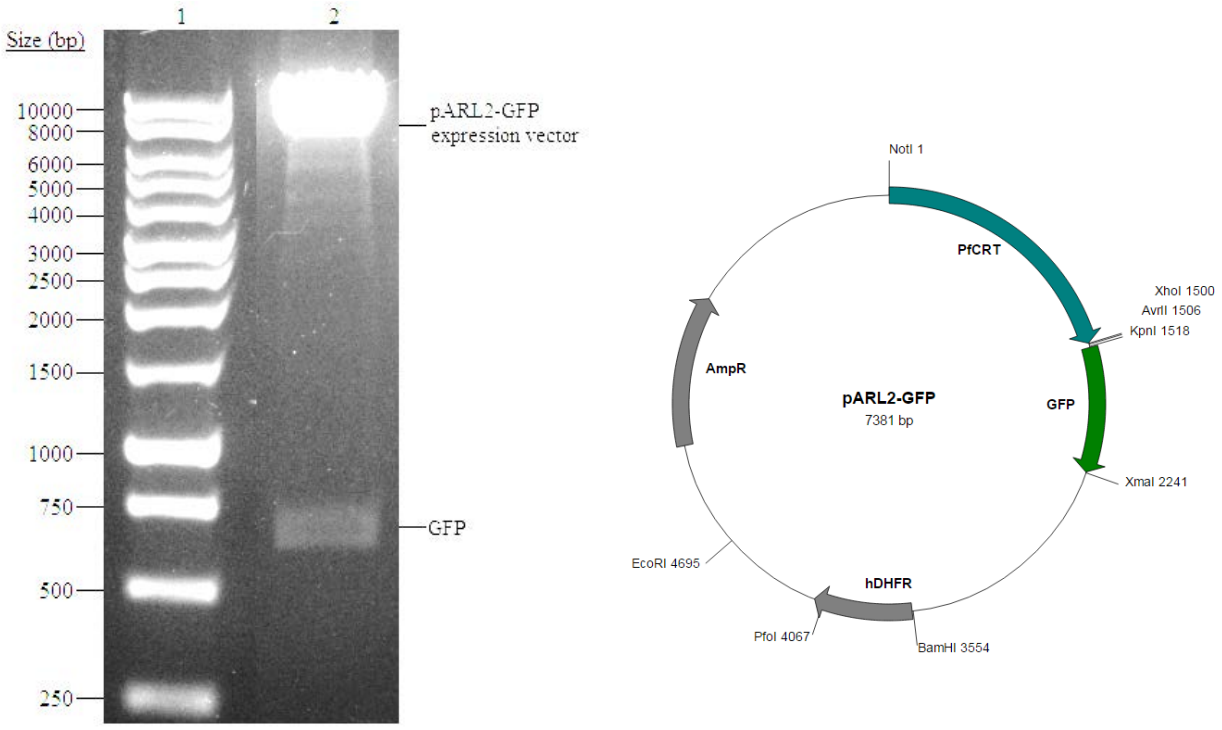

Figure 13. Restriction digest analysis of pARL2-GFP expression vector.

0.8% agarose gel showing the excised GFP coding sequence from the pARL2-GFP expression vector. The plasmid was digested with the restriction enzymes *Kpn*I and *Xma*I. The restriction sites for *Kpn*I and *Xma*I are found at the 5' and 3' end of the insert sequence respectively. This results in a fragment of 717 bp, and the plasmid backbone has a size of approximately 6664 bp. Lane 1: 1 kB DNA ladder. Lane 2: Restriction digest containing DNA fragments of predicted size.

3.2.6. Resultant pARL2-GFP P. falciparum expression plasmids

Once the pARL2-GFP expression vectors were prepared and the success of cloning determined based on the restriction digest patterns on agarose gels matching the predicted sizes, the plasmids were purified using a QIAfilter MaxiPrep kit and sequenced by Inqaba Biotech to confirm the inserts were successfully cloned, in the correct orientation, in frame and with no mutations (Appendix B). The high quantities of plasmid purified using the plasmid MaxiPrep kit (above 100 μg) was also required in order to perform the transfection reactions.

3.2.7. Transfection of P. falciparum parasites using the red blood cell preloading method

Uninfected RBCs were transfected with the high concentration, high purity expression vectors by electroporation. Pre-loaded RBCs were added to high parasitaemia, enriched trophozoite/schizont stage parasites. These transfected cultures were kept under selective drug pressure using RPMI 1640 media supplemented with WR99210 (antifolate inhibitor). Parasites that have successfully taken up the plasmids become resistant to the selection drug, due to the hDHFR gene expressed by the pARL2-GFP plasmid. Therefore, the successfully transfected parasites grow under constant drug pressure, while those parasites that have not, are cleared by the drug pressure. On average it took 3 weeks for transfected parasites to start to appear in culture, and 5 to 6 weeks for parasitaemia to reach high enough levels to allow for Western blot analysis and fluorescence microscopy.

3.2.8. Confirmation of expression by Western blotting

In order to confirm that the full-length GFP-tagged fusion proteins were being expressed in successfully transfected parasite cell lines, Western blotting was performed. High parasitaemia trophozoite /schizont stage parasites were released from infected RBCs by saponin lysis, and the parasite lysates were run on SDS-PAGE gels. Separated proteins were transferred to Hybond-ECL membrane by transblotting and incubated with commercially available mouse anti-GFP antibodies, followed by peroxidase-conjugated anti-mouse antibodies. Signals were detected

using a chemiluminescent peroxidase substrate. As can be seen below in Figure 14, Figure 15, Figure 16 and Figure 17, anti-GFP antibodies recognised specific proteins for control GFP, coronin-GFP, dynamin 2-GFP and μ4-GFP of sizes approximately 28 kDa, 100 kDa, 110 kDa and 75 kDa respectively. A comparison of the predicted protein sizes based on PlasmoDB predictions with the protein size observations from Western blotting can be found in Table 4. This table shows that the sizes predicted from the Western blotting correlates with the sizes predicted by PlasmoDB.

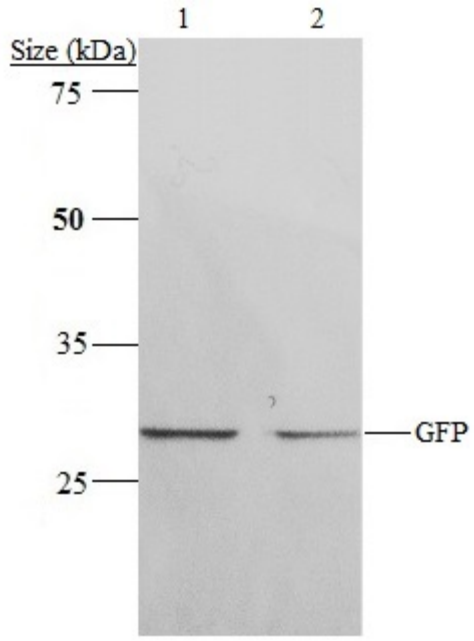

Figure 14. Western blot of *P. falciparum* parasite lysate transfected with pARL2-GFP using commercial mouse anti-GFP antibodies. Lanes 1 and 2 were loaded with the same lysates, with twice as much sample loaded into Lane 1.

Anti-GFP antibodies recognise a protein with an apparent molecular weight of approximately 28 kDa. NCBI protein prediction suggests that green fluorescent protein should have a size of 26.9 kDa.

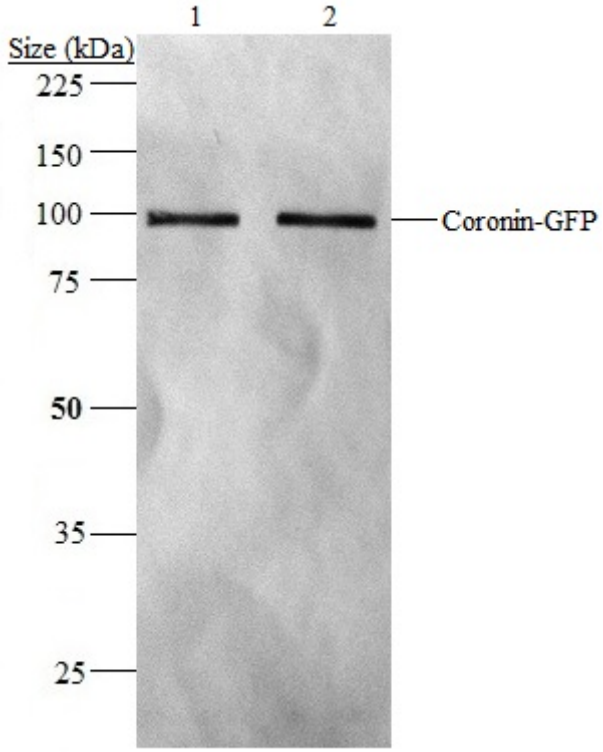

Figure 15. Western blot of *P. falciparum* parasite lysate transfected with pARL2-GFP-coronin using commercial mouse anti-GFP antibodies. Lanes 1 and 2 were loaded with equal amounts of lysate.

Anti-GFP antibodies recognise a GFP-tagged fusion protein with an apparent molecular weight of approximately 100 kDa. PlasmoDB protein prediction suggests that coronin should have a size of 69.016 kDa; therefore coronin fused to GFP should have a size of 95.916 kDa.

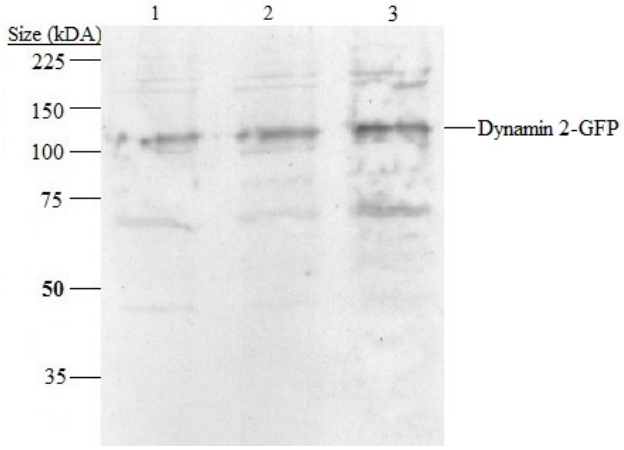

Figure 16. Western blot of *P. falciparum* parasite lysate transfected with pARL2-GFP-dynamin2 using commercial mouse anti-GFP antibodies. Lanes 1 to 3 were loaded with the same sample at increasing concentrations.

Anti-GFP antibodies recognise a GFP-tagged fusion protein with an apparent molecular weight of approximately 110 kDa. PlasmoDB protein prediction suggests that dynamin 2 should have a size of 69.016 kDa; therefore dynamin 2 fused to GFP should have a size of 108.427 kDa.

The source(s) of the additional faint bands are not clear. Lower molecular weight bands may represent proteolytic fragments of *Pf*DYN2-GFP. As mentioned in Chapter 1, dynamin and dynamin-like proteins form homo-oligomers that would have a higher mw than 110 kDa, but it is unlikely that they would remain intact under denaturing SDS-PAGE conditions. Longer incubations times were required to detect the *Pf*DYN2-GFP (possibly due to lower expression levels), which increases the possibility of non-specific binding of the antibodies to other parasite proteins.

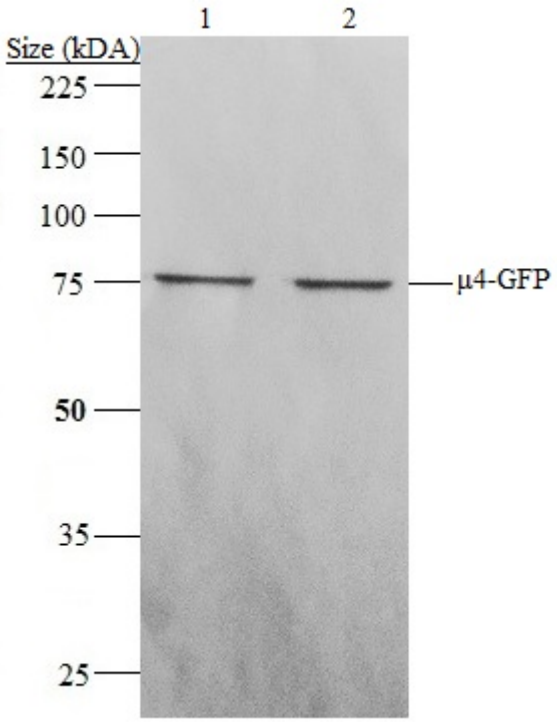

Figure 17. Western blot *P. falciparum* parasite lysate transfected with pARL2-GFP-µ4 using commercial mouse anti-GFP antibodies. Lanes 1 and 2 were loaded with an equal amount of lysate.

Anti-GFP antibodies recognise a GFP-tagged fusion protein with an apparent molecular weight of approximately 75 kDa. PlasmoDB protein prediction suggests that µ4 should have a size of 51.137 kDa; therefore µ4 fused to GFP should have a size of 78.037 kDa.

Table 4. Molecular weight values of GFP-tagged fusion proteins

The apparent molecular mass values estimated by Western blotting with anti-GFP antibodies and the molecular weight values predicted by PlasmoDB.

	Molecular weight values	
	Western Blotting (kDa) (Approximate)	Calculated (kDa)
GFP	28	26.9
Coronin-GFP	100	95.916
Dynamin2-GFP	110	108.427
μ4-GFP	75	78.037

3.3. Discussion

3.3.1. Sequence alignments

Coronin, dynamin 2 and μ4 homologues of *P. falciparum* were selected based on the close sequence homology to the mammalian versions. The identification and characterisation of these homologues is important as these homologues (or variants thereof) have been shown in mammalian cells to be involved in the endocytic process.

3.3.1.1. Coronin

P. falciparum coronin has a 27% amino acid identity and 51% similarity to coronin 1A over the 461 amino acid length of the human sequence. There is, however, an additional 120 amino acid extension at the C-terminal end of the parasite sequence. This region contains highly polar amino acid repeats consisting of aspartic acid, glutamic acid and asparagine. Interestingly, the arginine at position 30 of the human sequence which is critical for binding F-actin in Type I coronin (Cai *et al*. 2007; Chan *et al*. 2011; Gandhi *et al*. 2010), is conserved in the parasite sequence.

The random expansion of large amino acid repeats in the proteome of an organism is disfavoured. While the effects of these repeats on the structure of the host organism protein depends on the amino acid composition, the low complexity repeat regions tend to form loops or disordered structures (Muralidharan & Goldberg 2013). While most sequenced genomes have been shown to have a low abundance of amino acid repeats, *P. falciparum* proteins (along with *D. discoideum*) have a high abundance of amino acid repeats. In the *P. falciparum* proteome, approximately 30% of proteins contain amino acid repeats, primarily composed of asparagine residues (Singh *et al*. 2004). The asparagine-rich, low complexity regions are found in all protein families in all life stages of *P. 0*, and interestingly, these asparagine repeats are uncommon in other *Plasmodium* species (Muralidharan & Goldberg 2013).

The consequence of these large regions of asparagine repeats causes proteins to have a tendency to form insoluble aggregates (Halfmann *et al*. 2011). Formation of these insoluble aggregations does not have a deleterious effect in all cases. In fact, such protein aggregates have been shown to be important for mediating the inheritance of several phenotypes in yeast, antiviral innate

immunity and persistence of synaptic facilitation in mammals (Patino *et al*. 1996; Hou *et al*. 2011; Si *et al*. 2010). The effects of these aggregations can however be harmful. For example, the unregulated aggregation of proteins has been associated with various neurodegenerative diseases (Muralidharan & Goldberg 2013). In light of this data, it is still very interesting that *P. falciparum* has asparagine repeat sequences in 20-30% of all its proteins.

It would be assumed that *P. falciparum* has an abundance of these proteins containing asparagine repeats because it has a selective advantage or a function that these repeats provide. A number of hypotheses have been posed: asparagine repeats act as tRNA sponges, they have a role in immune response evasion and antigenic variation, and/or a role in protein-protein interactions (Muralidharan & Goldberg 2013). The challenge in finding a functional answer is highly unlikely since these repeats are present in all protein families, and involved in all metabolic pathways. If for example asparagine repeats had a specific function in a pathway, the asparagine repeats would be enriched specifically in that pathway (Muralidharan & Goldberg 2013). How the presence of asparagine and acidic amino acid repeats pertains to coronin function is not clear at present.

3.3.1.2. Dynamin 2

Human and *P. falciparum* dynamin 2 homologues were aligned to illustrate the similarities in the amino acid sequence of the two proteins and the regions that are evolutionarily conserved. Human dynamin contains five domains. These domains are labelled in Figure 4 as follows, (I) N-terminal GTPase domain (residues 1-299, shown as red and underlined). This domain induces the conformational changes that mediate vesicle fission by binding and hydrolyzing GTP. (II) Middle domain (residues 300-520, shown as light purple). (III) Pleckstrin homology (PH) domain (residues 521-622, shown as yellow and underlined), which binds to phosphorylated phosphatidylinositol lipids in the plasma membrane. (IV) GTPase effector domain (residues 623-745, shown as blue), which facilitates self-assembly of dynamin and stimulates GTP hydrolysis by the GTPase domain. (V) Proline-rich domain (PRD) (residues 746-866, shown as dark purple and underlined) which interacts with SH3 domains of accessory proteins (Hinshaw 2000).

The sequence alignment shows that the *P. falciparum* sequence displays a strong level of homology to the GTPase domain of the human counterpart (44% amino acid identity, and 66% similarity across this domain). The G1- G4 consensus motifs are also highly conserved in the parasite sequence (highlighted by the blue boxes in the alignment) - these consensus motifs are critical for GTP binding in dynamin (Praefcke & McMahon 2004). These motifs are: GxxxxGKS/T (residues 38-45 in the human sequence), T (residue 65), DxxG (136-139), and TKxD (205-208). This data suggests that the *P. falciparum* dynamin 2 protein displays prototypical dynamin-like GTPase activity. It must be noted, however, as is apparent from the alignment, the level of homology starts to decline over the remainder of the protein sequence. The middle domain has 29% identity and 46% similarity to the human sequence. The pleckstrin homology domain has 7% identity and 38% similarity, and the GTPase effector domain (GED) has 26% identity and 56% similarity to the human sequence. While this decline in homology is clear, the three amino acid residues that have been shown to be vital for the function of the GED in human dynamin 1 protein (Sever *et al*. 1999): K684, R715 and R720 (highlighted in green in the alignment) are semi-conserved in the parasite sequence. In the parasite sequence they are represented by R654, R684 and K689, respectively. The C-terminal proline-rich domain that binds SH-3 binding domain is absent from the parasite sequence.

The lack of the C-terminal domain as well as the use of an alternative lipid-binding domain in place of the pleckstrin homology domain is a feature of other dynamin-like proteins (Dlps) (Praefcke & McMahon 2004). These alterations do not necessarily compromise the ability of the *P. falciparum* dynamin 2 to mediate endocytic vesicle fission like its human counterpart. For example, the *D. discoideum* dynamin A lacks the PRD, and has an alternative sequence in the PH domain (here it has a glutamine-rich domain), but it is reported to function in endocytosis, cytokinesis and organelle morphology (Praefcke & McMahon 2004). Although Dlps are implicated in other cellular roles such as mitochondrial fission and cytokinesis (Konopka *et al*. 2006), the endocytic function of *D. discoideum* dynamin A and the lack of a *P. falciparum* dynamin homologue with an intact PRD and PH domain maintains the possibility that *P. falciparum* dynamin 2 is involved in endocytosis. Exploring this possibility is motivation to include dynamin 2 as a part of this study.

3.3.1.3. μ4 adaptin

The *P. falciparum* μ4 adaptin sequence shows a 30% amino acid identity and 59% similarity to its human counterpart over the entire length of the 436 amino acid sequence. The main function of the μ chain in their respective adaptor complexes is to trap and concentrate transmembrane cargo proteins in budding transport vesicles. They do this by recognizing amino acid motifs within the cytoplasmic tails of the cargo proteins, notably tyrosine motifs with a YXXϕ consensus sequence (ϕ refers to a bulky hydrophobic amino acid) (Canagarajah *et al*. 2013). The regions of the human μ4 sequence implicated in interacting with the tyrosine motifs are highlighted in green in Figure 5. The regions are: VFLD (residues 187-190 in the human sequence), K (residue 217), VRFL (residues 421-424) and KWVR (residues 438-441). These regions and the flanking amino acids are highly conserved in the *P. falciparum* sequence. These are highlighted in blue. The regions are: IFID (residues 179-182 in the *P. falciparum* sequence), K (residue 209), IKYL (residues 404-407) and RWVR (residues 420-423).

Extensive tyrosine motif-based sorting of cargo proteins has previously been demonstrated in apicomplexan parasites, such as *Toxoplasma gondii* (Hoppe & Joiner 2000). However, this has not been demonstrated in malaria parasites to date. The conservation of these regions in the *P. falciparum* μ4 sequence is nonetheless highly suggestive that tyrosine motif sorting of transmembrane cargo proteins is a feature of protein trafficking in the parasite and a function of the μ4 homologue.

3.3.2. Molecular cloning

As was described earlier, the coding sequences for these proteins of interest were successfully cloned using the pGEM-T Easy cloning vector system, and subcloned into the parasite expression vector, pARL2-GFP. Whilst this was finally achieved, the technique was fraught with difficulties and challenges. Cloning into the pGEM-T Easy vector was challenging on multiple occasions since it is possible for the cloning vector to lose the 3'-thymidine overhangs during storage, which meant that TA cloning was not possible and resulted in large numbers of background colonies due to re-circularization of the blunt-ended plasmids during ligation. Another challenge that was encountered was the formation of plasmid concatemers, - this is when multiple copies of the same DNA fragment are linked together. This occurred when multiple pGEM-T Easy plasmids were ligated to each other - likely due to ligation of blunt-ended plasmids that had lost the 3' overhangs as well as one copy of the insert. This resulted in unusual restriction digests patterns on agarose gels. In order to circumvent these issues, fresh pGEM-T Easy vector systems were required.

An additional solution to this issue would be to use a direct cloning method. In this method, PCR products would be digested with restriction enzymes, purified and cloned directly into the pARL2-GFP expression vector. Whilst this approach could prove successful, it isn't free of challenges. Restriction digests of restriction sites at the extreme ends of DNA fragments (PCR products in this case) may be less efficient, and the larger size of the pARL2-GFP vector (7381 bp, compared to 3015 bp for pGEM-T Easy) reduces transformation efficiency. Once inserts were successfully cloned into pGEM-T Easy vector, it meant that a renewable repository of the gene sequences could be stored as frozen transformed *E. coli* glycerol stocks.

After isolating the final pARL2-GFP recombinant plasmids in large volumes at a high concentration and purity, *P. falciparum* parasites were transfected with the expression vectors in order to generate transgenic parasite cells lines expressing full-length GFP-tagged fusion proteins using the RBC preloading method. Transgenic parasites were obtained 3 weeks after transfection, and took 5 to 6 weeks until parasite cultures reached a high enough parasitaemia to allow for western blotting and fluorescence microscopy. The fact that transgenic parasites were obtained in 3 to 6 weeks suggests that the modified electroporation protocol used is efficient for

transfections, and more significantly, that the overexpression of these GFP-tagged fusion proteins doesn't appear affect parasite viability.

Parasite lysates were prepared from a mixture of high parasitaemia trophozoite and schizont stage transfected parasites and analysed by Western blotting with anti-GFP antibodies. It confirmed that the full-length GFP-tagged fusion proteins are expressed. This suggests that gene transcription and translation accurately starts at the appropriate start codon and is not terminated prematurely. In addition to successful expression, there is no excessive proteolytic breakdown/truncation or turnover of the fusion proteins. The data is also encouraging because it suggests that the recombinant proteins are not inhibitory to parasite growth and transfectants weren't obtained due to plasmid re-arrangements that kept the hDHFR resistance cassette intact, but compromised the fusion protein expression region.

Now that transgenic parasite cell lines had been successfully produced, and it was confirmed that the full-length GFP-tagged fusion constructs were been expressed, it was possible to move onto the next step of the project: attempting to localize these proteins in live parasites using fluorescence and confocal microscopy.

CHAPTER FOUR: LOCALIZATION OF CANDIDATE ENDOCYTOSIS PROTEINS

4.1. Introduction

Coronin proteins are a family of highly conserved actin cytoskeleton regulators that have been shown to promote cell motility and modulate other actin-dependant process (Gandhi *et al*. 2010). *D. discoideum* coronin has been shown to be involved in phagocytosis, as well as cell locomotion, fluid-phase uptake and cytokinesis (Ishikawa-Ankerhold *et al*. 2010). The involvement in phagocytosis was the motivation to include coronin in this study, as an endocytosis candidate protein.

Dynamin proteins are a group of conserved large GTPase proteins that are found in many eukaryotic cell systems (Gaechter *et al*. 2008). Dynamin has been implicated in a variety of processes including the budding of transport vesicles, endocytosis, cytokinesis, pathogen resistance and the division of organelles (Praefcke & McMahon 2004; Zhou *et al*. 2009). Members of the dynamin superfamily are broadly divided into classical dynamins and dynamin-related or dynamin-like proteins (DRPs or DLPs). The most celebrated function of dynamin is its involvement in clathrin-mediated endocytosis. Dynamin is recruited to the plasma membrane during the early stages of endocytosis at clathrin-coated invaginations. Dynamin then self-assembles into rings at the necks of the invagination buds that become stacked and interconnected (Bottomley *et al*. 1999). The GTPase activity of dynamin drives the "pinchase" activity of these rings to pinch off the clathrin-coated vesicles (Hinshaw & Schmid 1995).

Adaptor proteins (AP) are a group of five closely related heterotetrameric complex that have been shown to have important functions in vesicle trafficking. They are made up of two large chains, one medium chain (μ) and one small chain (Hirst *et al*. 2013). The medium adpator protein chain of the AP-4 complex μ4 was selected for this study. AP-4 is widely expressed in mammalian tissues and is known to associate with the cellular membrane as a peripheral membrane protein. *Pf*μ4 has a high sequence homology to its human counterpart over the entire length of the 436 amino acid sequence. Medium chain adaptor proteins are known to trap and

concentrate transmembrane cargo proteins in budding transport vesicles by recognising amino acid motifs within the cytoplasmic tails of cargo proteins (Kibria *et al*. 2015).

Aims and Objectives

In the previous chapter, the expression of full-length GFP tagged fusion proteins in *P. falciparum* parasites was confirmed by Western blotting.

The aim of this section was to attempt to localize the GFP tagged fusion proteins in transfected *P. falciparum* parasites by fluorescence and confocal microscopy.

4.2. Results

4.2.1. Fluorescence microscopy analysis of transgenic parasites

Live *P. falciparum* parasites transfected with the pARL2-GFP, pARL2-GFP-coronin, pARL2-GFP-dynamin 2, and pARL2-GFP-μ4 vectors were stained with the nuclear stain DAPI, and visualized by fluorescence microscopy to determine the sub-cellular localization of these fluorescently tagged proteins. After DAPI staining, a small amount of packed red blood cells (RBCs) were pipetted onto a microscope slide, and covered with a glass cover slip. These slides were viewed using fluorescence microscopy, or confocal microscopy under oil immersion.

In most cases, single representative parasites were visible in the Bright Field panels (Bright Field was used in fluorescence microscopy and photomultiplier tube (PMT) during confocal microscopy). The surrounding erythrocyte was still visible as the parasites were not saponin lysed prior to viewing. The presence and localization of the food vacuole could be determined based on the position of the haemozoin crystal, which is prominent in the Bright Field panels. The same region can be inferred in the fluorescence images by the absence of fluorescence. The parasite nuclei were visible by blue fluorescence during UV illumination due to the DAPI staining which was performed prior to viewing the parasites.

A number of controls were used before attempting to localize the endocytosis candidate proteins. Wild-type *P. falciparum* 3D7 parasites not expressing any transgenic proteins or GFP were stained with DAPI and viewed using fluorescence microscopy. WT parasites not containing any construct showed no green or red auto-fluorescence, while staining of the nucleus was observed due to DAPI staining. These experiments also confirmed the absence of fluorescence bleed-through between channels.

In addition to the parasite cell lines transfected with a vector to express a GFP-tagged fusion protein, a cell line was generated where *P. falciparum* 3D7 parasites were transfected with pARL2-GFP. This generates a transgenic parasite line expressing GFP alone in order to investigate whether the fluorescent protein itself displays any preferential sub-cellular localization. This cell line was also used to ascertain that expressing GFP in these parasites did

not affect cell growth, and that the parasites survive, progress through the various life stages as expected, and multiply.

4.2.1.1. Localization of pARL2-GFP in transfected parasites

Parasites transfected with pARL2-GFP were used as a control. This was to ensure that localization of the GFP-tagged fusion proteins was not caused by the GFP-tag, but by the protein of interest itself. The sub-cellular localization of GFP was determined by confocal microscopy.

Figure 18, panel A and B show a single parasite in the trophozoite and schizont stage of the life cycle, respectively, viewed by confocal microscopy. In both instances, no distinct localization of GFP was observed. Instead, GFP was diffuse and appeared to be cytoplasmic in location. In addition, diffuse DAPI staining throughout the nucleus was also apparent. This information would lead one to make the assumption that the GFP is not localizing to any discreet regions in the parasite and, consequently, that alternative localization patterns seen with fusion proteins would be due to the proteins of interest.

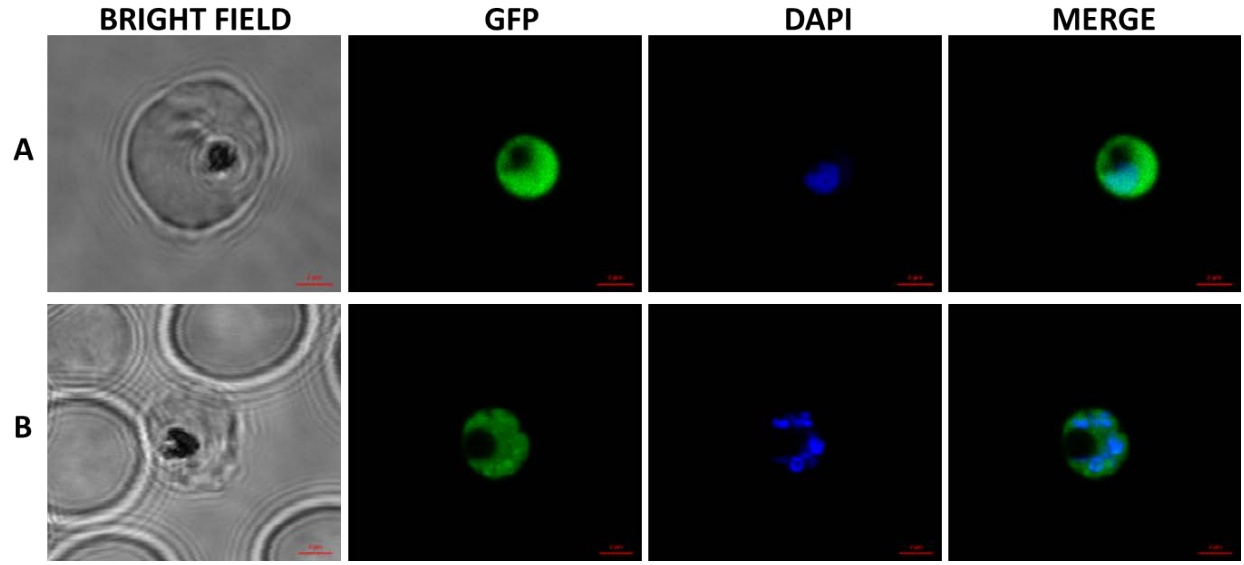

Figure 18. Confocal microscopy images of *P. falciparum* parasites expressing pARL2-GFP (control).

Confocal micrograph depicts the intracellular localization pattern for GFP in the parasite. The panels depict the fluorescence image (green) with the corresponding bright field image and the DAPI stained nuclei (blue). The merged image shows the area of overlap between the green and blue signals. **A** depicts a trophozoite stage parasite; and **B** depicts a schizont stage parasite. The red scale bar indicates 2 µm.

4.2.1.2. Localization of pARL2-GFP-coronin in transfected parasites

As was observed in the previous section with GFP alone, GFP-coronin did not localize to any discreet sub-cellular location in the trophozoite stage of the malaria parasite. (Figure 19A), but instead, displayed diffuse cytoplasmic/nuclear localization.

Figure 19, panels B, C, and D display multi-nucleated parasites in the schizont stage. A localization pattern distinct from that observed with GFP alone is clearly discernible, and the pattern was observed in all schizont stage parasites containing pARL2-GFP-coronin. Based on the patterns observed, the GFP-tagged coronin fusion protein appears to localize in discreet rings around individual nuclei in the parasite, most likely to the periphery of forming merozoites. The coronin could potentially be co-localizing with proteins of the inner membrane complex (IMC), as the localization patterns appear to be similar to what is observed with other proteins known to localize to the IMC (such as GAP45) (Kono *et al*. 2012).

The IMC has three major roles in apicomplexan parasites. It functions to confer stability and shape to the cell, it is important in the scaffolding compartment during the formation of daughter cells, and it has a major role in motility and invasion (Frénal *et al*. 2010; Gaskins *et al*. 2004; Kono *et al*. 2012; Tremp *et al*. 2008; Tremp & Dessens 2011). Coronin localization to the IMC could imply involvement in some of these roles that the IMC is known to be implicated in.

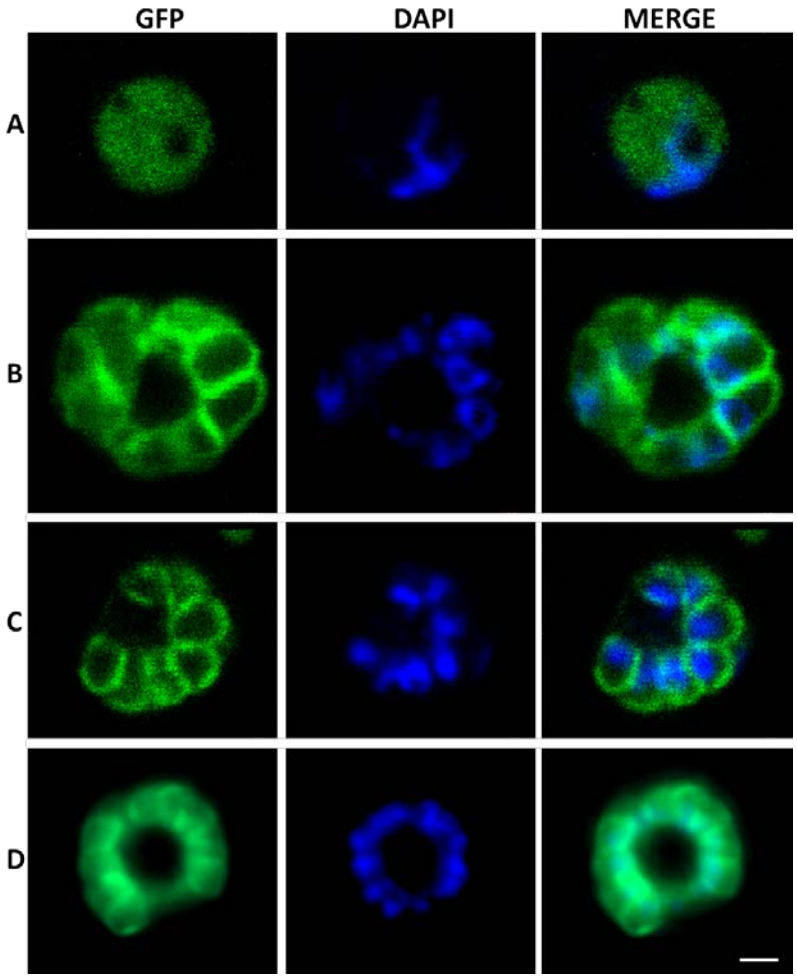

Figure 19. Fluorescence and Confocal microscopy images of *P. falciparum* parasites expressing pARL2-GFP-coronin.

Confocal micrograph depicts intracellular localization pattern for GFP in the parasite. The panels depict the fluorescence image (green) with the DAPI stained nuclei (blue). The merged image shows the area of overlap between the green and blue signals. Panel **A** depicts a trophozoite stage parasite; Panels **B**, **C** and **D** depict schizont stage parasites. Scale bar indicates 2 μM.

Figure 20 below shows an additional schizont in panel A clearly showing coronin localization around each nucleus in the multi-nucleated parasite. This further emphasizes the observed localization pattern of coronin, which was observed in all schizont stage parasites that were viewed by confocal or fluorescence microscopy. Localization was always distinct and bright, implying high expression levels of the coronin-GFP fusion protein.

Panels B and C in Figure 20 show confocal micrographs of the same parasite. The images in panel C were taken 5 minutes after those in panel B. The coronin localization in this late-schizont can be seen in the GFP and merge images, and as was previously observed, localization to regions around the nuclei is clearly visible. Following a 5 minute incubation at 37 °C in the heated chamber of the microscope assembly, the micrographs shown in panel C were taken. This is the resultant image after the RBC has lysed, releasing the daughter merozoites. The merge image clearly shows the daughter merozoites, it can be seen that the coronin-GFP is located at the membrane of these daughter merozoites, supporting the hypothesis that coronin could be involved in merozoite motility, and potentially the merozoite invasion of RBCs.

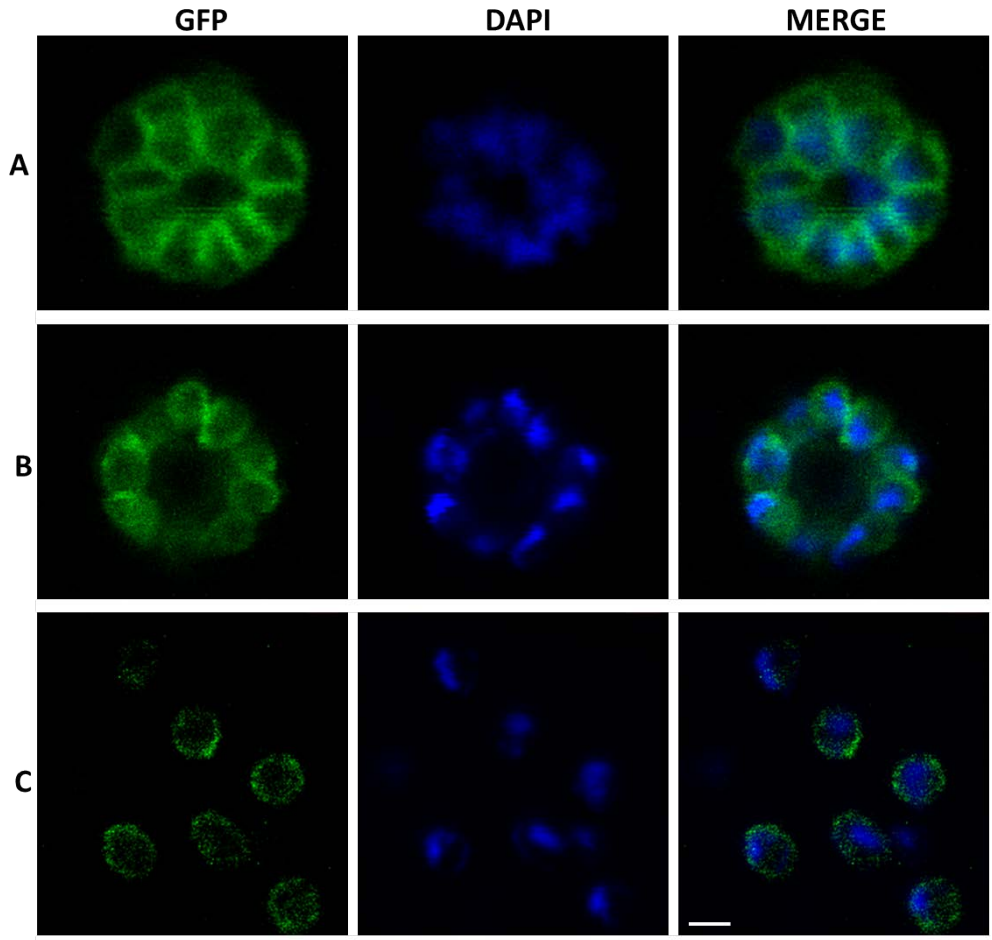

Figure 20. Confocal microscopy images of *P. falciparum* parasites expressing pARL2-GFP-coronin.

Confocal micrograph depicts intracellular localization pattern for GFP in the parasite. The panels depict the GFP fluorescence image (green) with the corresponding DAPI stained nuclei (blue). The merged image shows the area of overlap between the green and blue signals. Panels **A** and **B** depict schizont stage parasites, Panel **C** depicts free merozoites after lysis from the host RBC. Scale bar indicates 2 μM.

4.2.1.3. Localization of pARL2-GFP-dynamin2

Figure 21 depicts individual trophozoite and schizont stage parasites as bright field, GFP, DAPI and merge images. Red arrows are used to indicate areas where GFP was concentrated at the plasma membrane of the parasite. Blue arrows are used to indicate instances where GFP was concentrated at discreet punctuate regions within the parasite cytoplasm. White arrows are used to indicate instances where GFP was localization at the food vacuole/digestive vacuole.

Based on the GFP signals in trophozoite stage parasites containing pARL2-GFP-dynamin2 it would appear that dynamin localizes to the periphery of the parasites, potentially localizing to the parasite plasma membrane. These specific regions that the dynamin appears to localize to could be at sites of endocytosis, e.g. cytostomes. Panel A shows localization to the periphery of the parasite, as indicated by the red arrows. In this parasite, there also appears to be localization to discreet regions within the parasite cytoplasm (blue arrows). This localization could be at membrane bound organelles, such as the Golgi apparatus, endoplasmic reticulum or the apicoplast (Dourado *et al*. 2007).

Panels B and C show additional trophozoite stage parasites, with a number of discreet areas of GFP localization at the periphery of the parasite (as indicated by red arrows). There also appears to be areas of localization within the parasite cytoplasm (indicated by the blue arrows). In addition to these two areas of localization, there also appears to be punctuate regions of GFP localization at the food vacuole/digestive vacuole (indicated by white arrows). Panel D shows a schizont stage parasite with individual merozoites forming. Although there are areas of GFP punctate signals, a more precise localization is not discernible at present.

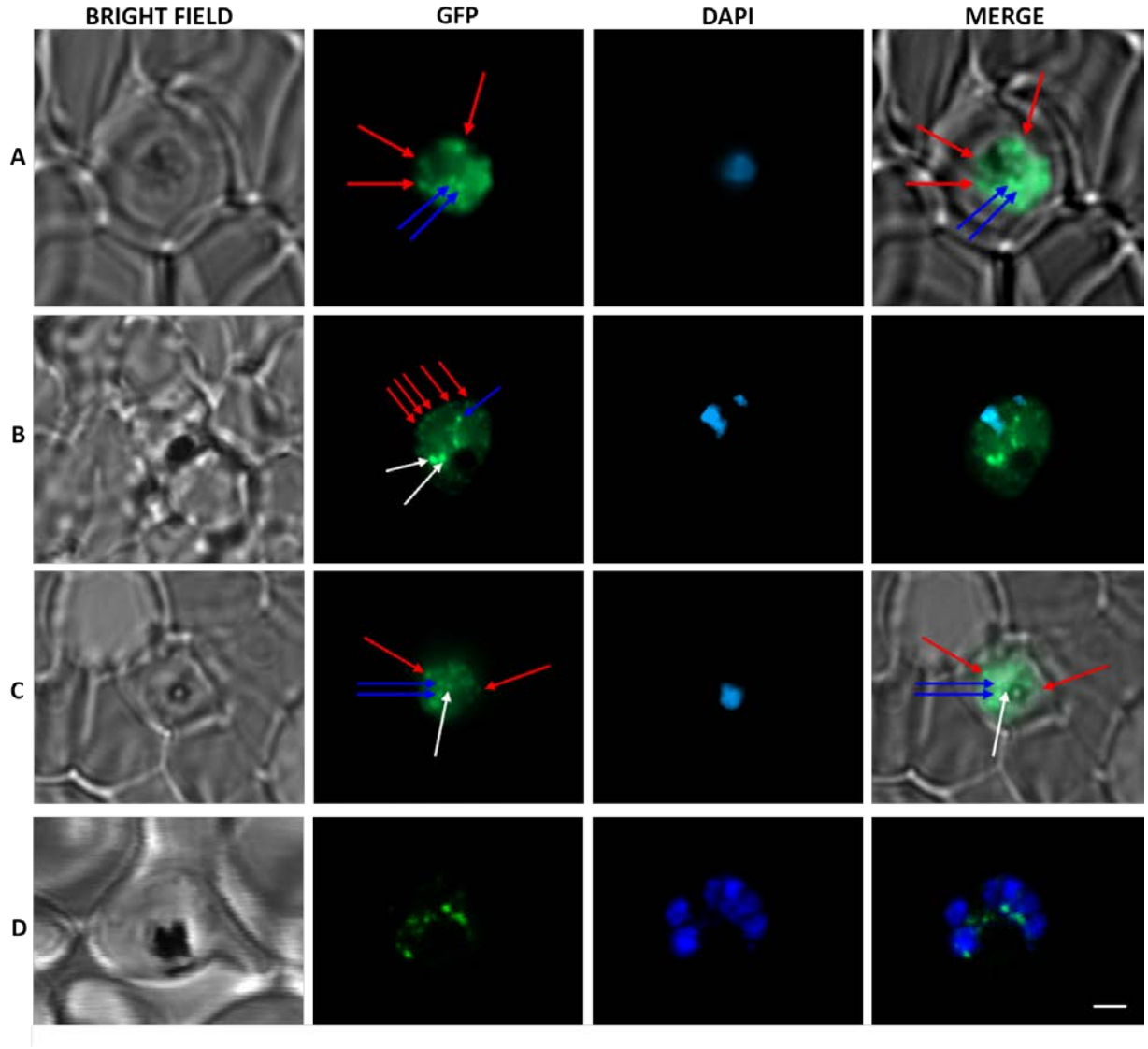

Figure 21. Fluorescence and confocal microscopy images of *P. falciparum* trophozoite and schizont stage parasites expressing pARL2-GFP-dynamin2.

Micrographs depict intracellular localization pattern for GFP in the parasite. The panels depict the fluorescence image (green) with the corresponding bright field image and the DAPI stained nuclei (blue). The merged image shows the area of overlap between the green and blue signals in panels **B** and **D**; green and bright field signals in panels **A** and **C**. Panels **A**, **B** and **C** were trophozoite stage parasites viewed by fluorescence microscopy, while panel **D** was a schizont stage parasite viewed by confocal microscopy. Red arrows indicate localization to the plasma membrane, blue arrows indicate localization to discreet locii in the parasite cytoplasm and white arrows indicated localization to the FV/DV. Scale bar indicates 2 μM.

4.2.1.4. Localization of pARL2-GFP-μ4

Figure 22 shows parasites containing pARL2-GFP-μ4. Two prominent patterns of μ4 adaptin localization were observed. As can be observed in Figure 22, the μ4 adaptin appeared to localize to specific regions along the parasite periphery in trophozoite stage parasites (indicated by red arrows). As observed in panels B and C, it appeared that the protein also localizes at, or near the food vacuole (indicated based on the proximity to the haemozoin crystal and by the white arrow). In addition to these specific regions of localization, there is also a large amount of cytoplasmic GFP signal observed. This was the case in the majority of the parasites containing pARL2-GFP-μ4. This is not surprising, given that adaptor proteins exist as a cytoplasmic pool that is transiently recruited to areas of vesicle budding (Dell'Angelica *et al*. 1999).

Panel D shows a multinucleated schizont stage parasite. The late schizont shows individual daughter merozoites (it appears that the parasite is on the verge of lysis from the RBC, and therefore, on the verge of the release of the daughter merozoites). There appears to be faint, but reasonably distinctive puncta near the periphery of each of these merozoites. However, as was previously mentioned for dynamin 2, a more precise conclusion on merozoite localization cannot be drawn at present.

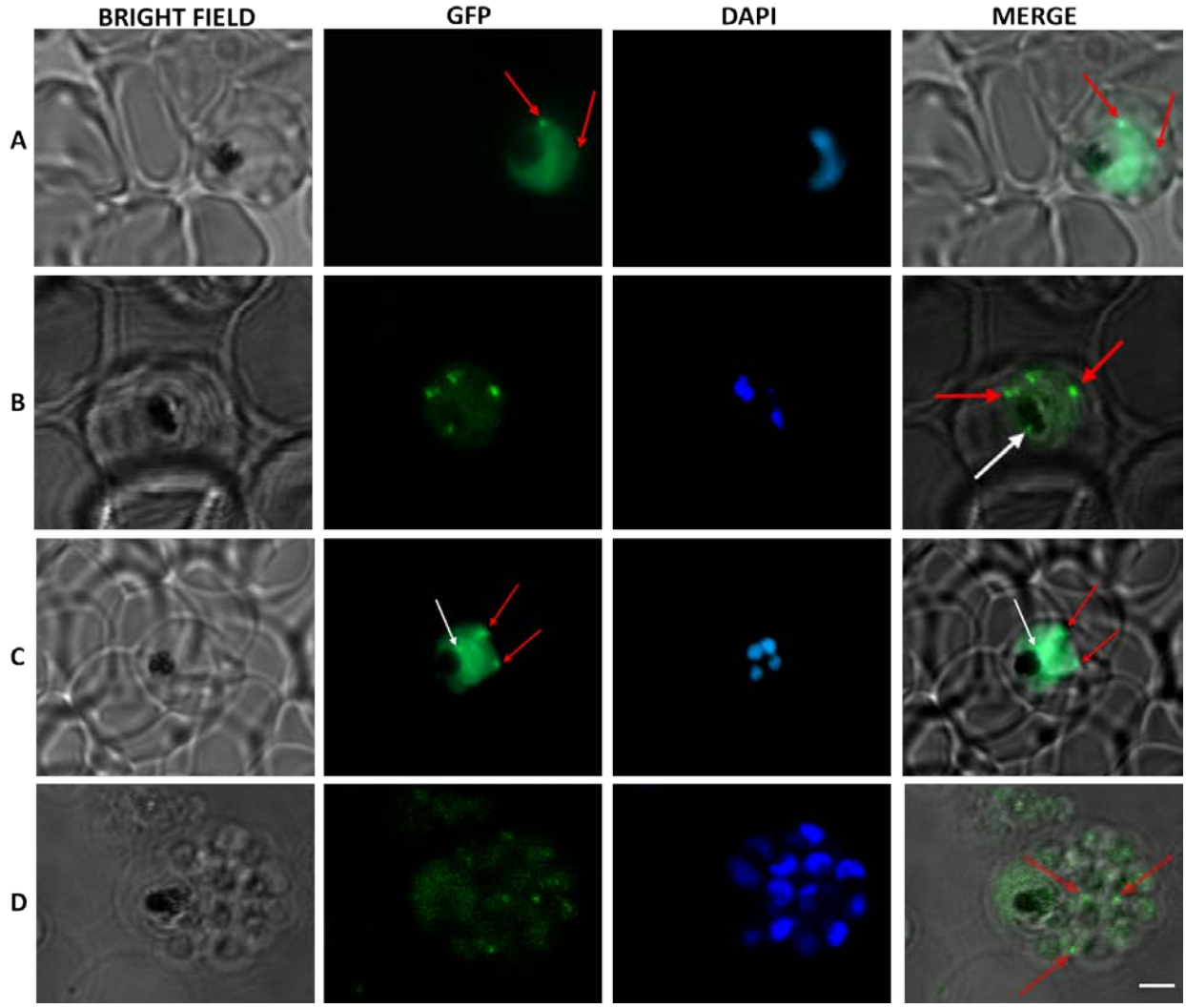

Figure 22. Fluorescence and confocal microscopy images of *P. falciparum* trophozoite and schizont stage parasites expressing pARL2-GFP-μ4.

Micrographs depict intracellular localization pattern for GFP in the parasite. The panels depict the fluorescence image (green) with the corresponding bright field image and the DAPI stained nuclei (blue). The merged image shows the area of overlap between green and bright field signals in panel **A**, viewed by fluorescence microscopy; and the green and bright field signals in panels **B**, **C** and **D**, viewed by confocal microscopy. Red arrows indicate localization to the plasma membrane; white arrows indicate localization to the FV/DV. Scale bar indicates 2 μM.

7.3. **Discussion**

Identifying and characterizing *P. falciparum* parasite homologues of genes potentially involved in endocytosis and other cellular events can provide valuable insight into the mechanisms the parasite uses in trafficking events. The proteins selected for this work were identified based on sequence homology to mammalian counterparts with known functionality. The parasite homologues of these proteins were expressed as GFP-tagged fusion proteins in blood stage parasites, and we attempted to localize these proteins by viewing live cells using fluorescence and confocal microscopy. The localization of these proteins within the parasite is a first step in identifying the functions of these proteins.

7.3.1. Coronin

One of the initial hypotheses was that coronin is involved in phagocytosis due to evidence in *D. discoideum* where coronin deficient mutants had a 60% decrease in phagocytic uptake levels (De Hostos *et al*. 1993). *P. falciparum* parasites digest more than 80% of the host erythrocyte haemoglobin to support parasite growth and asexual replication, and most of this occurs during the trophozoite stage (Lazarus *et al*. 2008). By exploring the localization of GFP-tagged coronin in transgenic parasites generated in this research, we aimed to investigate the possibility that coronin is involved in endocytosis in *P. falciparum* parasites. There was no distinct localization of coronin during the trophozoite stage of the parasite life cycle apart from a diffuse cytoplasmic/nuclear presence, while there was prominent distinct localization during schizont stages. Due to this lack of protein localization during the trophozoite stage when the parasite is most metabolically active, we were led to believe that the coronin protein we were working with is not involved in endocytosis.

Plasmodium species are members of the Alveolata, which is a group of unicellular eukaryotes which encompasses the traditional phyla of Ciliates, Dinoflagellates, and, important in this research, Apicomplexa. The inner membrane complex (IMC) is a defining characteristic of the Alveolata. This is a complex of membranous sacs underlying the plasma membrane that are connected to the cytoskeleton (Kono *et al*. 2012). This complex closely apposes the parasite plasma membrane (Frénal *et al*. 2010). The IMC has three major roles in apicomplexan

parasites. It functions to confer stability and shape to the cell, it is important in the scaffolding compartment during the formation of daughter cells, and it has a major role in motility and invasion (Frénal *et al*. 2010; Gaskins *et al*. 2004; Kono *et al*. 2012; Tremp *et al*. 2008; Tremp & Dessens 2011).

In terms of invasion of host cells, apicomplexans do not rely on endocytosis-based mechanisms to enter the host cells, as is the case for bacteria and other parasites. Instead, apicomplexans have developed a complex, efficient machinery that connects the receptor-ligand bridge with an actin-myosin motor inside the parasite (Baum *et al*. 2008). This substrate-dependent motility assists the parasite in actively penetrating and exiting host cells (Frénal *et al*. 2010). The gliding motility is powered by the actin-myosin motor, and requires the anchoring of a multi-protein complex known as the glideosome; this machinery allows the parasite to generate the necessary force for substrate-dependent gliding and invading (Baum *et al*. 2008; Frénal *et al*. 2010). The assembly of the glideosome is specifically coordinated in the narrow space between the plasma membrane and the IMC (Frénal *et al*. 2010). The glideosome is made up of class XIV myosin A, the associated myosin light chain, and two gliding-associated proteins; GAP45 and GAP50 (Frénal *et al*. 2010; Gaskins *et al*. 2004). According to Gaskins *et al*. (2004), both the myosin motor and actin have been shown to localize to the space between the IMC and the plasma membrane of *Plasmodium* and *Toxoplasma* parasites. The localization of actin to this space is therefore essential as actin polymerization is a critical requirement of gliding motility (Wetzel *et al*. 2003). Cytochalasin D (cytoD) prevents actin polymerization and promotes the depolymerization of existing actin filaments (Sampath & Pollard 1991). It has been shown in *Toxoplasma gondii* that cytoD blocks both parasite motility and host cell invasion (Wetzel *et al*. 2003).

During schizogony, replication of the parasite is initiated by DNA replication and mitosis, which results in a multinucleated schizont stage parasite (Bannister *et al*. 2000). The replication of organelles takes place within the cytoplasm, encapsulated by plasma membrane from the mother cell (Ridzuan *et al*. 2012). Once the parasite organelles have replicated, merozoites are pinched off from the schizont by the plasma membrane surrounding the individual merozoites (Bannister *et al*. 2000; Ridzuan *et al*. 2012). Based on the localization of GAP45 to the IMC, Ridzuan *et al*. (2012) suggest that formation of the inner membrane complex occurs simultaneously with

plasma membrane encapsulation of daughter merozoites. This supports the hypothesis that the IMC functions as a scaffolding compartment during the formation of daughter cells.

Live fluorescent imaging data for GFP-tagged coronin presented here shows that expression of the protein occurs throughout the parasitic life cycle (due to the use of the PfCRT promoter in the pARL2-GFP expression vector). However, during the trophozoite stage of the parasite life cycle, the localization of coronin is seen to be diffuse, and spread throughout the parasite cytoplasm. When schizogony occurs and the parasite progresses into the schizont stage of development, the localization becomes very distinct and clearly visible. Coronin appears to be located in complete rings around newly replicated nuclei in the fully segmented schizont. This contrasts the trophozoite stage parasites where fluorescence of GFP-coronin is evenly distributed throughout the parasite rather than in discrete foci, and there were no ring-like structures evident. The sub-cellular localization of GFP-tagged coronin in malaria parasites clearly resembles the published localization data of many IMC associated proteins, such as GAP45, GAP50, GAPM1 and GAPM2 (Bannister *et al*. 2000; Kono *et al*. 2012; Ridzuan *et al*. 2012).

Once the possibility arose that coronin was associated with the IMC (based on the preliminary data), we attempted to co-localize GFP-coronin with GAP45 fused to mCherry. The approach we took in cloning the GAP45 coding sequence was very important - it is preferential to insert the mCherry coding sequence within the coding sequence of GAP45. This is due to the presence of the 29 amino acids at the N-terminal domain, which contains two acylation sites that have been suggested to drive the localization of GAP45 to the IMC. The C-terminal of GAP45 contains important motifs that have been shown in *T. gondii* to be important in the binding of GAP45 to the motor complex (Johnson *et al*. 2007). They found that inserting a YFP tag to the C-terminus of *Tg*GAP45 eliminated its binding to the rest of the motor complex, and the only way they could circumvent this, was to use an internally located epitope tag (Gilk *et al*. 2009; Johnson *et al*. 2007).

Ridzuan *et al*. (2012) suggests inserting the mCherry coding sequence into the ORF, 29 amino acids downstream from the N-terminal, followed by the remaining amino acids coding for GAP45. They showed that by using this approach, the GAP45 successfully localized to the IMC. We chose to follow the protocol suggested by Ridzuan *et al*. (2012), rather than using an epitope tag approach. This would allow us to co-transfect parasites with GFP-tagged coronin and

mCherry-tagged GAP45. The proteins could then be viewed in live parasites by fluorescence microscopy to potentially observe co-localization of the two proteins. The cloning of pARL2-mCherry-GAP45 was successful. However difficulties were encountered with the growth conditions of the parasites in the presence of blasticidin-S (blasticidin deaminase is the selection marker present in the pARL2-mCherry plasmid). This caused parasites in culture to appear and disappear sporadically. Once parasites had appeared in culture, they were viewed by fluorescence microscopy, however mCherry signals were extremely faint and it was not possible to confidently localize the GAP45.

While we are confident that our data suggests that coronin has an involvement in the IMC or associated actin cytoskeleton based on the localization to the merozoite periphery in late schizonts and after the rupture of daughter merozoites from the RBC, it is not clear exactly what the functions of coronin might be. In other cell types, coronins are most celebrated for their roles as actin cytoskeleton regulators, mediating actin-dependent processes like cell motility, cytokinesis and phagocytosis. One possibility therefore is that coronin is required to orchestrate the formation and dynamics of the actin network between the merozoite IMC and plasma membrane on which the glideosome depends for generating the motile force to invade RBCs and which is also likely required for cytokinesis and merozoite formation.

Future work regarding coronin is required. The first step would be to confirm the localization of coronin. If coronin does indeed localize to the IMC, this needs to be confirmed by co-localization. The approach of attempting to co-transfect parasites with coronin-GFP and GAP-45-mCherry should be revisited. Since the cloning data suggested that the expression vector is correctly constructed, repeating the transfections could be a possible approach to follow.

It has been widely described in literature that mammalian coronin homologues have a function in actin-dependant processes; it would therefore be valuable to perform co-localization studies of *Pf* coronin and actin. Immunofluorescence assays of parasites expressing the pARL2-GFP-coronin vector could be probed using anti-actin antibodies and viewed by fluorescence microscopy. This would potentially show that *Pf* coronin does associate with parasite actin filaments. In addition to co-localization studies using anti-actin antibodies, the association of *Pf* coronin with actin filaments could be confirmed using co-sedimentation assays. This was the approach originally used by Tardieux *et al*. (1998), who first suggested that *Pf* coronin associates with actin

filaments. However, this was performed using anti-coronin antibodies, which were raised against *D. discoideum* coronin. Whilst these experiments were successful, it would be valuable to use the coronin-GFP parasite cell line we generated here, to confirm that *Pf* coronin co-sediments with parasite actin using anti-GFP antibodies.

If the localization of coronin can be elucidated for certain, then it will be possible to follow up with functional assays to determine what function(s) coronin has in *P. falciparum* parasites. Gene knockdown (silencing) experiments could provide valuable insight into the function of coronin. Gene knockdown could be performed using RNA interference techniques, however, the ability to use RNAi to silence gene expression in malaria parasites is generally accepted not to work (Baum *et al*. 2009). A more recently described technique for the inducible knockdown of *Plasmodium* gene expression using the *glmS* ribozyme could be attempted (Prommana *et al*. 2013). In this technique, the coding sequence for the *glmS* ribozyme is introduced into the 3' untranslated region of the target gene. Parasites are transfected with this expression plasmid, and should episomally express the coronin-GFP proteins as previous. In order to reduce the expression of the target gene (coronin), glucosamine is added to the parasite culture, this causes the *glmS* ribozyme to cleave reporter mRNA, leading to the reduction in protein levels (Prommana *et al*. 2013). This can be rapidly reversed by removing the glucosamine inducer, after which protein expression reverts to normal levels (Prommana *et al*. 2013).

In order for this technique to be used for gene silencing, it is necessary to perform homologous recombination to replace the endogenous coronin gene with the coronin-GFP-ribozyme. This technique could prove to be challenging. Homologous recombination is a rare event in *P. falciparum* parasites and requires extensive periods of culturing and selection drug cycling. If the coronin-GFP-ribozyme sequence doesn't adequately compensate for the disruption of the endogenous coronin gene, reduced parasite growth or parasite lethality might be the outcome. However, if successful it will provide a valuable tool in assessing coronin function, since it provides a mechanism for the inducible knockdown of protein expression levels.

Since we are proposing a potential role for coronin in merozoite motility and host cell invasion, following the knock down of coronin protein expression levels, the effects could be visualized by monitoring the success of invasion of erythrocytes by merozoites. Weiss *et al*. (2015) filmed live cells in order to monitor the temporal changes in invasion of erythrocytes following the

treatment of parasites with small molecules that block receptor-ligand interactions required for host-cell invasion. A similar technique could be used to monitor the effects that knockdown of *Pf* coronin has on the parasite. Following the treatment of parasites with glucosamine to induce ribozyme-mediated silencing of coronin expression, live cells would be filmed. Analysis of the films would show if there was any impact on receptor-ligand interactions between merozoites and erythrocytes, and if there is any effect on the success of erythrocyte invasion by merozoites

7.3.2. Dynamin 2

Based on the primary structure displayed in the sequence alignments shown previously (Chapter 3), *Pf*DYN2 belongs to the Dynamin-like protein (Dlp) group of the dynamin superfamily. According to Praefcke & McMahon (2004), dynamins are usually recruited and localized to specific sites of action by protein and lipid interactions of the PH (pleckstrin homology) domain and the PR (proline rich) domain. While these domains are absent in *Pf*DYN2, this doesn't necessarily compromise the ability of *Pf*DYN2 to mediate endocytic vesicle fission like its human counterpart.

According to Dourado *et al*. (2007), dynamin 2 is only expressed during the schizont stage of parasite growth. This was determined by harvesting identical quantities of synchronised parasites at various time intervals post-invasion (ring, early trophozoite, mature trophozoite, and schizont stages). These parasite lysates were then separated using SDS-PAGE, followed by immunodetection using anti-*Pf*DYN2 antibodies. Dourado *et al*. (2007) found that signals on the Western blots were only present in the schizont stage of parasite development. In addition to these observations by Western blot, the authors reported that during immunofluorescence assays using anti-PfDYN2 sera on asynchronous parasites, the specific expression of *Pf*DYN2 at the schizont stage was confirmed.

However, in our research, we found that the dynamin 2 GFP-tagged fusion protein was localized during both the trophozoite, and schizont stages. We expected *Pf*DYN2 to be expressed throughout the parasite life cycle due to the PfCRT promoter in the pARL2-GFP expression vector. However if dynamin 2 had no functional purpose during the trophozoite stage, one possibility would be that the *Pf*DYN2-GFP would not localize, and instead be present as a cytoplasmic pool. Our data suggests that during trophozoite stages, dynamin 2 localizes to numerous punctuate structures within the parasite. Three potential locations for dynamin 2 were identified and these were: localization to the parasite periphery, localization to the food vacuole/digestive vacuole, and localization to punctuate structures in the parasite cytoplasm.

When studying the localization and function of proteins, a powerful technique is to knockout the gene, or to chemically inhibit the function of the protein. We attempted to inhibit the function of dynamin 2 using Hydroxy-dynasore. According to Zhou *et al*. (2009), Hydroxy-dynasore is a

small molecule that inhibits dynamins GTPase activity. The authors report that this inhibited the uptake of haemoglobin by the parasite, which suggests that dynamin may be involved in haemoglobin trafficking. According to Zhou *et al*. (2009), *Pf*DYN1 and *Pf*DYN2 were sensitive to the inhibitor, with *Pf*DYN1 found to be more sensitive to dynasore. We explored this experiment in wild-type 3D7 parasites, as well as parasites over-expressing *Pf*DYN2-GFP. Using the concentrations suggested by Zhou *et al* (2009) we were unable to see the same effects that the authors noted. The authors propose that concentrations of dynasore between 20 μmol/L and 40 μmol/L delayed parasite growth, but the parasites could still develop to later life stages. Using dynasore at a concentration of 80 μmol/L completely inhibited the growth of the parasites and arrested their development at the ring stage of growth. We used the recommended concentrations of dynasore to determine whether it had any effect on the localization patterns of *Pf*DYN2-GFP. No changes were observed; we therefore attempted to determine the IC_{50} for dynasore using the enzymatic pLDH assay. After numerous attempts, no IC_{50} could be determined, due to the inability of dynasore to inhibit parasite growth at the expected concentrations. In addition, there is a very real possibility that using such high concentrations of the inhibitor (80 μmol/L) could cause multiple inhibitory off-target effects in the parasite, unrelated to the GTPase activity of dynamin. Further pursuit of this approach would require sourcing of more potent dynasore derivatives or other dynamin inhibitors.

The most common localization presented in this chapter appears to indicate that GFP-tagged dynamin 2 localizes to punctate regions at the parasite periphery, likely the plasma membrane. This could be indicative of a function similar to that of human dynamin. Dynamin and dynamin-like proteins are proposed to be essential vesicle-scission molecules. Dynamin is involved in the scission of a range of organelles and vesicles, including clathrin-coated vesicles (CCVs), caveolae, mitochondria, and phagosomes (Praefcke & McMahon 2004). The reason for *Pf*DYN2 localizing to the parasite plasma membrane could suggest an involvement in vesicle scission at sites of endocytosis. The model for vesicle scission in higher eukaryotes involves the formation of a helical polymer of dynamin surrounding the constricted membrane neck of a clathrin- coated pit. Upon GTP hydrolysis, the neck of the membrane is pinched off, releasing the CCV to the interior of the cell (Doherty & McMahon 2009; Praefcke & McMahon 2004). Our localization of *Pf*DYN2 at the parasite periphery, and the suggestion that this is due to its involvement in vesicle scission, would indicate that it has a function usually attested to that of classical

dynamins. Immunofluorescence assays performed by Dourado *et al*. (2007) did not indicate the same localization of *Pf*DYN2 to the parasite periphery that we observed. Dourado *et al*. (2007) used anti-DYN2 sera, and instead found that dynamin 2 localization was limited to the cytoplasm of the parasite.

*Pf*DYN2-GFP was also found to localize to distinct punctuate structures within the cytoplasm, and there also appeared to be localization at the food vacuole/digestive vacuole (FV). Based on the localization data presented it here, it is possible to speculate to which organelles dynamin is localizing to, although it is not possible to clearly conclude these locii without further co-localization experiments. The localization of dynamin 2 to the FV could be indicative of a possible role for dynamin in the scission of transport vesicles from the FV. These vesicles would be destined for the parasite periphery in order to recycle plasma membrane. Recycling of endocytosed membrane has not been reported in malaria parasites, but is a prominent feature of endocytic pathways in other organisms. Membrane recycling from the FV would be required to recover plasma membrane lipids and proteins lost during endocytosis, and to ensure FV homeostasis. Considering that up to 80% of the RBC cytoplasm is ingested and delivered to the FV, this implies a large influx of membrane which would have to be recycled to maintain the integrity and composition of the plasma membrane and to prevent the FV from expanding inordinately.

Dourado *et al*. (2007) used co-localization marker antibodies to determine that *Pf*DYN2 partially co-localizes with *Pf*BIP (endoplasmic reticulum resident protein), *Pf*ERD2 (Golgi apparatus marker), and *Pf*ACP (apicoplast marker). The association of dynamin with the ER and Golgi apparatus could suggest a role in the fission of vesicles from these organelles. In the mammalian system of secretion, newly synthesized proteins and lipids are translocated into the ER before transport in coated vesicles from the ER to the Golgi complex for sorting and processing, followed by transport to the plasma membrane, in clathin-coated vesicles to endosomes, or formation of secretory granules (Baines & Zhang 2007). The classical secretory pathway similar to that in eukaryotes has been suggested for the malaria parasite. A parasite Golgi apparatus has been identified, but its morphology and organization is not fully understood. Cooke *et al*. (2004) describe this Golgi-like complex as ‘rudimentary’, and it appears as a collection of a few tubular or flat cisternae surrounded by various sized vesicles. Research has also suggested that the Golgi

is unstacked and consists of individual compartments (Van Wye *et al*. 1996). The parasite endoplasmic reticulum proliferates extensively throughout the parasite cytoplasm and is connected with the nuclear envelope (Atkinson & Aikawa 1990; Bannister *et al*. 2004).

Dourado *et al*. (2007) constructed a phylogenetic tree to illustrate the position of *Pf*DYN2 in the dynamin superfamily. This tree proves very interesting, as it could provide insight into the localization of the GFP-tagged *Pf*DYN2 that we generated in our work. According to this phylogenetic tree, *Pf*DYN2 clusters closely with *Tb*DLP, *At*ADL2a, *Sc*DNM1 and *Hs*DRP1. *Trypanosoma brucei* DLP is a unique Dlp that has been found to be involved in endocytosis as well as mitochondrial fission; *Arabidopsis thaliana* Dlp is involved in plant mitochondria division; *Saccharomyces cerevisiae* DNM1 is involved in both endosome dynamics and mitochondrial outer membrane division; *Homo sapiens* Drp1 has been found to regulate ER and mitochondria division (Chanez *et al*. 2006; Arimura 2004; Hoepfner *et al*. 2001; Sesaki 1999; Pitts *et al*. 1999). The striking similarity amongst all those functions is the inclusion of these dynamins in mitochondrial division. This could potentially provide an insight into the function of *Pf*DYN2. It is possible that the localization we are seeing in our data for *Pf*DYN2-GFP, is due to this conserved function of Dlps in mitochondria, and that *Pf*DYN2 is involved in mitochondrial fission. Since mitochondria are dynamic organelles and in a constant state of division and fusion within the cell (Pitts *et al*. 1999), it would therefore be an explanation for the localization of *Pf*DYN2-GFP in multiple live stages of the parasite, and not just during schizogony. Confirmation that *Pf*DYN2-GFP is indeed localizing to the mitochondria would be an important future prospect for this work. This could be achieved by using organelle stains (e.g. mitotracker), or with marker antibodies specific for mitochondria.

Based on the evidence presented here, our preliminary conclusions and basis for future work is that *Pf*DYN2 localizes to the parasite periphery where it is potentially involved in the scission of endocytic vesicles, to the FV where it mediates the formation of recycling vesicles, and to the mitochondria where it is potentially involved in the division of this organelle. These conclusions are speculative, and are based on the assumption that *Pf*DYN2 displays functions similar to those eukaryotic dynamin 1, and dynamin 2 and dynamin-like proteins.

7.3.3. μ4

As was the case for coronin and dynamin 2, live cell imagining using fluorescence and confocal microscopy was the approach employed to determine the subcellular localization of μ4. The data we present here suggests that μ4 localizes to the plasma membrane and the digestive vacuole/food vacuole of the parasite. Localization to the plasma membrane was the more commonly observed result on the live parasites viewed. There were also a large number of occurrences where distinct localization was not observed in individual parasites - instead, GFP fluorescence was observed as a diffuse pool in the cytoplasm. This would support the notion that the recruitment of adaptins to membranes is transient. The existence of both cytosolic and membrane-bound pools of μ4 supports the hypothesis that it forms part of a complex (AP-4) that is a component of a protein coat, which cycles between the cytosol and membranes, as is the case with other coat proteins (Dell'Angelica *et al*. 1999).

Localization of μ4 to the parasite plasma membrane and to the digestive vacuole supports the hypothesis that μ4 could be involved in protein trafficking as well as having a role in the mediation of endocytosis. AP-4 is closely related to the AP-2 complex, and therefore it would be acceptable to assume that the parasite AP-4 complex could be similar in localization and function to both the mammalian AP-2 and AP-4 complexes.

The AP-2 complex is involved in clathrin-mediated endocytosis. In mammalian systems, AP-2 recruits clathrin, triggers clathrin assembly, recruits numerous endocytic accessory factors and interacts directly with cargo molecules (Sean D. Conner & Schmid 2003). This recruitment of clathrin to the plasma membranes initiates endocytosis. The localization of *Pf*μ4 to the plasma membrane could be indicative of the parasite AP-4 complex being responsible for recruitment of clathrin to initiate endocytosis in a similar fashion to that of the mammalian AP-2 complex.

In order to discern whether this is the case in parasites, a valuable experimental procedure to follow would be the co-localization of μ4 with clathrin. This could be achieved by co-expressing clathrin as a fusion protein with mCherry, or by performing immunofluorescence microscopy with anti-clathrin antibodies.

If areas of co-localization are observed between clathrin and μ4, this would support the hypothesis that μ4, based on similarities to mammalian systems, could be involved in

endocytosis in a similar manner to AP-2 complexes. Previous work by a researcher associated with our research group has shown that *Pf*μ4 co-localizes with *P. falciparum* clathrin. Antiserum raised in rabbit to a recombinant fusion of GST and the C-terminal hub of *P. falciparum* clathrin heavy chain homologue (PFL0930w) was used in co-localization immunofluorescence assays, with anti-μ4 raised in mice. The findings showed that *Pf*μ4 and the clathrin heavy chain co-localized, markedly at peripheral sites of the parasite (Sandra Meredith: PhD thesis, 2008). Based on this data, we should follow the mCherry-tagged fusion protein approach with clathrin to determine whether localization occurs when using fusion proteins, and if this localization confirms and complements what was found by Meredith (2008). In the latter study, μ4 was localized at the parasite periphery, as well as at the food vacuole. This is very interesting since this work made use of antisera raised to recognise μ4, and observed the same localization as we did using GFP-tagged fusion protein expression.

Since we found that both *Pf*μ4-GFP and *Pf*DYN2-GFP appeared to localize to puncta at the parasite plasma membrane, an attractive hypothesis was that these two proteins are co-localizing. This is a reasonable hypothesis if we assume that the parasite AP-4 complex is recruiting clathrin to the periphery, and then *Pf*DYN2 is responsible for clathrin-coated vesicle scission. In order to show this, we attempted to generate transfectants expressing both *Pf*μ4-GFP, and *Pf*DYN2-mCherry. The pARL2-mCherry-DYN2 expression vector was successfully cloned and a parasite cell line episomally expressing μ4-GFP was transfected with this mCherry vector. After culturing this parasite cell line with complete media supplemented with both WR99210 (to select for GFP transfectants) and blasticidin-S (to select for mCherry transfectants), parasites appeared in culture, however, in a similar manner to the GAP45-mCherry transfectants, these parasites tended to appear, and then disappear from culture sporadically. Attempts were made to perform fluorescence microscopy when parasites were visible in culture. *Pf*μ4-GFP parasites were observed, and the localization of this μ4 was consistent with previously observed localization. However no expression of *Pf*DYN2-mCherry was observed.

In addition to localization indicating that μ4 is present at the parasite periphery, we found that *Pf*μ4-GFP also appeared to localize to the parasite food vacuole. This acidic compartment is comparable to the mammalian lysosome, and is the site of haemoglobin degradation (Elliott *et al*. 2008). The reason for this association is not clear at present, but – as was discussed for *Pf*DYN2

above – it could indicate that μ4 forms part of a coat complex that mediates the formation of vesicles that recycle membrane from the FV to the plasma membrane.

Immunoelectron microscopy studies in mammalian cells have shown that μ4 localizes to a post-Golgi compartment (thought to correspond to the *trans*-Golgi network) (Hirst *et al*. 2013). The data suggests that AP-4 mediates trafficking between the TGN and an endosomal and lysosomal-like compartment. Dell'Angelica *et al*. (1999) showed with immunofluorescence of mammalian cells that μ4 is associated with the TGN, and that this association is sensitive to the Golgi-disrupting agent, brefeldin A. This treatment caused AP-4 to disassociate from the TGN into the cytosol. Based on this data, Dell'Angelica *et al*. (1999) proposed that AP-4 has a role in the signal-mediated trafficking of integral membrane proteins in mammalian cells. Simmen *et al*. (2002) propose that alternatively, or in addition to, AP-4 may be involved in mediating a direct route of trafficking from the TGN to the plasma membrane. According to Hirst *et al*. (2013), it is not possible to unequivocally distinguish between the two scenarios based on the current evidence that is available.

AP-1 has been shown to be involved in the sorting of proteins from the TGN to compartments of the endosomal and lysosomal systems (Dell'Angelica *et al*. 1999). This raises an interesting question - if AP-4 also mediates export from the TGN and targeting to the endosomes, why would these two parallel pathways exist? This subject was addressed by Hirst *et al*. (2013). Interestingly, AP-1 is 30 times more abundant than AP-4 in HeLa cells, and appears to be more highly expressed in most human tissues. This could suggest that AP-4 is a specialized cargo adaptor which is involved in preferential TGN export for a specific set of proteins (Hirst *et al*. 2013). A study has shown that when the formation of clathrin-coated vesicles from the TGN is abolished by knockdown of the clathrin heavy chain, or auxilin, AP-4 vesicle formation is considerably stimulated, whilst no increase in AP-4 expression was observed (Borner *et al*. 2012). This led Hirst *et al*. (2013) to hypothesize that the AP-4 pathway is very sensitive to disturbances in clathrin-mediated trafficking, and in response to a lack of clathrin-coated vesicle formation, AP-4 provides the compensation mechanism that ensure there is no backup of cargo in the TGN. This finding may then show that while AP-4 is thought to be responsible for specialized transport for a select set of proteins, it may also be capable of sorting a number of

cargos that normally rely on clathrin-coated vesicle trafficking. Our data does, however lead to the conclusion that *Pf*μ4 functions like mammalian AP-2, and not AP-4.

Future prospects for the characterization of μ4 would be to revisit the co-localization studies with *Pf*DYN2-GFP. Since we struggled to generate mCherry transfectants with both GAP45, and dynamin 2, the blasticidin-S culture conditions need to be optimised further. Whilst we used concentrations of blasticidin-S that have been widely used and published previously, we were still unsuccessful. As discussed previously in this section, it would be a valuable future prospect to co-localize μ4 with the clathrin-heavy chain to attempt to show that μ4 (as a part of the AP-4 complex) is responsible for recruiting clathrin to the parasite periphery, where *Pf*DYN2 then mediates vesicle scission.

With all research into the localization and function of proteins, silencing or gene-knockdown experiments are vitally important. Using RNAi or the previously discussed *glm*S ribozyme inducible knockdown technique, silencing μ4 could provide insight into the function of μ4. An example of this would be to knockdown μ4 expression, and determine if this has an effect on the endocytosis of haemoglobin. If haemoglobin levels in the parasite were reduced after knocking down or silencing μ4, this would be further evidence to suggest that μ4 is involved in endocytosis. Abnormal FV morphology may also be indicative of a role for μ4 in the formation of membrane recycling vesicles.

CHAPTER FIVE: GENERAL CONCLUSION

In this study we aimed to identify and localize three proteins potentially involved in endocytosis in the malaria parasite, *P. falciparum*. These proteins were selected based on sequence homology to mammalian proteins previously shown to be involved in endocytosis. The selected candidate endocytosis proteins were coronin, dynamin 2, and the medium chain adaptor protein μ4. The coding sequences for these proteins were amplified using PCR and cloned into the malaria expression vector, pARL2-GFP. *P. falciparum* 3D7 parasites were transfected with high concentrations of purified plasmid by electroporation using the RBC preloading method. Transfected parasites were cultured in complete media supplemented with WR99210. Parasites began to appear in culture after approximately 3 weeks, and Western blots were performed using commercially available anti-GFP antibodies after 5 weeks to confirm the expression of full-length GFP-tagged fusion proteins. Live parasites were analysed using fluorescence and confocal microscopy in order to determine the subcellular localization of the candidate endocytosis proteins.

5.1. Coronin

Coronins are a family of highly conserved actin cytoskeleton regulators that have been shown to promote cell motility and modulate other actin-dependant process. *D. discoideum* coronin has been shown to be involved in phagocytosis, as well as cell locomotion and cytokinesis. The involvement in phagocytosis was the motivation to include coronin in this study, as an endocytosis candidate protein. *P. falciparum* coronin has a 27% amino acid identity and 51% similarity to coronin 1A over the 461 amino acid length of the human sequence. The arginine at position 30 of the human sequence, which is critical for F-actin binding, is conserved in the parasite sequence. This suggests that F-actin binding properties are conserved for parasite coronin.

Localization of *Pf*coronin-GFP by fluorescence and confocal microscopy showed that during the trophozoite stages of parasite development, GFP is present as a cytoplasmic pool. The lack of localization of coronin during the trophozoite stage of the parasite life cycle, when the parasite is

most metabolically active, suggests that *Pf*coronin is not involved in endocytosis. During schizogony when parasites progress into the schizont stage of development, the localization of *Pf*coronin became distinct. It appeared to be localized in rings encircling newly replicated nuclei in the fully segmented schizont. The localization patterns observed closely resembles the localization of proteins known to associate to the inner membrane complex (IMC), such as GAP45 (Bannister *et al*. 2000; Kono *et al*. 2012; Ridzuan *et al*. 2012). We also believe that *Pf*coronin has a role in merozoite motility and invasion of RBCs. Based on the similarity of *Pf*coronin to mammalian coronins, which are well-known actin cytoskeleton regulators, and known to be mediators of actin-dependant processes, we propose that in *P. falciparum* parasites, coronin is required to coordinate the formation of the actin network between the merozoite IMC and the plasma membrane. The glideosome is dependent on this network for generating the motile forces necessary for the invasion of RBCs by merozoites.

5.2. Dynamin 2

Dynamin proteins are a group of conserved large GTPase proteins that are found in many eukaryotic cell systems (Praefcke & McMahon 2004; Gaechter *et al*. 2008). Dynamins are known to be involved in a number processes including the budding of transport vesicles, division of organelles, endocytosis, cytokinesis and pathogen resistance (Praefcke & McMahon 2004; Zhou *et al*. 2009). Members of the dynamin superfamily are broadly divided into classical dynamins and dynamin-related or dynamin-like proteins (DRPs or DLPs). The most well known function of dynamin is its involvement in clathrin-mediated endocytosis. During the early stages of the endocytic process, dynamin localizes to the plasma membrane at clathrin-coated invaginations. Dynamin then self-assembles into rings at the necks of the invagination buds that become stacked and interconnected (Bottomley *et al*. 1999). The GTPase activity of dynamin drives the constriction of these rings to pinch off the clathrin-coated vesicles (Hinshaw & Schmid 1995).

Based on the primary structure sequence homology, *Pf*DYN2 in grouped into the dynamin-like protein (Dlp) group of the dynamin superfamily. As was presented in Chapter 3, the sequence alignment shows that the *P. falciparum* sequence displays a strong level of homology in the GTPase domain of its human counterpart (44% amino acid identity, and 66% similarity across the GTPase domain). The G1- G4 consensus motifs (critical for GTP binding in dynamin) are also highly conserved. The data suggests that *Pf*DYN2 displays prototypical dynamin-like GTPase activity.

Fluorescence microscopy analysis of live parasites expressing *Pf*DYN2-GFP presented three localization patterns. These were: localization to the parasite periphery, localization to the food vacuole, and localization at punctuate structures in the parasite cytoplasm. Localization of *Pf*DYN2 to the parasite plasma membrane was the localization pattern most commonly observed during the study. This indicates a potential, conserved role as an endocytic vesicle scission molecule. This would lead to the assumption that *Pf*DYN2 functions in a similar manner to the classical dynamin family of proteins, as is observed in many higher eukaryotes.

Two addition localization patterns for *Pf*DYN2-GFP were observed. These were at punctuate structures within the parasite cytoplasm, and at the parasite food vacuole. Speculative reasons

for localization at these sites have been proposed in this study. The localization of dynamin 2 at the FV could be indicative of a role in the scission of transport vesicles from the FV. The potential reason for this vesicular trafficking is to recycle endocytosed membrane back to the plasma membrane, in order to maintain the integrity and composition of the plasma membrane, as well as preventing the FV from expanding inordinately due to the large influx of membrane from transport vesicles. One of the conserved functions that have been observed in many dynamin-like proteins in the dynamin superfamily is the involvement of dynamin in mitochondrial division. Our data showed localization of *Pf*DYN2-GFP to distinct locii in the parasite cytoplasm. We propose that this localization could be at mitochondria, implicating parasite dynamin 2 in mitochondrial fission.

5.3. μ4

Adaptor proteins (AP) are a group of five closely related heterotetrameric complex that have been shown to have important functions in vesicle trafficking. They are made up of two large chains, one medium chain (μ) and one small chain (Hirst *et al*. 2013). The medium adpator protein chain of the AP-4 complex μ4 was selected for this study. AP-4 is widely expressed in mammalian tissues and is known to associate with the cellular membrane as a peripheral membrane protein. The *Pf*μ4 sequence has a 30% amino acid identity and 59% similarity to its human counterpart over the entire length of the 436 amino acid sequence. Medium chain adaptor proteins are known to trap and concentrate transmembrane cargo proteins in budding transport vesicles by recognising amino acid motifs within the cytoplasmic tails of cargo proteins (Kibria *et al*. 2015). Important motifs in μ4 for this recognition are the regions: VFLD, K217, VRFL and KWVR (Canagarajah *et al*. 2013). These regions are highly conserved in *Pf*μ4. This suggests that tyrosine motif sorting of transmembrane cargo proteins is a feature of *Pf*μ4.

Live *P. falciparum* parasites expressing pARL2-GFP-μ4 viewed by fluorescence microscopy indicated that *Pf*μ4-GFP localizes to the parasite plasma membrane and to the food vacuole. The more frequently observed localization of *Pf*μ4-GFP was to the parasite plasma membrane. There were also numerous cases where GFP localization was not distinct, and instead *Pf*μ4-GFP was found as a diffuse pool in the parasite cytoplasm. This supports the notion by Dell'Angelica *et al*. (1999) that μ4 forms part of an AP-4 complex, that is part of a protein coat which cycles between the membrane and the cytosol. This is the transient recruitment of adaptins to membranes. The mammalian AP-2 complex is involved in clathrin-mediated endocytosis by recruiting clathrin to the plasma membrane, triggering clathrin assembly and recruiting numerous endocytic accessory factors and interacting with cargo molecules (Conner & Schmid 2003). We believe that the localization of *Pf*μ4 to the plasma membrane is indicative of the parasite AP-4 complex being responsible for recruitment of clathrin to initiate endocytosis in a similar manner to that of the mammalian AP-2 complex.

In addition to the localization to the parasite periphery, localization of *Pf*μ4-GFP to the food vacuole was observed. The exact reasons for this localization are not clear at this stage. However we believe it could be indicative of a function for μ4 as part of a coat complex that mediates the formation of vesicles that recycle membrane from the FV to the plasma membrane.

An involvement in this process could also be a reason that *Pf*µ4-GFP and *Pf*DYN2-GFP appeared to present a similar localization.

Overall, the objectives for this study were achieved. We aimed to identify candidate endocytosis proteins based on homology to mammalian counterparts, known to be involved in endocytosis. We aimed to amplify the coding sequences for these proteins and clone them into the malaria expression vector, pARL2-GFP and transfect *P. falciparum* 3D7 parasites with this vector. Following the transfection with these constructs, we aimed to confirm that full-length GFP-tagged fusion protein expression was taking place in the parasite. Following confirmation of protein expression, the next objective was to localize these proteins using fluorescence microscopy. All of these aims and objectives were achieved over the course of the project, and the study showed that expressing endocytosis candidate proteins as full-length GFP-tagged fusion constructs is an effective approach in the first steps of determining the localization and function of malaria proteins *in vitro*.

5.4. Future prospects

There are a number of follow up experiments regarding the localization and function of the proteins. In order to confirm the proposed localization of coronin to the IMC, co-localization studies are required, and the known IMC resident protein, GAP45 would be a good candidate for this study. Furthermore, to confirm that *Pf*coronin is an actin associated protein, and is involved in actin-dependant processes, co-sedimentation assays as well as co-localization studies could be performed. Protein silencing using the *glmS* ribozyme approach is another proposed future study to determine the affects on merozoite formation, motility and invasion.

Data suggested *Pf*DYN2-GFP and *Pf*μ4-GFP were localizing to similar regions in the parasite, so co-localization of these two proteins is another proposed future experiment. The study would involve transfecting *P. falciparum* 3D7 parasites with both the pARL2-DYN2-mCherry, and the pARL2-μ4-GFP expression plasmids. Fluorescence microscopy will be used to determine areas of overlap between the mCherry and GFP signals which would suggest co-localization. In addition to performing co-localization studies for *Pf*DYN2 and *Pf*μ4, immuno-electron microscopy studies would provide valuable insight into the localization of these proteins at a much higher magnification than is possible with fluorescence microscopy. The *glmS* ribozyme gene knockdown proposed for *Pf*coronin should also be performed for *Pf*DYN2 and *Pf*μ4 in order to study the affects of the knockdown of these proteins has on endocytosis.

REFERENCES

Van Agtmael, M. a, Eggelte, T. a & Van Boxtel, C.J., 1999. Artemisinin drugs in the treatment of malaria: from medicinal herb to registered medication. *Trends in Pharmacological Sciences*, 20(5), pp.199–205.

Aguilar, R.C., Boehm, M., Gorshkova, I., Crouch, R.J., Tomita, K., Saito, T., Ohno, H. & Bonifacino, J.S., 2001. Signal-binding specificity of the mu4 subunit of the adaptor protein complex AP-4. *The Journal of biological chemistry*, 276(16), pp.13145–52.

Appleton, B.A., Wu, P. & Wiesmann, C., 2006. The crystal structure of murine coronin-1: A regulator of actin cytoskeletal dynamics in lymphocytes. *Structure*.

Arimura, S. -i., 2004. Arabidopsis Dynamin-Like Protein 2a (ADL2a), Like ADL2b, is Involved in Plant Mitochondrial Division. *Plant and Cell Physiology*, 45(2), pp.236–242.

Atkinson, C.T. & Aikawa, M., 1990. Ultrastructure of malaria-infected erythrocytes. *Blood cells*, 16(2-3), pp.351–68.

Baines, A.C. & Zhang, B., 2007. Receptor-mediated protein transport in the early secretory pathway. *Trends in biochemical sciences*, 32(8), pp.381–8.

Bannister, L.., Hopkins, J.., Fowler, R.., Krishna, S. & Mitchell, G.., 2000. A Brief Illustrated Guide to the Ultrastructure of Plasmodium falciparum Asexual Blood Stages. *Parasitology Today*, 16(10), pp.427–433.

Bannister, L.H., Hopkins, J.M., Margos, G., Dluzewski, A.R. & Mitchell, G.H., 2004. Three-dimensional ultrastructure of the ring stage of Plasmodium falciparum: evidence for export pathways. *Microscopy and microanalysis : the official journal of Microscopy Society of America, Microbeam Analysis Society, Microscopical Society of Canada*, 10(5), pp.551–62.

Baum, J., Gilberger, T.-W., Frischknecht, F. & Meissner, M., 2008. Host-cell invasion by malaria parasites: insights from Plasmodium and Toxoplasma. *Trends in parasitology*, 24(12), pp.557–63.

Baum, J., Papenfuss, A.T., Mair, G.R., Janse, C.J., Vlachou, D., Waters, A.P., Cowman, A.F., Crabb, B.S. & de Koning-Ward, T.F., 2009. Molecular genetics and comparative genomics reveal RNAi is not functional in malaria parasites. *Nucleic acids research*, 37(11), pp.3788–98.

Bear, J.E. & Gertler, F.B., 2009. Ena/VASP: towards resolving a pointed controversy at the barbed end. *Journal of cell science*, 122(Pt 12), pp.1947–1953.

Beier, J.C., 1998. Malaria parasite development in mosquitoes. *Annual review of entomology*, 43, pp.519–543.

Birkholtz, L.-M., Blatch, G., Coetzer, T.L., Hoppe, H.C., Human, E., Morris, E.J., Ngcete, Z., Oldfield, L., Roth, R., Shonhai, A., Stephens, L. & Louw, A.I., 2008. Heterologous expression of plasmodial proteins for structural studies and functional annotation. *Malaria journal*, 7(1), p.197.

Boehm, M., Aguilar, R.C. & Bonifacino, J.S., 2001. Functional and physical interactions of the adaptor protein complex AP-4 with ADP-ribosylation factors (ARFs). *The EMBO journal*, 20(22), pp.6265–76.

Borgne, R. Le & Hoflack, B., 1998. Mechanisms of protein sorting and coat assembly: insights from the clathrin-coated vesicle pathway. *Current Opinion in Cell Biology*, 10(4), pp.499–503.

Borner, G.H.H., Antrobus, R., Hirst, J., Bhumbra, G.S., Kozik, P., Jackson, L.P., Sahlender, D.A. & Robinson, M.S., 2012. Multivariate proteomic profiling identifies novel accessory proteins of coated vesicles. *The Journal of cell biology*, 197(1), pp.141–60.

Bottomley, M.J., Surdo, P.L. & Driscoll, P.C., 1999. Endocytosis: How dynamin sets vesicles PHree! *Current Biology*, 9(8), pp.0–3.

Bretscher, M.S., 1982. Surface uptake by firbroblasts and its consequences. *Cold Spring Harbor Symposia on Quantitative Biology*, 46(2), pp.707–712.

Cai, L., Makhov, A.M. & Bear, J.E., 2007. F-actin binding is essential for coronin 1B function in vivo. *Journal of cell science*.

Canagarajah, B.J., Ren, X., Bonifacino, J.S. & Hurley, J.H., 2013. The clathrin adaptor complexes as a paradigm for membrane-associated allostery. *Protein science : a publication of the Protein Society*, 22(5), pp.517–29.

Carreno, R.A., Kissinger, J.C., McCutchan, T.F. & Barta, J.R., 1997. Phylogenetic analysis of haemosporinid parasites (apicomplexa: Haemosporina) and their coevolution with vectors and intermediate hosts. *Archiv für Protistenkunde*, 148(3), pp.245–252.

Chan, K.T., Creed, S.J. & Bear, J.E., 2011. Unraveling the enigma: progress towards understanding the coronin family of actin regulators. *Trends in cell biology*, 21(8), pp.481–8.

Chanez, A.-L., Hehl, A.B., Engstler, M. & Schneider, A., 2006. Ablation of the single dynamin of T. brucei blocks mitochondrial fission and endocytosis and leads to a precise cytokinesis arrest. *Journal of cell science*, 119(Pt 14), pp.2968–74.

Conner, S.D. & Schmid, S.L., 2003. Differential requirements for AP-2 in clathrin-mediated endocytosis. *Journal of Cell Biology*, 162(5), pp.773–779.

Conner, S.D. & Schmid, S.L., 2003. Regulated portals of entry into the cell. *Nature*, 422(6927), pp.37–44.

Cooke, B.M., Lingelbach, K., Bannister, L.H. & Tilley, L., 2004. Protein trafficking in Plasmodium falciparum-infected red blood cells. *Trends in Parasitology*, 20(12), pp.581–589.

Damke, H., Baba, T., Warnock, D.E. & Schmid, S.L., 1994. Induction of mutant dynamin specifically blocks endocytic coated vesicle formation. *Journal of Cell Biology*, 127(4), pp.915–934.

Deitsch, K.W., Driskill, C.L. & Wellems, T.E., 2001. Transformation of malaria parasites by the spontaneous uptake and expression of DNA from human erythrocytes. *Nucleic Acids Research*, 29(3), pp.850–853.

Dell'Angelica, E.C., Mullins, C. & Bonifacino, J.S., 1999. AP-4, a novel protein complex related to clathrin adaptors. *Journal of Biological Chemistry*, 274(11), pp.7278–7285.

Dell'Angelica, E.C., Ohno, H., Ooi, C.E., Rabinovich, E., Roche, K.W. & Bonifacino, J.S., 1997. AP-3: an adaptor-like protein complex with ubiquitous expression. *The EMBO journal*, 16(5), pp.917–28.

Doherty, G.J. & McMahon, H.T., 2009. Mechanisms of endocytosis. *Annual review of biochemistry*, 78, pp.857–902.

Van Dooren, G.G., Marti, M., Tonkin, C.J., Stimmler, L.M., Cowman, A.F. & McFadden, G.I., 2005. Development of the endoplasmic reticulum, mitochondrion and apicoplast during the asexual life cycle of Plasmodium falciparum. *Molecular Microbiology*, 57(2), pp.405–419.

Dourado, I.M., Mouray, E., Morais, B., Santana, J.M., Grellier, P. & Florent, I., 2007. Characterization of PfDYN2 , a dynamin-like protein of Plasmodium falciparum expressed in schizonts. , 9, pp.797–805.

Elliott, D. a, McIntosh, M.T., Hosgood, H.D., Chen, S., Zhang, G., Baevova, P. & Joiner, K. a, 2008. Four distinct pathways of hemoglobin uptake in the malaria parasite Plasmodium falciparum. *Proceedings of the National Academy of Sciences of the United States of America*, 105(7), pp.2463–8.

Fattorusso, E. & Taglialatela-Scafati, O., 2009. Marine antimalarials. *Marine drugs*, 7(2), pp.130–52.

Feng, B., 2002. Furrow-Specific Endocytosis during Cytokinesis of Zebrafish Blastomeres. *Experimental Cell Research*, 279(1), pp.14–20.

Fidock, D. a, Rosenthal, P.J., Croft, S.L., Brun, R. & Nwaka, S., 2004. Antimalarial drug discovery: efficacy models for compound screening. *Nature Reviews Drug Discovery*, 3(6), pp.509–520.

Frénal, K., Polonais, V., Marq, J.-B., Stratmann, R., Limenitakis, J. & Soldati-Favre, D., 2010. Functional dissection of the apicomplexan glideosome molecular architecture. *Cell host & microbe*, 8(4), pp.343–57.

Gaechter, V., Schraner, E., Wild, P. & Hehl, A.B., 2008. The single dynamin family protein in the primitive protozoan Giardia lamblia is essential for stage conversion and endocytic transport. *Traffic (Copenhagen, Denmark)*, 9(1), pp.57–71.

Gandhi, M., Achard, V., Blanchoin, L. & Goode, B.L., 2009. Coronin Switches Roles in Actin Disassembly Depending on the Nucleotide State of Actin. *Molecular Cell*, 34(3), pp.364–374.

Gandhi, M., Jangi, M. & Goode, B.L., 2010. Functional surfaces on the actin-binding protein coronin revealed by systematic mutagenesis. *Journal of Biological Chemistry*.

Gaskins, E., Gilk, S., DeVore, N., Mann, T., Ward, G. & Beckers, C., 2004. Identification of the membrane receptor of a class XIV myosin in Toxoplasma gondii. *The Journal of cell biology*, 165(3), pp.383–93.

Gerald, N., Mahajan, B. & Kumar, S., 2011. Mitosis in the human malaria parasite Plasmodium falciparum. *Eukaryotic Cell*, 10(4), pp.474–482.

Gilk, S.D., Gaskins, E., Ward, G.E. & Beckers, C.J.M., 2009. GAP45 phosphorylation controls assembly of the Toxoplasma myosin XIV complex. *Eukaryotic cell*, 8(2), pp.190–6.

Ginsburg, H., 1990. Some reflections concerning host erythrocyte-malarial parasite interrelationships. *Blood cells*, 16(2-3), pp.225–35.

Giobbia, M., Tonon, E., Zanatta, A., Cesaris, L., Vaglia, A. & Bisoffi, Z., 2005. Late recrudescence of Plasmodium falciparum malaria in a pregnant woman: a case report. *International journal of infectious diseases : IJID : official publication of the International Society for Infectious Diseases*, 9(4), pp.234–5.

Haldar, K., 1998. Intracellular trafficking in Plasmodium-infected erythrocytes. *Current Opinion in Microbiology*, 1(4), pp.466–471.

Halfmann, R., Alberti, S., Krishnan, R., Lyle, N., O'Donnell, C.W., King, O.D., Berger, B., Pappu, R. V & Lindquist, S., 2011. Opposing effects of glutamine and asparagine govern prion formation by intrinsically disordered proteins. *Molecular cell*, 43(1), pp.72–84.

Heldwein, E.E., Macia, E., Wang, J., Yin, H.L., Kirchhausen, T. & Harrison, S.C., 2004. Crystal structure of the clathrin adaptor protein 1 core. *Proceedings of the National Academy of Sciences of the United States of America*, 101(39), pp.14108–13.

Hempelmann, E., 2007. Hemozoin biocrystallization in Plasmodium falciparum and the antimalarial activity of crystallization inhibitors. *Parasitology research*, 100(4), pp.671–6.

Heuser, J., 1980. Three-dimensional visualization of coated vesicle formation in fibroblasts. *The Journal of Cell Biology*, 84(3), pp.560–583.

Hinshaw, J.E., 2000. Dynamin and its role in membrane fission. *Annual review of cell and developmental biology*, 16, pp.483–519.

Hinshaw, J.E. & Schmid, S.L., 1995. Dynamin self-assembles into rings suggesting a mechanism for coated vesicle budding. *Nature*, 374(6518), pp.190–2.

Hirst, J., Barlow, L.D., Francisco, G.C., Sahlender, D.A., Seaman, M.N.J., Dacks, J.B. & Robinson, M.S., 2011. The fifth adaptor protein complex. *PLoS biology*, 9(10), p.e1001170.

Hirst, J., Irving, C. & Borner, G.H.H., 2013. Adaptor protein complexes AP-4 and AP-5: new players in endosomal trafficking and progressive spastic paraplegia. *Traffic (Copenhagen, Denmark)*, 14(2), pp.153–64.

Hoepfner, D., van den Berg, M., Philippsen, P., Tabak, H.F. & Hettema, E.H., 2001. A role for Vps1p, actin, and the Myo2p motor in peroxisome abundance and inheritance in Saccharomyces cerevisiae. *The Journal of cell biology*, 155(6), pp.979–90.

Holton, T.A. & Graham, M.W., 1991. A simple and efficient method for direct cloning of PCR products using ddT-tailed vectors. *Nucleic acids research*.

Hoppe, H.C. & Joiner, K. a, 2000. Cytoplasmic tail motifs mediate endoplasmic reticulum localization and export of transmembrane reporters in the protozoan parasite Toxoplasma gondii. *Cellular microbiology*, 2(6), pp.569–78.

De Hostos, E.L., 1999. The coronin family of actin-associated proteins. *Trends in Cell Biology*, 9(9), pp.345–350.

De Hostos, E.L., Bradtke, B., Lottspeich, F., Guggenheim, R. & Gerisch, G., 1991. Coronin, an actin binding protein of Dictyostelium discoideum localized to cell surface projections, has sequence similarities to G protein beta subunits. *The EMBO journal*.

De Hostos, E.L., Rehfueß, C., Bradtke, B., Waddell, D.R., Albrecht, R., Murphy, J. & Gerisch, G., 1993. Dictyostelium mutants lacking the cytoskeletal protein coronin are defective in cytokinesis and cell motility. *Journal of Cell Biology*.

Hou, F., Sun, L., Zheng, H., Skaug, B., Jiang, Q.-X. & Chen, Z.J., 2011. MAVS forms functional prion-like aggregates to activate and propagate antiviral innate immune response. *Cell*, 146(3), pp.448–61.

Huang, W., Ghisletti, S., Saijo, K., Gandhi, M., Aouadi, M., Tesz, G.J., Zhang, D.X., Yao, J., Czech, M.P., Goode, B.L., Rosenfeld, M.G. & Glass, C.K., 2011. Coronin 2A mediates actin-dependent de-repression of inflammatory response genes. *Nature*, 470(7334), pp.414–418.

Insall, R.H. & Machesky, L.M., 2009. Actin dynamics at the leading edge: from simple machinery to complex networks. *Developmental cell*, 17(3), pp.310–22.

Ishikawa-Ankerhold, H.C., Gerisch, G. & Müller-Taubenberger, A., 2010. Genetic evidence for concerted control of actin dynamics in cytokinesis, endocytic traffic, and cell motility by coronin and Aip1. *Cytoskeleton (Hoboken, N.J.)*, 67(7), pp.442–55.

Janse, C.J., Van der Klooster, P.F.J., Van der Kaay, H.J., Van der Ploeg, M. & Overdulve, J.P., 1986. Rapid repeated DNA replication during microgametogenesis and DNA synthesis in young zygotes of Plasmodium berghei. *Transactions of the Royal Society of Tropical Medicine and Hygiene*, 80(1), pp.154–157.

Johnson, T.M., Rajfur, Z., Jacobson, K. & Beckers, C.J., 2007. Immobilization of the type XIV myosin complex in Toxoplasma gondii. *Molecular biology of the cell*, 18(8), pp.3039–46.

Kappe, S.H.I., Vaughan, A.M., Boddey, J. a & Cowman, A.F., 2010. That was then but this is now: malaria research in the time of an eradication agenda. *Science*, 328(5980), pp.862–866.

Karl, S., Wong, R.P., St Pierre, T.G. & Davis, T.M., 2009. A comparative study of a flow-cytometry-based assessment of in vitro Plasmodium falciparum drug sensitivity. *Malaria Journal*, 8, p.294.

Keen, J.H., Willingham, M.C. & Pastan, I.H., 1979. Clathrin-coated vesicles: Isolation, dissociation and factor-dependent reassociation of clathrin baskets. *Cell*, 16(2), pp.303–312.

Kerr, M.C. & Teasdale, R.D., 2009. Defining macropinocytosis. *Traffic*, 10(4), pp.364–371.

Kibria, K.M.K., Rawat, K., Klinger, C.M., Panchal, M. & Singh, S., 2015. A role for Adaptor Protein complex 1 in biogenesis and protein targeting to rhoptry organelles in Plasmodium falciparum.

Kirchhausen, T., Bonifacino, J.S. & Riezman, H., 1997. Linking cargo to vesicle formation: receptor tail interactions with coat proteins. *Current Opinion in Cell Biology*, 9(4), pp.488–495.

Kirkham, M. & Parton, R.G., 2005. Clathrin-independent endocytosis: new insights into caveolae and non-caveolar lipid raft carriers. *Biochimica et biophysica acta*, 1745(3), pp.273–86.

Kobayashi, T., Sato, S., Takamiya, S., Komaki-Yasuda, K., Yano, K., Hirata, A., Onitsuka, I., Hata, M., Mi-ichi, F., Tanaka, T., Hase, T., Miyajima, A., Kawazu, S., Watanabe, Y. & Kita, K., 2007. Mitochondria and apicoplast of Plasmodium falciparum: behaviour on subcellular fractionation and the implication. *Mitochondrion*, 7(1-2), pp.125–32.

Kono, M., Herrmann, S., Loughran, N.B., Cabrera, A., Engelberg, K., Lehmann, C., Sinha, D., Prinz, B., Ruch, U., Heussler, V., Spielmann, T., Parkinson, J. & Gilberger, T.W., 2012.

Evolution and architecture of the inner membrane complex in asexual and sexual stages of the malaria parasite. *Molecular biology and evolution*, 29(9), pp.2113–32.

Konopka, C.A., Schleede, J.B., Skop, A.R. & Bednarek, S.Y., 2006. Dynamin and cytokinesis. *Traffic (Copenhagen, Denmark)*, 7(3), pp.239–47.

Labrousse, A.M., Zappaterra, M.D., Rube, D.A. & van der Bliek, A.M., 1999. C. elegans Dynamin-Related Protein DRP-1 Controls Severing of the Mitochondrial Outer Membrane. *Molecular Cell*, 4(5), pp.815–826.

Lazarus, M.D., Schneider, T.G. & Taraschi, T.F., 2008. A new model for hemoglobin ingestion and transport by the human malaria parasite Plasmodium falciparum. *Journal of cell science*, 121(Pt 11), pp.1937–49.

Lee, A., Frank, D.W., Marks, M.S. & Lemmon, M.A., 1999. Dominant-negative inhibition of receptor-mediated endocytosis by a dynamin-1 mutant with a defective pleckstrin homology domain. *Current Biology*, 9(5), pp.261–265.

Lenz, M., Morlot, S. & Roux, A., 2009. Mechanical requirements for membrane fission: common facts from various examples. *FEBS letters*, 583(23), pp.3839–46.

Li, H., Han, Z., Lu, Y., Lin, Y., Zhang, L., Wu, Y. & Wang, H., 2004. Isolation and functional characterization of a dynamin-like gene from Plasmodium falciparum. *Biochemical and Biophysical Research Communications*, 320, pp.664–671.

Li, X. & Gould, S.J., 2003. The dynamin-like GTPase DLP1 is essential for peroxisome division and is recruited to peroxisomes in part by PEX11. *The Journal of biological chemistry*, 278(19), pp.17012–20.

Marks, M.S., Ohno, H., Kirchhausen, T. & Bonifacino, J.S., 1997. Protein sorting by tyrosine-based signals: Adapting to the Ys and wherefores. *Trends in Cell Biology*, 7(March), pp.124–128.

Marshall, T.W., Aloor, H.L. & Bear, J.E., 2009. Coronin 2A regulates a subset of focal-adhesion-turnover events through the cofilin pathway. *Journal of cell science*, 122(Pt 17), pp.3061–3069.

Martin, R.E., Henry, R.I., Abbey, J.L., Clements, J.D. & Kirk, K., 2005. The "permeome" of the malaria parasite: an overview of the membrane transport proteins of Plasmodium falciparum. *Genome biology*, 6(3), p.R26. A

Mullins, C., Hartnell, L.M. & Bonifacino, J.S., 2000. Distinct requirements for the AP-3 adaptor complex in pigment granule and synaptic vesicle biogenesis in Drosophila melanogaster. *MGG - Molecular and General Genetics*, 263(6), pp.1003–1014.

Muralidharan, V. & Goldberg, D.E., 2013. Asparagine Repeats in Plasmodium falciparum Proteins : Good for Nothing ? , 9(8), pp.8–11.

Ngô, H.., Yang, M., Paprotka, K., Pypaert, M., Hoppe, H. & Joiner, K.., 2003. AP-1 in Toxoplasma gondii mediates biogenesis of the rhoptry secretory organelle from a post-Golgi compartment. *Journal of Biological Chemistry*, 278(7), pp.5343–5352.

Niedergang, F. & Chavrier, P., 2004. Signaling and membrane dynamics during phagocytosis: many roads lead to the phagos(R)ome. *Current opinion in cell biology*, 16(4), pp.422–8.

Niemann, H.H., Knetsch, M.L., Scherer, A., Manstein, D.J. & Kull, F.J., 2001. Crystal structure of a dynamin GTPase domain in both nucleotide-free and GDP-bound forms. *The EMBO journal*, 20(21), pp.5813–21.

Nothwehr, S.F., 1995. Golgi and vacuolar membrane proteins reach the vacuole in vps1 mutant yeast cells via the plasma membrane. *The Journal of Cell Biology*, 129(1), pp.35–46.

Owen, D.J., 1998. A Structural Explanation for the Recognition of Tyrosine-Based Endocytotic Signals. *Science*, 282(5392), pp.1327–1332.

Owen, D.J. & Luzio, J.P., 2000. Structural insights into clathrin-mediated endocytosis. *Current Opinion in Cell Biology*, 12(4), pp.467–474.

Patino, M.M., Liu, J.-J., Glover, J.R. & Lindquist, S., 1996. Support for the Prion Hypothesis for Inheritance of a Phenotypic Trait in Yeast. *Science*, 273(5275), pp.622–626..

Pimenta, P.F., Touray, M. & Miller, L., 1994. The Journey of Malaria Sporozoites in the Mosquito Salivary Gland. *The Journal of Eukaryotic Microbiology*, 41(6), pp.608–624.

Pitts, K.R., Yoon, Y., Krueger, E.W. & McNiven, M.A., 1999. The Dynamin-like Protein DLP1 Is Essential for Normal Distribution and Morphology of the Endoplasmic Reticulum and Mitochondria in Mammalian Cells. *Molecular Biology of the Cell*, 10(12), pp.4403–4417.

Pollard, T.D., Blanchoin, L. & Mullins, R.D., 2003. Molecular Mechanisms Controlling Actin Filament Dynamics in Nonmuscle Cells.

Praefcke, G.J.K. & McMahon, H.T., 2004. The dynamin superfamily: universal membrane tubulation and fission molecules? *Nature reviews. Molecular cell biology*, 5(2), pp.133–47.

Price, R.N., Tjitra, E., Guerra, C. a, Yeung, S., White, N.J. & Anstey, N.M., 2007. Vivax malaria: neglected and not benign. *The American journal of tropical medicine and hygiene*, 77(6 Suppl), pp.79–87.

Prommana, P., Uthaipibull, C., Wongsombat, C., Kamchonwongpaisan, S., Yuthavong, Y., Knuepfer, E., Holder, A.A. & Shaw, P.J., 2013. Inducible knockdown of Plasmodium gene expression using the glmS ribozyme. *PloS one*, 8(8), p.e73783.

Przyborski, J.M., Miller, S.K., Pfahler, J.M., Henrich, P.P., Rohrbach, P., Crabb, B.S. & Lanzer, M., 2005. Trafficking of STEVOR to the Maurer's clefts in Plasmodium falciparum-infected erythrocytes. *The EMBO journal*, 24(13), pp.2306–17.

Ramachandran, R., 2011. Vesicle scission: dynamin. *Seminars in cell & developmental biology*, 22(1), pp.10–7.

Rapoport, I., Chen, Y.C., Cupers, P., Shoelson, S.E. & Kirchhausen, T., 1998. Dileucine-based sorting signals bind to the beta chain of AP-1 at a site distinct and regulated differently from the tyrosine-based motif-binding site. *The EMBO journal*, 17(8), pp.2148–55.

Rappleye, C.A., Paredez, A.R., Smith, C.W., McDonald, K.L. & Aroian, R. V, 1999. The coronin-like protein POD-1 is required for anterior-posterior axis formation and cellular architecture in the nematode caenorhabditis elegans. *Genes & development*, 13(21), pp.2838–51.

Ridzuan, M. a M., Moon, R.W., Knuepfer, E., Black, S., Holder, A. a & Green, J.L., 2012. Subcellular location, phosphorylation and assembly into the motor complex of GAP45 during Plasmodium falciparum schizont development. *PloS one*, 7(3), p.e33845.

Riglar, D.T., Richard, D., Wilson, D.W., Boyle, M.J., Dekiwadia, C., Turnbull, L., Angrisano, F., Marapana, D.S., Rogers, K.L., Whitchurch, C.B., Beeson, J.G., Cowman, A.F., Ralph, S.A. & Baum, J., 2011. Super-resolution dissection of coordinated events during malaria parasite invasion of the human erythrocyte. *Cell host & microbe*, 9(1), pp.9–20.

Roberts, L., Egan, T.J., Joiner, K. a & Hoppe, H.C., 2008. Differential effects of quinoline antimalarials on endocytosis in Plasmodium falciparum. *Antimicrobial Agents and Chemotherapy*, 52(5), pp.1840–1842.

Robinson, M.S. & Bonifacino, J.S., 2001. Adaptor-related proteins. *Current Opinion in Cell Biology*, 13(4), pp.444–453.

Rosenthal, P.J., 1995. Plasmodium falciparum: effects of proteinase inhibitors on globin hydrolysis by cultured malaria parasites. *Experimental parasitology*, 80(2), pp.272–281.

Rybakin, V., Stumpf, M., Schulze, A., Majoul, I. V, Noegel, A.A. & Hasse, A., 2004. Coronin 7, the mammalian POD-1 homologue, localizes to the Golgi apparatus. *FEBS letters*, 573(1-3), pp.161–7.

Sampath, P. & Pollard, T.D., 1991. Effects of cytochalasin, phalloidin and pH on the elongation of actin filaments. *Biochemistry*, 30(7), pp.1973–1980.

Schmid, E.M., Ford, M.G.J., Burtey, A., Praefcke, G.J.K., Peak-Chew, S.-Y., Mills, I.G., Benmerah, A. & McMahon, H.T., 2006. Role of the AP2 beta-appendage hub in recruiting partners for clathrin-coated vesicle assembly. *PLoS biology*, 4(9), p.e262.

Schmid, E.M. & McMahon, H.T., 2007. Integrating molecular and network biology to decode endocytosis. *Nature*, 448(7156), pp.883–888.

Schrevel, J., Asfaux-Foucher, G., Hopkins, J.M., Robert, V., Bourgouin, C., Prensier, G. & Bannister, L.H., 2008. Vesicle trafficking during sporozoite development in Plasmodium

berghei: ultrastructural evidence for a novel trafficking mechanism. *Parasitology*, 135(Pt 1), pp.1–12.

Sesaki, H., 1999. Division versus Fusion: Dnm1p and Fzo1p Antagonistically Regulate Mitochondrial Shape. *The Journal of Cell Biology*, 147(4), pp.699–706. A

Sever, S., Muhlberg, A.B. & Schmid, S.L., 1999. Impairment of dynamin's GAP domain stimulates receptor-mediated endocytosis. *Nature*, 398(6727), pp.481–6.

Shim, J., Sternberg, P.W. & Lee, J., 2000. Distinct and Redundant Functions of 1 Medium Chains of the AP-1 Clathrin-Associated Protein Complex in the Nematode Caenorhabditis elegans. *Molecular Biology of the Cell*, 11(8), pp.2743–2756.

Shina, M.C., Unal, C., Eichinger, L., Müller-Taubenberger, A., Schleicher, M., Steinert, M. & Noegel, A.A., 2010. A Coronin7 homolog with functions in actin-driven processes. *The Journal of biological chemistry*, 285(12), pp.9249–61.

Si, K., Choi, Y.-B., White-Grindley, E., Majumdar, A. & Kandel, E.R., 2010. Aplysia CPEB can form prion-like multimers in sensory neurons that contribute to long-term facilitation. *Cell*, 140(3), pp.421–35.

Sigismund, S., Confalonieri, S., Ciliberto, a., Polo, S., Scita, G. & Di Fiore, P.P., 2012. Endocytosis and Signaling: Cell Logistics Shape the Eukaryotic Cell Plan. *Physiological Reviews*, 92(1), pp.273–366.

Simmen, T., Höning, S., Icking, A., Tikkanen, R. & Hunziker, W., 2002. AP-4 binds basolateral signals and participates in basolateral sorting in epithelial MDCK cells. *Nature cell biology*, 4(2), pp.154–9.

Simpson, F., 1996. A novel adaptor-related protein complex. *The Journal of Cell Biology*, 133(4), pp.749–760.

Simpson, F., Peden, a a, Christopoulou, L. & Robinson, M.S., 1997. Characterization of the adaptor-related protein complex, AP-3. *The Journal of cell biology*, 137(4), pp.835–45..

Singh, G.P., Chandra, B.R., Bhattacharya, A., Akhouri, R.R., Singh, S.K. & Sharma, A., 2004. Hyper-expansion of asparagines correlates with an abundance of proteins with prion-like domains in Plasmodium falciparum. *Molecular and biochemical parasitology*, 137(2), pp.307–19.

Smirnova, E., Shurland, D.-L., Ryazantsev, S.N. & Van der Bliek, a M., 1998. A human dynamin-related protein controls the distribuition of mitochondria. *J. Cell Biol.*, 143(2), pp.351–358.

Stephens, D. & Banting, G., 1998. Specificity of interaction between adaptor-complex medium chains and the tyrosine-based sorting motifs of TGN38 and lgp120. *Biochem. J*, 335, pp.567–572.

Stowell, M.H.B., Marks, B., Wigge, P. & McMahon, H.T., 1999. Nucleotide-dependent conformational changes in dynamin: evidence for a mechanochemical molecular spring. *Nature Cell Biology*, 1(1), pp.27–32.

Sweitzer, S.M. & Hinshaw, J.E., 1998. Dynamin Undergoes a GTP-Dependent Conformational Change Causing Vesiculation. *Cell*, 93(6), pp.1021–1029.

Talman, A.M., Domarle, O., McKenzie, F.E., Ariey, F. & Robert, V., 2004. Gametocytogenesis : the puberty of Plasmodium falciparum. *Malaria Journal*, 3(1), p.24.

Taraschi, T.F., O'Donnell, M., Martinez, S., Schneider, T., Trelka, D., Fowler, V.M., Tilley, L. & Moriyama, Y., 2003. Generation of an erythrocyte vesicle transport system by Plasmodium falciparum malaria parasites. *Blood*, 102(9), pp.3420–6.

Tardieux, I., Liu, X., Poupel, O., Parzy, D., Dehoux, P. & Langsley, G., 1998. A Plasmodium falciparum novel gene encoding a coronin-like protein which associates with actin filaments. *FEBS letters*, 441(2), pp.251–6.

Thompson, H.M., Skop, A.R., Euteneuer, U., Meyer, B.J. & McNiven, M.A., 2002. The Large GTPase Dynamin Associates with the Spindle Midzone and Is Required for Cytokinesis. *Current Biology*, 12(24), pp.2111–2117.

Trampuz, A., Jereb, M., Muzlovic, I. & Prabhu, R.M., 2003. Clinical review: Severe malaria. *Critical Care*, 7(4), pp.315–323.

Traub, L.M., 2009. Tickets to ride: selecting cargo for clathrin-regulated internalization. *Nature reviews. Molecular cell biology*, 10(9), pp.583–96.

Tremp, A.Z. & Dessens, J.T., 2011. Malaria IMC1 membrane skeleton proteins operate autonomously and participate in motility independently of cell shape. *Journal of Biological Chemistry*, 286(7), pp.5383–5391.

Tremp, A.Z., Khater, E.I. & Dessens, J.T., 2008. IMC1b is a putative membrane skeleton protein involved in cell shape, mechanical strength, motility, and infectivity of malaria ookinetes. *Journal of Biological Chemistry*, 283(41), pp.27604–27611.

Trowbridge, I.S., Collawn, J.F. & Hopkins, C.R., 1993. Signal-dependent membrane protein trafficking in the endocytic pathway. *Annual review of cell biology*, 9, pp.129–61.

Tse, S.M.L., Furuya, W., Gold, E., Schreiber, A.D., Sandvig, K., Inman, R.D. & Grinstein, S., 2003. Differential role of actin, clathrin, and dynamin in Fc gamma receptor-mediated endocytosis and phagocytosis. *The Journal of biological chemistry*, 278(5), pp.3331–8.

Uetrecht, A.C. & Bear, J.E., 2006. Coronins: the return of the crown. *Trends in cell biology*, 16(8), pp.421–6.

Ungewickell, E.J. & Hinrichsen, L., 2007. Endocytosis: clathrin-mediated membrane budding. *Current opinion in cell biology*, 19(4), pp.417–25.

Vallis, Y., Wigge, P., Marks, B., Evans, P.R. & McMahon, H.T., 1999. Importance of the pleckstrin homology domain of dynamin in clathrin-mediated endocytosis. *Current Biology*, 9(5), pp.257–263.

Vetter, I.R. & Wittinghofer, A., 2001. The guanine nucleotide-binding switch in three dimensions. *Science (New York, N.Y.)*, 294(5545), pp.1299–304.

Weiss, G.E., Gilson, P.R., Taechalertpaisarn, T., Tham, W.-H., de Jong, N.W.M., Harvey, K.L., Fowkes, F.J.I., Barlow, P.N., Rayner, J.C., Wright, G.J., Cowman, A.F. & Crabb, B.S., 2015. Revealing the Sequence and Resulting Cellular Morphology of Receptor-Ligand Interactions during Plasmodium falciparum Invasion of Erythrocytes. *PLoS Pathogens*, 11(2), p.e1004670.

Wetzel, D.M., Håkansson, S., Hu, K., Roos, D. & Sibley, L.D., 2003. Actin filament polymerization regulates gliding motility by apicomplexan parasites. *Molecular biology of the cell*, 14(2), pp.396–406.

Wong, E.D., Wagner, J. a., Scott, S. V., Okreglak, V., Holewinske, T.J., Cassidy-Stone, A. & Nunnari, J., 2003. The intramitochondrial dynamin-related GTPase, Mgm1p, is a component of a protein complex that mediates mitochondrial fusion. *Journal of Cell Biology*, 160(3), pp.303–311.

Wu, Y., Sifri, C.D., Lei, H.H., Su, X.Z. & Wellems, T.E., 1995. Transfection of Plasmodium falciparum within human red blood cells. *Proceedings of the National Academy of Sciences of the United States of America*, 92(4), pp.973–7.

Van Wye, J., Ghori, N., Webster, P., Mitschler, R.R., Elmendorf, H.G. & Haldar, K., 1996. Identification and localization of rab6, separation of rab6 from ERD2 and implications for an “unstacked” Golgi, in Plasmodium falciparum. *Molecular and Biochemical Parasitology*, 83(1), pp.107–120.

Yoon, H.-G., Chan, D.W., Huang, Z.-Q., Li, J., Fondell, J.D., Qin, J. & Wong, J., 2003. Purification and functional characterization of the human N-CoR complex: the roles of HDAC3, TBL1 and TBLR1. *The EMBO journal*, 22(6), pp.1336–46.

Zhou, H., Gao, Y., Zhong, X. & Wang, H., 2009. Dynamin like protein 1 participated in the hemoglobin uptake pathway of Plasmodium falciparum. *Chinese medical journal*, 122(14), pp.1686–91.

APPENDIX A

Composition of non-commercial reagents

All reagents used were made up using purified water produced by the MilliQ Water System (Millipore Corp, USA), unless otherwise stated. Heat sterilizations were carried out in an autoclave (Sturdy, Taiwan). Filter sterilizations were performed using 0.22 μM filters (Gilson, United Kingdom). pH values were measured and adjusted using a Crison 20 pH meter (Crison Instruments, Spain). All reagents were stored at room temperature unless otherwise stated.

Acrylamide (30%)

Dissolve 30 g Acrylamide and 0.8 g *bis*-acrylamide in 100 mL, stored at 4 °C

Agar Plates (Luria agar)

30.5g of Luria Broth Agar was dissolved in 1 L water and autoclaved

Once cooled to below 60 °C, ampicillin or kanamycin was added to a final concentration of 100 μg/mL

Whilst working under a flame, solution was poured into sterile petri dishes and allowed to cool

Stored at 4 °C

Agarose Gel (0.8%)

0.4 g agarose and dissolved in 50 mL 1x TBE buffer (by heating in a microwave)

Once cooled to below 60 °C, add 12 μL of 10 mg/mL ethidium bromide

Ammonium persulphate (10%)

0.1 g APS was dissolved in 1 mL water immediately before use

Ampicillin (1 mg/mL)

10 mg of ampicillin was dissolved in 10 mL water

Aliquots stored at -20 °C for long-term and 4 °C for short-term

Complete RPMI 1640 culture medium

Whilst working under aseptic conditions in a laminar flow hood:

2.5 g Albumax II dissolved in 25 mL incomplete RPMI 1640 medium

2 g glucose dissolved in 25 mL incomplete RPMI 1640 medium

44 mg hypoxanthine dissolved in 500 µL 1M NaOH

500 µL gentamicin solution

The above constituents were combined and filtered sterilized into 450 mL incomplete RPMI 1640 medium, and stored at 4 °C

Cytomix (2x)

1.789 g KCl, 300 µL of a 0.1 M stock of $CaCl_2$, 95.2 mg $MgCl_2$, 152 mg EGTA, 0.595 g Hepes and 384 mg of K_2PO_4 was dissolved in 100 mL water.

Adjust pH to 7.6 using KOH, filter sterilize and stored at 4 °C

Cytomix (1x)

2x cytomix was diluted in half with 25 mM Hepes to obtain 1x cytomix and stored at 4 °C

DAPI

1 µg/mL DAPI in 1x PBS, stored at -20 °C

D-sorbitol (5%)

2.5 g D-sorbitol dissolved in 50 mL water, filter sterilized and stored at 4 °C

Ethanol (70%)

7 mL absolute ethanol was made up to a total volume of 10 mL

Ethidium bromide

100 mg ethidium bromide dissolved in 10 mL water and stored in the dark

Freezing solution (28% glycerol)

14 mL glycerol dissolved in 36 mL PBS and filter sterilized, stored at 4 °C

Giemsa stain

1 mL Giemsa modified solution made up to 10 mL with PBS and stored in the dark

GTE buffer (pH 8.0)

30 mM glucose, 25 mM Tris, 10 mM EDTA, up to 10 μg/mL RNase A

Stored at 4 °C

Hepes (25 mM)

0.595 g of Hepes dissolved in 100 mL water

Adjust pH to 7.6 with KOH, filter sterilized and stored at 4 °C

Hoechst (*bis*-Benzemide H 33258)

1 μg/mL in 1x PBS and stored at -20°C

Incubation buffer (for Western blot)

TBS-Tween 20 containing 1% BSA and 2% milk powder and stored at 4°C

Lower Gel buffer

Dissolve 18.2.g Tris, and 0.4 g SDS in 100 mL water.

Adjust pH to 8.8 with HCl

Luria Broth (Contains 10 g/L tryptone, 5 g/L yeast extract and 5 g/L NaCl)

Dissolve 20 g of the LB broth powder in 1 L water

Autoclaved and stored at 4 °C

NaOH/SDS Lysis solution

0.2 N NaOH and SDS 1% (w/v)

Percoll (60%)

6 mL Percoll was mixed with 4 mL 2.5x RPMI/12.5% sorbitol

The solution was filter sterilized and stored at 4 °C

Phosphate buffered saline (PBS, pH 7.4)

Dissolve 1 PBS tablet in 200 mL water

Autoclaved, and stored at 4 °C

Ponceau S stain

0.1% Ponceau S in 1% acetic acid

Ponceau S destain

1% acetic acid

Potassium acetate solution (5M, pH 4.8)

29.5 mL acetic acid made up to 70 mL in water, and KOH pellets were added until the pH reaches 4.8

The solution is made up to a total volume of 100 mL in water

2.5x RPMI/12.5% sorbitol

1.045 g RPMI 1640 powder and 5.0 g sorbitol was dissolved in 40 mL water

pH adjusted to 7.0 with KOH, the solution was filter sterilized and stored at 4 °C

Sample loading buffer (for AGE)

7 mL 1x TBE added to 3 mL glycerol and 0.025 g bromophenol blue and stored at 4 °C

Sample loading buffer (4x, for SDS-PAGE)

0.8 g SDS, 0.8 mL 2-mercaptoethanol and 0.2 mg bromophenol blue was dissolved in 10 mL stacking buffer, 8 mL glycerol, and 1.2 mL water

Saponin (5%)

0.5 g saponin dissolved in 10 mL water and stored at 4 °C

SDS-PAGE running buffer (5x)

Dissolve 15.1 g Tris, 72 g Glycine and 5 g SDS in 1 litre water and adjusted to pH 8.4

Sodium dodecyl sulphate (SDS, 18%)

9 g SDS dissolved in 50 mL water

Sodium chloride (12%)

6 g NaCl dissolved in 50 mL water, filter sterilized and stored at 4 °C

Sodium chloride (1.2%)

0.6 g NaCl dissolved in 50 mL water, filter sterilized and stored at 4 °C

Sodium hydroxide (1M)

1 g NaOH dissolved in 50 mL water

Stacking Gel buffer

Dissolve 6.05.g Tris, and 0.4 g SDS in 100 mL water, adjusted pH to 6.8 with HCl

TBE buffer (10x)

27.5 g Tris, 13.75 g boric acid, and 3.72 g EDTA dissolved in 1 L water. Dilute to 1x in water

Transblot buffer

3.029 g Tris and 14.4 g glycine dissolved in 800 mL and 200 mL methanol

Tris buffered saline

1.2 g Tris and 4.5 g NaCl dissolved in 500 mL water, adjusted pH to 7.4 with HCl

TBS-T (Western blot washing solution)

Add 0.1% Tween 20 to Tris buffered saline

Triton X-100 (0.1%)

15 µL Triton X-100 dissolved in 15 mL PBS

WR99210 (10 µM)

A 10 mM stock was first prepared by dissolving 3.95 mg in 1 mL DMSO and stored at -20 °C.

10 µL of this stock was diluted in 10 mL complete culture media resulting in a 10 µM stock and stored at 4 °C.

In order to obtain a final concentration of 2.5 nM in complete media for selecting transfectants, 125 µL of the 10 µM stock was added to 500 mL of complete RPMI 1640 media.

APPENDIX B

Amino acid sequences used for generating sequence alignments

Coronin

Human coronin 1A

>gi|300934762|ref|NP_001180262.1| coronin-1A [Homo sapiens]
MSRQVVRSSKFRHVFGQPAKADQCYEDVRVSQTTWDSGFCAVNPKFVALICEASGGGAFLVLPLGKTGRVDKNAPTV
CGHTAPVLDIAWCPHNDNVIASGSEDCTVMVWEIPDGGLMLPLREPVVTLEGHTKRVGIVAWHTTAQNVLLSAGCDN
VIMVWDVGTGAAMLTLGPEVHPDTIYSVDWSRDGGLICTSCRDKRVRIIEPRKGTVVAEKDRPHEGTRPVRAVFVSE
GKILTTGFSRMSERQVALWDTKHLEEPLSLQELDTSSGVLLPFFDPDTNIVYLCGKGDSSIRYFEITSEAPFLHYLS
MFSSKESQRGMGYMPKRGLEVNKCEIARFYKLHERRCEPIAMTVPRKSDLFQEDLYPPTAGPDPALTAEEWLGGRDA
GPLLISLKDGYVPPKSRELRVNRGLDTGRRRAAPEASGTPSSDAVSRLEEEMRKLQATVQELQKRLDRLEETVQAK

Parasite coronin

PlasmoDB: PF3D71251200
MYNVPLIKNLYPDPSNNLYGDLRICSRATETCGIACSAGYIAVPWQVEGGGMIGVIRLENQVRNPPVIKLKSHTSPI
LDLSFNPCYSEILASCSEDMSIRIWEIRHEDENVNEVKDPLCILNGHKKKVNILSWNPMNYFILSSTSFDSSVNIWD
IENEKKAFEINMPKKLSSLQWDIGGNLLSGTCQNKQIHIIDPRKQEICNSFLIHDGGKSTKCIWIDGFGGEDKCILT
TGFSKNNMRELKLWSLKNTTSPLTTITLDNAASPLLPHYDESVGMIYLIGKGDGNCRYYQYSQGSIRKVDEYKSCLP
FRSFGFLPKRMCDVYKCEIGRVYKNENNTDIRPISFYVPRKNSSIFQEDLYPPIIMRDPERSTNKWIDGINLDIKRV
SIKDLTEDDLLITKKFKQLPKESKSILIQDNNNPKKGSVMRQFTKKFTFRKKKETTEIQGEIMGETKSSIEADFEPQ
ECKENKKGNKLNEAPKFLFACEDVEICHLKDNVDDDDYLIVNGTNEPYEETVIKTNENENYKENNDSSIQSIRSNSK
SIEKNDDDNNNNNDNDNTLQSEENEEHLKHISSIHEENNFKNFFKNVLDNILDMKMCKSTATVL

Dynamin 2

Human dynamin 2

>gi|56549119|ref|NP_004936.2| dynamin-2 isoform 3 [Homo sapiens]
MGNRGMEELIPLVNKLQDAFSSIGQSCHLDLPQIAVVGGQSAGKSSVLENFVGRDFLPRGSGIVTRRPLILQLIFSK
TEHAEFLHCKSKKFTDFDEVRQEIEAETDRVTGTNKGISPVPINLRVYSPHVLNLTLIDLPGITKVPVGDQPPDIEY
QIKDMILQFISRESSLILAVTPANMDLANSDALKLAKEVDPQGLRTIGVITKLDLMDEGTDARDVLENKLLPLRRGY
IGVVNRSQKDIEGKKDIRAALAAERKFFLSHPAYRHMADRMGTPHLQKTLNQQLTNHIRESLPALRSKLQSQLLSLE
KEVEEYKNFRPDDPTRKTKALLQMVQQFGVDFEKRIEGSGDQVDTLELSGGARINRIFHERFPFELVKMEFDEKDLR
REISYAIKNIHGVRTGLFTPDLAFEAIVKKQVVKLKEPCLKCVDLVIQELINTVRQCTSKLSSYPRLREETERIVTT
YIREREGRTKDQILLLIDIEQSYINTNHEDFIGFANAQQRSTQLNKKRAIPNQVIRRGWLTINNISLMKGGSKEYWF
VLTAESLSWYKDEEEKEKKYMLPLDNLKIRDVEKGFMSNKHVFAIFNTEQRNVYKDLRQIELACDSQEDVDSWKASF
LRAGVYPEKDQAENEDGAQENTFSMDPQLERQVETIRNLVDSYVAIINKSIRDLMPKTIMHLMINNTKAFIHHELLA
YLYSSADQSSLMEESADQAQRRDDMLRMYHALKEALNIIGDISTSTVSTPVPPPVDDTWLQSASSHSPTPQRRPVSS
IHPPGRPPAVRGPTPGPPLIPVPVGAAASFSAPPIPSRPGPQSVFANSDLFPAPPQIPSRPVRIPPGIPPGVPSRRP
PAAPSRPTIIRPAEPSLLD

Parasite dynamin 2

PlasmoDB: PF3D71037500
MDKLVPIVNKLQNVLSSFISSETLSLPHIAVVGAQSVGKTSLLESLVGLSFMPKGEDIVTRTPIIIQLTNSKSDDCY
CTLTYCDYDNNRVEKHIDDFSILNEILIDVTEEITGGNKCIKETPIIIEIHKNDVLDLTLIDLPGLTKVPVGNQPQN
VEEQIVNLVNKYIKNPNCIILAVSSANIDLANSDSLKMARNVDPKHERTIGVITKCDMVEKPEIWKKMISGSLYPLK
KGFVAVVCRSQKDVEDDITIEMSIKKEEEYFSQCIDFSNQMECIMECGIKNLAKKLNNILIEHIKNTVPFLKPKIDS
LKSIEEERLLELGEPMDNMNRSEYLAVLVNYITKFSQQYQDIIDGKVFYKDRVDELKGGARIHYIFNDWYIKSLNDF
SPLEMLTDEEIRIAIRNSSGPRGALFVPESAFETLIKKLINCLKEPSLRCADQVYEELLKIVDNCRIADMERFTNLK
SAINEQVKILLKDCLQPTKEMIKNLMLIELSYINTSHPDFLNEHFMKNVYDKDNDYIDELDTVVHPKHNHKMLQRPK
REYQETCGSNMNYSTIHHNNTYKEEMKMWKHKEDAKSFRNKEGTKITNINNNRENVFVLPVIPEKIIPEYSSSSKEI
IEIDLIKSLINNYFNIVRKHIADAVPKAIMHFMVNTSRKTMQKVLISNLHNGELFNLFNECSSIKVKRNNCKKNLES
LNQAIKMLAEIRNQEV

μ4 adaptin

Human μ4

>sp|O00189|AP4M1_HUMAN AP-4 complex subunit mu-1 OS=Homo sapiens GN=AP4M1
PE=1 SV=2
MISQFFILSSKGDPLIYKDFRGDSGGRDVAELFYRKLTGLPGDESPVVMHHHGRHFIHIRHSGLYLVVTTSENVSPF
SLLELLSRLATLLGDYCGSLGEGTISRNVALVYELLDEVLDYGYVQTTSTEMLRNFIQTEAVVSKPFSLFDLSSVGL
FGAETQQSKVAPSSAASRPVLSSRSDQSQKNEVFLDVVERLSVLIASNGSLLKVDVQGEIRLKSFLPSGSEMRIGLT
EEFCVGKSELRGYGPGIRVDEVSFHSSVNLDEFESHRILRLQPPQGELTVMRYQLSDDLPSPLPFRLFPSVQWDRGS
GRLQVYLKLRCDLLSKSQALNVRLHLPLPRGVVSLSQELSSPEQKAELAEGALRWDLPRVQGGSQLSGLFQMDVPGP
PGPPSHGLSTSASPLGLGPASLSFELPRHTCSGLQVRFLRLAFRPCGNANPHKWVRHLSHSDAYVIRI

Parasite μ4

PlasmoDB: PF3D71119500
MVISQFYILSPRGDTIINRDFRGDIIKGSAEVFFRNVKLYKGDAPPVFYLNGINFTYLKSNSLYFVVTSLFNISPSY
LIELLHRLLKIFKDFCGQITEELIRTNFILIYEIIDEIIDYGYLQNSNTEYIKNLIHNEIATNNNTVKKFANLPNFS
IKNTNTLPSNASQKPIQINDKKNEIFIDIVEKINLIMNSNGEIVYSYIDGVIQIKSYLLGNPFIKIALNDDLYIKNI
HHDNSNNIIIDDCNFNHLVNLSQFEKDKILSLYQPDGECVLMNYRINNNFKAPFKIYANVIYNQNHTVELCIRIRLD
IPSQYTCTNVFVYCNLCKHITNVHLDLNTNSDLFSAQYISNENKLLWTIKKFKGEHEYSIRSKITLSPHYAFSKRDF
GPIYILFEIPMFNLSKLRIKYLRIIENYKTSNTHRWVRYITQSSSYVYRLN

Summary of sequencing (sequencing performed by Inqaba Biotech, South Africa)

pARL2-GFP multiple cloning site

```
                                                                      XhoI
1441   TCATATTATTTATTATACATTCATTTATTATTTTGTTTTTTTTAATTTCTTACATATAA**C**
       AGTATAATAAATAATATGTAAGTAAATAATAAAACAAAAAAAATTAAAGAATGTATATT**G**

            AvrII       KpnI
1501   **TCGAG**CCTAGGGCGCGC**GGTACC** ATG AGT AAA GGA GAAGAACTTTTCACTGGAGTTGTCC
       **AGCTC**GGATCCCGCGCG**CCATGG** TAC TCA TTT CCT CTTCTTGAAAAGTGACCTCAACAGG
```

Sequencing result aligned with the Coronin sequence (from PlasmoDB)

```
Upper line: Plasmid 2_F, from 52 to 600
Lower line: Coronin, from 1 to 549
                                                        XhoI
1      TWWCATTCATTTATTATTTTGTTTTTTTTAATTTCTTACATATAACTCGAC**ATGTATAAT**
                                                           |||||||||
1      .....................................................**ATGTATAAT**
                                                  **Start of COR coding sequence**
61     GTTCCTTTAATCAAGAATTTATATCCTGATCCGTCAAATAACCTGTACGGAGACTTGAGG
       ||||||||||||||||||||||||||||||||||||||||||||||||||||||||||||
10     GTTCCTTTAATCAAGAATTTATATCCTGATCCGTCAAATAACCTGTACGGAGACTTGAGG

121    ATTTGCTCGAGAGCAACCGAAACATGTGGTATAGCTTGTAGTGCTGGATATATTGCTGTA
       ||||||||||||||||||||||||||||||||||||||||||||||||||||||||||||
70     ATTTGCTCGAGAGCAACCGAAACATGTGGTATAGCTTGTAGTGCTGGATATATTGCTGTA

181    CCATGGCAAGTTGAAGGGGGAGGAATGATCGGAGTTATCAGATTAGAAAATCAAGTGAGA
       ||||||||||||||||||||||||||||||||||||||||||||||||||||||||||||
130    CCATGGCAAGTTGAAGGGGGAGGAATGATCGGAGTTATCAGATTAGAAAATCAAGTGAGA

241    AATCCCCCTGTAATAAAATTGAAGAGTCATACATCTCCCATCCTTGATTTGTCATTTAAC
       ||||||||||||||||||||||||||||||||||||||||||||||||||||||||||||
190    AATCCCCCTGTAATAAAATTGAAGAGTCATACATCTCCCATCCTTGATTTGTCATTTAAC

301    CCGTGTTATAGTGAGATATTAGCTTCATGTTCAGAAGATATGTCTATAAGAATATGGGAG
       ||||||||||||||||||||||||||||||||||||||||||||||||||||||||||||
250    CCGTGTTATAGTGAGATATTAGCTTCATGTTCAGAAGATATGTCTATAAGAATATGGGAG

361    ATACGTCATGAGGATGAGAATGTGAATGAGGTAAAGGATCCTTTATGTATATTAAATGGT
       ||||||||||||||||||||||||||||||||||||||||||||||||||||||||||||
310    ATACGTCATGAGGATGAGAATGTGAATGAGGTAAAGGATCCTTTATGTATATTAAATGGT

421    CATAAGAAAAAAGTAAATATATTATCATGGAATCCTATGAATTATTTTATATTATCATCT
       ||||||||||||||||||||||||||||||||||||||||||||||||||||||||||||
370    CATAAGAAAAAAGTAAATATATTATCATGGAATCCTATGAATTATTTTATATTATCATCT

481    ACCTCTTTTGATTCTTCTGTTAATATATGGGATATAGAAAATGAGAAGAAAGCCTTTGAA
       ||||||||||||||||||||||||||||||||||||||||||||||||||||||||||||
430    ACCTCTTTTGATTCTTCTGTTAATATATGGGATATAGAAAATGAGAAGAAAGCCTTTGAA

541    ATAAATATGCCAAAGAAATTAAGTTCTTTACAATGGGATATCGGTGGTAATTTATTAAGT
       ||||||||||||||||||||||||||||||||||||||||||||||||||||||||||||
490    ATAAATATGCCAAAGAAATTAAGTTCTTTACAATGGGATATCGGTGGTAATTTATTAAGT
```

>2_pARL-R sequence exported from 2_pARL-R_A01_01.ab1

Reverse complimentary

```
                                                    coronin
1      TGCGGTGGAA GATCAACGTA TTGTAACAYG GTTTTTCAAA GGATAATATT GAAGAGGAAC
61     TGAACTATGA GTTAAAAGAA ATACGACATC ACCATAACTA CTATTACATT AGATAATGCT
121    GCTTCACCTT TATTACACAT TATGATGAGA GCGTAGGTAT GATTTATTTT GATAGGTAAA
181    GGTGATGGTA ATTGTCGTTA TTATCAATAT TCACAAGGTT CCATACGTAA AGTCGATGAA
241    TATAAATCGT GCTTACCTTT TAGATCTTTT GGATTTTTAC CTAAACGTAT GTGTGACGTA
301    TACAAATGTG AAATTGGTAG AGTATATAAA AATGAAAATA ACACAGATAT TAGACCCATA
361    TCTTTTTATG TACCTAGAAA GAATTCATCA ATATTTCAAG AAGATTTATA TYCTCCTATT
421    ATTATGAGAG ATCCTGAACG TAGTACAAAC AAATGGATTG ATGGTATAAA CCTAGATATT
481    AAAAGGGTGT YTATAAAGGA TTTAACCGAA GACGATTTAT TAATTACAAA AAAATTTAAA
541    CAACTTCCTA AGGAATCCAA AAGTATTYTT ATTCAAGATA ACAATAATCC TAAGAAGGGT
601    TYTGTCATGA GACAGTTTAC CAAAAAATTT ACCTTYAGAA AAAAAAAAGA AACTACAGAG
661    ATACAAGGAG AAATAATGGG GGAAACCAAA TCTTCGATTG AAGCTGATTT TGAACCACAA
721    GAATGTAAAG AAAATAAAAA AGGAAATAAA TTAAATGAAG CACCCAAATT TTTATTTGCT
781    TGTGAGGACG TTGAAATATG TCATTTGAAA GACAACGTGG ACGATGATGA CTATCTCATA
841    GTTAATGGAA CAAATGAGCC ATACGAAGAA ACTGTTATTA AAACAAATGA AAATGAGAAT
901    TATAAAGAAA ATAATGATAG TAGTATACAA AGTATAAGAA GTAATAGTAA AAGTATAGAA
961    AAGAATGATG ATGATAATAA TAATAATAAT AATGATAACA CACTCCAATC TGAAGAAAAT
1021   GAAGAACATC TTAAACATAT ATCTTCAATA CATGAAGAAA ATAATTTTAA GAATTTCTTC
1081   AAAAATGTAT TAGATAATAT ACTAGACATG AAAATGTGTA AAAGTACAGC AACGGTATTA
1141   GGTACCATGA GTAAAGGAGA AGACTGC            coronin
       KpnI  GFP coding sequence
```

Sequencing result aligned with the Dynamin 2 sequence (from PlasmoDB)

Upper line: Plasmid 1_F sequence, from 52 to 540
Lower line: Dynamin 2, from 1 to 489

```
                                                      AvrII
1      TWWCATTCATTTATTATTTTGTTTTTTTTAATTTCTTACATATAACTCGAGATGGATAAA
                                                           |||||||||
1      .....................................................ATGGATAAA
                                                 Start of DYN2 coding sequence
61     TTAGTACCGATTGTAAACAAATTACAGAATGTTTTATCATCTTTTATTAGTAGTGAAACC
       ||||||||||||||||||||||||||||||||||||||||||||||||||||||||||||
10     TTAGTACCGATTGTAAACAAATTACAGAATGTTTTATCATCTTTTATTAGTAGTGAAACC

121    TTGAGCTTACCACATATAGCAGTGGTAGGGGCTCAATCAGTTGGAAAAACCTCATTACTA
       ||||||||||||||||||||||||||||||||||||||||||||||||||||||||||||
70     TTGAGCTTACCACATATAGCAGTGGTAGGGGCTCAATCAGTTGGAAAAACCTCATTACTA

181    GAATCATTAGTAGGTTTAAGTTTTATGCCTAAAGGAGAAGATATAGTAACTCGGACTCCA
       ||||||||||||||||||||||||||||||||||||||||||||||||||||||||||||
130    GAATCATTAGTAGGTTTAAGTTTTATGCCTAAAGGAGAAGATATAGTAACTCGGACTCCA

241    ATAATAATTCAGCTAACGAATTCTAAATCAGATGATTGTTATTGTACCTTAACATATTGT
       ||||||||||||||||||||||||||||||||||||||||||||||||||||||||||||
190    ATAATAATTCAGCTAACGAATTCTAAATCAGATGATTGTTATTGTACCTTAACATATTGT

301    GATTATGATAATAATAGAGTAGAAAAACATATAGATGATTTTTCTATTTTGAATGAAATA
       ||||||||||||||||||||||||||||||||||||||||||||||||||||||||||||
250    GATTATGATAATAATAGAGTAGAAAAACATATAGATGATTTTTCTATTTTGAATGAAATA
```

```
361   TTAATTGACGTTACAGAAGAAATTACTGGGGGTAATAAATGCATTAAAGAAACTCCTATT
      |||||||||||||||||||||||||||||||||||||||| ||||||||||||||||||
310   TTAATTGACGTTACAGAAGAAATTACTGGGGGTAATAAATGTATTAAAGAAACTCCTATT

421   ATAATTGAGATTCATAAAAATGATGTTTTAGATTTAACTTTAATTGATTTACCTGGTTTA
      |||||||||||||||||||||||||||||||||||||||||||||||||||||||||||
370   ATAATTGAGATTCATAAAAATGATGTTTTAGATTTAACTTTAATTGATTTACCTGGTTTA

481   ACAAAAGTCCCTGTTGGGAATCAGCCACAAAATGTAGAGGAGCAAATAGTAAATTTAGTA
      |||||||||||||||||||||||||||||||||||||||||||||||||||||||||||
430   ACAAAAGTCCCTGTTGGGAATCAGCCACAAAATGTAGAGGAGCAAATAGTAAATTTAGTA
```

>1_pARL-R sequence exported from 1_pARL-R_H12_24.ab1

Reverse complimentary sequence

dynamin 2

```
1      GTTTATTTAG GTTAATTTWT ATTTAACAAA ACTTTCACAC CAGWATCCAG AWTAATAGAT
61     GGAAAGTTTT TATAAGATAG AGTGATGATA AAGGGTGGCG CAAGAATACA TATATATTTA
121    ATGATTGGTA TATAAAATCA TTAAATGATT TTTCACCATT AGAAATGTTA ACAGATGAAG
181    AAATTCGAAT AGCTATAAGA AATTCTAGTG GTCCAAGAGG AGCATTATTC GTACCAGAAA
241    GTGCTTTTGA AACTTTAATA AAAAAAATTA ATAAATTGTT TAAAGGAACC TTCACTTCGT
301    TGTGCTGATC AGGTATATGA AGAATTATTA AAAATAGTTG ATAATTGTCG TATAGCAGAT
361    ATGGAAAGAT TTACTAATTT AAAGAGTGCT ATAAATGAAC AAGTCAAAAT ATTATTAAAA
421    GATTGTTTAC AACCAACCAA AGAAATGATA AAAAATTTAA TGCTAATTGA ATTATCATAT
481    ATTAATACAA GTCATCCTGA CTTTTTAAAT GAACATTTTA TGAAAAATGT ATATGATAAA
541    GATAATGATT ATATAGATGA ATTAGATACA GTAGTTCACC CTAAACATAA TCATAAAATG
601    TTACAGCGTC CAAAAAGAGA ATATCAAGAA ACTTGTGGAA GTAATATGAA TTATTCAACT
661    ATACACCATA ATAATACATA TAAAGAAGAA ATGAAAATGT GGAGACATAA AGAAGATGCT
721    AAATCTTTTA GAAATAAAGA AGGTACCAAA ATTACTAATA TAAATAATAA TAGAGAAAAT
781    GTTTTTGTTT TACCAGTGAT TCCAGAAAAA ATTATACCAG AATATTCATC TTCATCTAAA
841    GAAATAATAG AAATTGACTT AATAAAATCG TTAATTAATA ATTATTTTAA TATTGTTAGA
901    AAACATATAG CAGATGCGGT ACCTAAAGCA ATTATGCATT TTATGGTTAA TACATCGAGA
961    AAAACTATGC AGAAAGTTTT AATATCAAAT TTACATAATG GGGAACTTTT CAACTTATTT
1021   AATGAATGTT CATCTATTAA AGTAAAAAGA AAWAACTGCA AAAAAAATCT GGAATCTTTA
1081   AATCAAGCAA TAAAAATGTT GGCCGAAATT AGAAACCAAG AAGTTCCTAG GGCGCGCGGT
1141   ACCATGAGTA AAGGAGAAGA CTTGC
```

dynamin 2 AvrII KpnI

GFP coding sequence

Sequencing result aligned with the μ4 sequence (from PlasmoDB)

```
Upper line: plasmid 3_F, from 52 to 420
Lower line: Mu4, from 1 to 369

                                                        XhoI
1     AWCATTCATTTTATTATTTTGTTTTTTTTAATTTCTTACATATAACTCGAGATGGTGATA
                                                          |||||||||
1     ..................................................ATGGTGATA
                                                  Start of μ4 coding sequence
61    TCCCAATTTTATATTTTGTCTCCAAGAGGGGATACCATTATTAATAGAGATTTTCGTGGA
      ||||||||||||||||||||||||||||||||||||||||||||||||||||||||||||
10    TCCCAATTTTATATTTTGTCTCCAAGAGGGGATACCATTATTAATAGAGATTTTCGTGGA

121   GATATAATAAAAGGTAGTGCCGAAGTATTTTTTCGAAATGTAAAATTATATAAAGGTGAT
      ||||||||||||||||||||||||||||||||||||||||||||||||||||||||||||
70    GATATAATAAAAGGTAGTGCCGAAGTATTTTTTCGAAATGTAAAATTATATAAAGGTGAT

181   GCACCTCCAGTTTTTTATTTGAATGGTATAAATTTTACATATTTGAAAAGTAATAGTTTA
      ||||||||||||||||||||||||||||||||||||||||||||||||||||||||||||
130   GCACCTCCAGTTTTTTATTTGAATGGTATAAATTTTACATATTTGAAAAGTAATAGTTTA

241   TATTTTGTAGTAACATCATTGTTTAATATTTCTCCAAGTTATTTAATTGAATTATTACAT
      ||||||||||||||||||||||||||||||||||||||||||||||||||||||||||||
190   TATTTTGTAGTAACATCATTGTTTAATATTTCTCCAAGTTATTTAATTGAATTATTACAT

301   CGGTTGCTAAAAATATTTAAAGATTTTTGTGGACAAATTACAGAAGAATTAATACGAACC
      ||||||||||||||||||||||||||||||||||||||||||||||||||||||||||||
250   CGGTTGCTAAAAATATTTAAAGATTTTTGTGGACAAATTACAGAAGAATTAATACGAACC

361   AATTTTATTTTAATATATGAAATAATAGATGAAATAATAGATTATGGTTATTTACAAAAT
      ||||||||||||||||||||||||||||||||||||||||||||||||||||||||||||
310   AATTTTATTTTAATATATGAAATAATAGATGAAATAATAGATTATGGTTATTTACAAAAT

>3_pARL-R sequence exported from 3_pARL-R_B01_04.ab1
```

Reverse complimentary

```
                          μ4
1      AGTAAAAACM ATTCATTGTT TTAATATTTC TGCAAGTATT TAGTTGACAT ACATCGCTGC
61     TAAAAAATAT TAAAGATTTC GTGGACAAAT TACAGAAGAA ATAAATACGA ACCAATTTTA
121    TTTTAATATA TGAAATAATA GATGAAATAA TAGATTATGG TTATTTACAA AATAGTAATA
181    CAGAATATAT AAAAAAATCT AATACATAAT GAAATAGCAA CAAATAATAA TACAGTGAAA
241    AAAATTTGCC AACCTACCTA ATTTTTCTAT AAAAAATACA AATACATTAC CATCAAATGC
301    ATCCCAAAAA CCTATACAAA TTAATGATAA AAAAAATGAA ATATTTATAG ATATAGTTGA
361    AAAAATTAAT TTAATTATGA ATTCGAATGG AGAAATAGTA TATTCATATA TTGATGGTGT
421    TATACAAATA AAATCTTATT TATTAGGAAA TCCATTTATC AAAATAGCTT TGAATGATGA
481    TTTATATATT AAAAATATTC ATCATGATAA TTCAAATAAT ATTATTATTG ACGATTGTAA
541    TTTTAATCAT CTAGTTAATT TATCACAATT TGAAAAAGAT AAAATTCTAT CTTTATACCA
601    ACCAGATGGT GAATGTGTAC TTATGAATTA TCGAATCAAT AATAACTTTA AAGCGCCTTT
661    TAAAATATAT GCTAATGTTA TATATAACCA AAATCATACG GTAGAATTGT GTATAAGAAT
721    ACGGCTAGAT ATCCCTTCTC AATATACATG CACAAATGTA TTTGTTTATT GCAATTTATG
781    TAAACACATA ACTAATGTAC ATTTGGACTT GAATACGAAT TCGGATTTAT TCTCAGCTCA
841    ATATATATCA AATGAGAACA AATTATTATG GACCATCAAA AAATTCAAGG GAGAACACGA
901    ATATAGTATT CGATCAAAAA TTACCTTAAG TCCTCATTAT GCCTTTTCAA AACGAGATTT
961    TGGACCTATA TATATTTTAT TTGAAATACC AATGTTTAAT TTATCAAAAC TTAGAATAAA
1021   ATATCTGAGG ATAATTGAAA ATTACAAAAC AAGTAATACG CACCGATGGG TGSGTTATAT
1081   AACTCAATCT TCTTCATATG TTTACCGTTT GAACGGTACC ATGAGTAAAG GAGAAGACTT
1141   GMC              μ4                  KpnI   GFP coding sequence
```